

© 2014, S.M. Haaker
Alle rechten voorbehouden
All rights reserved
ISBN: 978-90-8891-951-0

Cover design: Lau & Shanna (Inspired by the Fibonacci sequence)
Printed by: Proefschriftmaken.nl || Uitgeverij BOXPress
Published by: Uitgeverij BOXPress, 's-Hertogenbosch

Contact: shannahaaker@gmail.com

TOPOLOGICAL PHASES IN CONDENSED MATTER SYSTEMS

A study of symmetries, quasiparticles and phase transitions

ACADEMISCH PROEFSCHRIFT

ter verkrijging van de graad van doctor
aan de Universiteit van Amsterdam
op gezag van de Rector Magnificus
prof. dr. D.C. van den Boom
ten overstaan van een door het college voor promoties
ingestelde commissie,
in het openbaar te verdedigen in de Agnietenkapel
op vrijdag 3 oktober 2014, te 10:00 uur

door

Shanna Merinde Haaker

geboren te Amsterdam

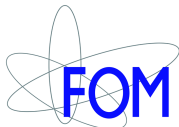
PROMOTIECOMMISSIE

Promotores: Prof. dr. C.J.M. Schoutens
Prof. dr. ir. F.A. Bais

Overige leden: Prof. dr. J. de Boer
Prof. dr. J.-S. Caux
Prof. dr. C. Morais Smith
Dr. V. Gritsev
Dr. B.D.A. Estienne

Faculteit der Natuurwetenschappen, Wiskunde en Informatica

The research described in this thesis is part of the research programme of the *Foundation for Fundamental Research on Matter* (FOM), which is part of the *Netherlands Organisation for Scientific Research* (NWO) and was carried out at the *Institute of Physics, University of Amsterdam* in The Netherlands.



This thesis is based on the following papers:

F.A. Bais, J.K. Slingerland, and S.M. Haaker, THEORY OF TOPOLOGICAL EDGES AND DOMAIN WALLS, *Phys. Rev. Lett.* **102**, 220403 (2009).

B. Estienne, S.M. Haaker, and K. Schoutens, PARTICLES IN NON-ABELIAN GAUGE POTENTIALS: LANDAU PROBLEM AND INSERTION OF NON-ABELIAN FLUX, *New J. Phys.* **13**, 045012 (2011).

S.M. Haaker, F.A. Bais, and K. Schoutens, NONCOMPACT DYNAMICAL SYMMETRY OF A SPIN-ORBIT-COUPLED OSCILLATOR, *Phys. Rev. A* **89**, 032105 (2014).

F.A. Bais and S.M. Haaker, TOPOLOGICAL SYMMETRY BREAKING: DOMAIN WALLS AND PARTIAL INSTABILITY OF CHIRAL EDGES, arXiv:1407.5790.

S.M. Haaker, F.A. Bais, and J.K. Slingerland, A QUANTUM GROUP APPROACH TO FRACTIONAL QUANTUM HALL HIERARCHIES, *working title*.

Contents

| | |
|---|-----------|
| A very short introduction to this thesis | 1 |
| 1 Topology, condensed matter systems and artificial gauge fields | 5 |
| 1.1 Topological phases of matter | 5 |
| 1.2 Quantum Hall physics and topology | 8 |
| 1.2.1 Landau problem | 8 |
| 1.2.2 Laughlin argument | 9 |
| 1.2.3 Berry phase | 10 |
| 1.2.4 Parallel transport | 12 |
| 1.2.5 Chern numbers | 12 |
| 1.3 Artificial gauge fields | 14 |
| 1.3.1 Rotating cold atoms | 14 |
| 1.3.2 Atom-laser coupling | 16 |
| 1.3.3 Optical lattices | 17 |
| 1.4 Non-Abelian gauge fields | 18 |
| 1.4.1 Basic features of non-Abelian gauge fields | 19 |
| 1.4.2 Berry matrix | 20 |
| 1.4.3 Cold atoms | 22 |
| 1.5 Topological insulators | 22 |
| 1.5.1 2D time-reversal invariant topological insulator | 23 |
| 1.5.2 Majorana fermions | 25 |
| 2 Topological symmetry breaking and fractional quantum Hall states | 27 |
| 2.1 Topological excitations in $(2 + 1)$ dimensions | 27 |
| 2.1.1 Fusion and splitting | 28 |
| 2.1.2 Braiding and topological spin | 29 |
| 2.2 Topological symmetry breaking | 31 |
| 2.3 Effective theory FQH states | 34 |
| 2.3.1 K matrix formalism | 35 |
| 2.3.2 CFT description | 36 |
| 3 Noncompact dynamical symmetry of a spin-orbit coupled oscillator | 39 |
| 3.1 Spin-orbit coupled harmonic oscillator | 40 |
| 3.2 Symmetry algebra | 43 |
| 3.2.1 Rescaled operators | 44 |
| 3.2.2 $SO(3, 2)$ representation theory | 47 |

| | | |
|----------|---|------------|
| 3.2.3 | Representations of the physical operators | 49 |
| 3.3 | Spectrum generating algebra | 50 |
| 3.A | Representation theory $SO(3)$ versus $SO(2, 1)$ | 53 |
| 3.B | Commutation relations physical operators | 57 |
| 4 | Non-Abelian gauge potentials: Landau problem and non-Abelian flux | 59 |
| 4.1 | The non-Abelian Landau problem | 60 |
| 4.1.1 | On the plane | 61 |
| 4.1.2 | On the sphere | 63 |
| 4.2 | Adiabatic insertion of non-Abelian flux | 67 |
| 4.A | Landau levels on the plane | 77 |
| 4.B | Landau levels on the sphere | 78 |
| 4.C | Details about the non-Abelian field on the sphere | 80 |
| 4.D | Generic non-Abelian field configuration | 82 |
| 5 | Topological symmetry breaking: Domain walls and an instability of chiral edges | 85 |
| 5.1 | Unstable chiral $U(1)$ states | 86 |
| 5.1.1 | Unstable bosonic Laughlin states | 86 |
| 5.1.2 | Unstable fermionic Laughlin states | 88 |
| 5.2 | Domain walls and confinement | 89 |
| 5.2.1 | Vertex operators and Wilson loops | 89 |
| 5.2.2 | Vacuum expectation value and ground state degeneracy | 91 |
| 5.2.3 | Domain walls | 93 |
| 5.2.4 | Confined particles | 94 |
| 5.2.5 | Unstable general Laughlin states | 97 |
| 5.A | CFT description of $U(1)$ chiral states | 98 |
| 5.B | Laughlin states | 99 |
| 5.B.1 | Bosonic Laughlin states | 99 |
| 5.B.2 | Fermionic Laughlin states | 99 |
| 6 | Boundaries between topological phases induced by a multilayer Bose condensate | 101 |
| 6.1 | Multilayer condensation | 102 |
| 6.2 | Phase transition between non-Abelian states | 104 |
| 6.2.1 | Kitaev's honeycomb and the toric code | 104 |
| 6.2.2 | The Pfaffian/NASS interface | 107 |
| 6.3 | Phase transitions between different levels of the HH hierarchy | 109 |
| 6.A | General HH hierarchy | 116 |
| 6.A.1 | From the 0th to the 1st level | 116 |

| | | |
|----------|---|------------|
| 6.A.2 | Transitions to k th level of the HH hierarchy | 119 |
| 7 | Outlook | 123 |
| | Bibliography | 127 |
| | Samenvatting | 139 |
| | Summary | 147 |
| | Dankwoord | 155 |

A very short introduction to this thesis

The content of this thesis is based on the research I did during my time as a Ph.D. student and it focuses on *topological phases* in condensed matter systems from a theoretical physics point of view. This is a rapidly developing branch of low-energy physics and started with the unexpected observations of the quantized Hall conductance $\sigma_H = n \frac{e^2}{h}$ in an experiment performed by von Klitzing et al. in 1980 [1]. What makes this branch of physics so exciting in my opinion, is the beautiful interplay between theoretical and experimental physics. I will illustrate this symbiotic relationship by highlighting several experimental observations and theoretical predictions which followed from one another that are all in some way related to the subject of topological phases, and will appear at certain stages of this thesis.

Initially the quantization of the Hall conductance was not well understood until the theorist Laughlin gave a plausible argument explaining this precise quantization [2], which was later reformulated by several different theorists and cast into a general framework of topology [3–6]. Mathematicians developed the concept of topology to classify different spaces by invariant properties under continuous deformations. The classic example is that a coffee cup is topologically equivalent to a donut, as both of the objects have one hole and can be transformed into each other by stretching and bending. Only two years after the discovery of the integer quantum Hall effect, the experimentalists obtained another surprising result, when Tsui et al. observed plateaus of the Hall conductance at fractional values $\sigma_H = \nu \frac{e^2}{h}$ [7]. These results inspired Laughlin to propose a multi-particle wave function explaining the observations [8]. If one were to believe his proposal, an immediate consequence would be that the low-lying excitations must have fractional charge of $e^* = e/3$, with e the electron charge. This was indeed confirmed by two experimental groups in 1997 [9, 10].

In the meantime, the theory of the quantum Hall effect had developed at a rapid pace and concepts from many different fields in physics were adopted and put to use. In 1991, Moore and Read wrote a seminal paper in which they express Laughlin's wave function in terms of conformal field theory correlators [11]. This enabled them to propose many other trial quantum Hall wave functions by using different conformal field theories, with their most prominent outcome being a wave function which is now a leading candidate for the plateau observed at $\nu = 5/2$ [12]. This result in turn predicted that the fundamental quasiparticles of the $\nu = 5/2$ phase must have non-Abelian statistics, which gave a huge boost to the research on fractional quantum Hall states, as these theoretically predicted quasiparticles could serve as qubits of a fault-tolerant (topological) quantum computer [13].

It might not have escaped the reader with a background in this field that yet another boost came after the turn of the millennium. This time it was the theorists who realized

that certain band insulators with spin-orbit coupling were topologically different from trivial insulators. These time-reversal invariant *topological insulators* have an insulating bulk and topologically protected edge modes which are helical instead of chiral [14, 15]. Shortly after this realization, these topological phases were indeed observed [16]. This eventually led to an entire classification of topological noninteracting fermionic phases in every spatial dimension [17–19]. Some of these phases have been predicted to carry Majorana particles [20–22], which are highly sought-after particles in many branches of physics. Not only would the observation of such a particle confirm the predictions made by Ettore Majorana in 1937 [23], they also have non-Abelian statistics in the present context. In 2012 the group of Kouwenhoven from Delft reported on strong signatures that they had observed these Majorana particles at the endpoints of a one-dimensional topological wire [24] and more experiments obtaining similar results followed subsequently [25–29].

With this short overview of some selected topics within the framework of topological phases in condensed matter system, I hope to have convinced the reader of the rapid development and utmost importance of this branch of physics.

Let me conclude this very short introduction by guiding the reader through the outline of this thesis. The first two chapters are introductory, meaning that the stage is set and notation fixed for the chapters to follow.

In chapter 1 we focus on the topological phases that stem from an underlying noninteracting system. We start by showing how the concept of topology emerges in physics and focus mainly on the integer quantum Hall effect. By introducing concepts like the Berry phase, parallel transport and Chern numbers we demonstrate how the quantized Hall plateaus can be explained by topological invariants. Then we digress from condensed matter physics to ultracold atomic systems, which may function as quantum simulators. We show how artificial gauge fields arise from such systems and how they can generalize to non-Abelian gauge fields. The different components of non-Abelian gauge fields do not commute with each other unlike the conventional $U(1)$ Maxwell theory. In the final part of this chapter we return to topological phases and discuss topological insulators and the emergence of Majorana fermions.

In chapter 2 the focus lies on $(2 + 1)$ -dimensional topological phases that have an underlying strongly correlated microscopic theory. We show how the topological excitations of these phases may be labeled by irreducible representations of a quantum group and that these particles together with their interactions form an anyonic model. The quantum numbers associated with their fusion and braiding interactions are presented, and we show how a phase transition between two topological phases can be driven by the condensation of a nontrivial quasiparticle, thus breaking the underlying symmetry. This formalism is called topological symmetry breaking and the main ingredients are discussed. The chapter is concluded with a section on the effective field theory of the fractional quantum Hall

phases and how it is related to conformal field theory.

After these introductory chapters we move to chapter 3, where the symmetry algebra of a spin-orbit coupled harmonic oscillator in three dimensions is derived. This model was proposed as a continuum model of a three-dimensional topological insulator. Its spectrum has finite and infinite degeneracies and we determine the symmetry operators that are associated with these degeneracies. The operators form a nonlinear algebra, but after a simple rescaling $SO(3, 2)$ commutation relations are obtained. At the end of the chapter the algebra of operators that connect the different energy levels is derived.

In chapter 4 the effect of non-Abelian gauge potentials on two-dimensional integer quantum Hall states is investigated. First we discuss the problem of a spin- $\frac{1}{2}$ particle confined to a sphere in a perpendicular $U(2)$ background magnetic field. Its spectrum is derived and falls into $SU(2)$ irreps reflecting the rotational symmetry of the system. The large radius limit is obtained and we retrieve the corresponding configuration on the plane. In the second part of this chapter we probe a planar quantum Hall system by inserting a non-Abelian flux. Starting from a spin-polarized state, the adiabatic insertion of the flux results in a state with nontrivial spin-texture which is recognized as a quantum Hall skyrmion.

Chapter 5 focuses on fractional quantum Hall states and topological symmetry breaking. Certain states with chiral edge modes may undergo a phase transition to a state at higher filling fraction. We then show that a careful treatment of topological symmetry breaking results in a possible degeneracy of ground states in the broken phase. The system chooses one of these ground states resulting in a spontaneous breaking of the symmetry. As a consequence different domains may appear with domain walls in between. We discuss this phenomenon in detail on the edge as well as in the bulk of the system. A thorough study of confined particles is presented where we show that they are indeed confined in the bulk, but not on the edge. Even though they are not confined they do become massive and break the chiral symmetry.

In chapter 6 we study phase transitions induced by multilayered condensates, which vastly increases the number of phases topological symmetry breaking can be applied to. In the first part we examine non-Abelian phases and in the second part we address an entire hierarchy of fractional quantum Hall states. A special focus is given to the study of the one-dimensional boundary between the two phases.

This thesis is concluded in chapter 7, where we give an outlook of open problems and suggest possible interesting topics for future research.

CHAPTER 1

Topology, condensed matter systems and artificial gauge fields

In this first chapter we present the main concepts that part of the research dealt with in this thesis was based on and inspired by. As such this chapter does not contain any original results, but serves to set the stage for later chapters. In one way or another these topics are linked to noninteracting topological systems. We start, in section 1.1, by recalling how the concept of topology recently reemerged in condensed matter physics in a novel guise referred to as *topological ordered phases of matter*. In section 1.2 we show how topological invariants come about by guiding the reader through diverse concepts including the quantum Hall effect, Berry phases and Chern numbers. Section 1.3 addresses *artificial gauge fields* and how they can be created in cold atomic systems. These cold atoms are not actual dynamical degrees of freedom of the condensed matter system but rather furnish an effective highly controllable setup to represent specific effects that are present in the system. They even allow for a generalization in the form of non-Abelian gauge fields, which is presented in section 1.4. Finally, in section 1.5, we briefly touch upon a new class of topological phases, called *topological insulators*, which were discovered less than a decade ago.

1.1 Topological phases of matter

The topic that binds all the chapters of this thesis together is the notion of topological phases of matter, which has matured over the last two decades into an important field of condensed matter physics. But let us take a step back and start with topology. It is a branch of mathematics which studies certain global properties of a space. Roughly stated, it studies the properties of a space that stay invariant under continuous deformations of the geometry of the space, which excludes cutting or gluing. Manifolds that are locally different are considered to have the same topology if they can be transformed into each other by the aforementioned continuous deformations. Perhaps the simplest example of two spaces which are topologically different is a cylinder of finite length versus the Möbius strip. Both objects are depicted in fig. 1.1 along with a finite strip from which they can be obtained. At any point, i.e. locally, the Möbius strip can be smoothed in such a way that it is identical to the cylinder. But globally we can never get rid of the twist, which makes the Möbius strip topologically different from the cylinder.

Topology arises in many different fields of physics. An excellent historical discussion

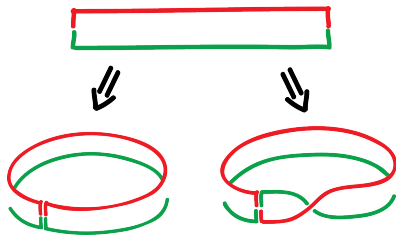


Figure 1.1: The difference in topology between a finite cylinder and the Möbius strip is shown. Starting from a finite strip we can either glue the short edges together in such a way that the red part connects to the red and the green to the green, giving a cylinder which has trivial topology. Alternatively, we can glue the red to the green part, thus obtaining a Möbius strip. Note that there has to be a twist somewhere along the Möbius strip resulting in a nontrivial topology. Moreover the cylinder has two sides, whereas the Möbius strip has only one.

of the connection between topology and physics is given by Nash in chapter 12 of [30]. Here we give one well-known example: the possible existence of a magnetic monopole¹ due to Dirac [31]. Consider the magnetic field of a magnetic monopole with charge q_m , which is of the form

$$\mathbf{B}(\mathbf{r}) = \frac{q_m}{r^2} \hat{r}. \quad (1.1)$$

It obeys Maxwell's equations everywhere except at the origin. We may choose an appropriate gauge and express the field in terms of a vector potential

$$\mathbf{A}_+(\mathbf{r}) = \frac{q_m}{r} \frac{1 - \cos \theta}{\sin \theta} \hat{\phi}, \quad (1.2)$$

which satisfies $\mathbf{B} = \nabla \times \mathbf{A}_+$ and is expressed in spherical coordinates, with r the distance to the origin, θ the polar coordinate, and ϕ the azimuthal coordinate. Note that this field configuration has a line singularity which runs from the monopole along the negative \hat{z} -axis, i.e. for $\theta = \pi$. This reflects the singularity of the magnetic field at the origin and it is called the *Dirac string*. Of course, we could have chosen a different gauge-equivalent vector potential

$$\mathbf{A}_-(\mathbf{r}) = \frac{q_m}{r} \frac{-1 - \cos \theta}{\sin \theta} \hat{\phi}, \quad (1.3)$$

¹The existence of a magnetic monopole implies that electric charge is quantized. Even though magnetic monopoles have not yet been observed, the quantization of electric charge is a fact.

which has a singularity at $\theta = 0$. These two potentials are related by a gauge transformation $U = e^{2iq_m\phi}$. If we now use \mathbf{A}_+ for the upper hemisphere and \mathbf{A}_- for the lower hemisphere, we have a well-defined field covering the entire space. The Dirac string can be moved around, but cannot be removed: it is a gauge artifact.

If we have a particle with electric charge q_e subject to this field configuration, a gauge transformation influences the wave function of the particle. In the upper hemisphere we have $\psi_+(\mathbf{r})$ and in the lower part $\psi_-(\mathbf{r})$. In the region where the two configurations overlap, the two wave functions have to be related by a gauge transformation

$$\psi_+ = e^{\frac{2iq_e q_m}{\hbar c} \phi} \psi_- . \quad (1.4)$$

The wave function of this particle should be single-valued, leading to $\frac{2iq_e q_m}{\hbar c} \in \mathbb{Z}$, which is *Dirac's quantization condition*. These integers can be understood by considering a mapping between different topological spaces, called a *homotopy group*. In the present case the mapping is from the overlap region which is a circle in real space S^1 , to the $U(1) \sim S^1$ gauge group, i.e. $\pi_1(S^1) = \mathbb{Z}$.

The connection between topology and physics that we are interested in, is what is called *topological phases of matter*. These are phases in condensed matter that are not characterized by some local order parameter, but still can be distinguished from a trivial phase (which has the same symmetry) by some topological invariant [3, 32, 33]. It is a relatively young subject, and the definition of a topological phase of matter varies in the literature [34]. Some say it is a phase which has a low energy effective description in terms of a topological field theory. Others state that if such a phase shares an edge with a different topological phase (which could be a trivial phase), it must carry robust gapless edge excitations. Yet another definition might be that it is a phase whose quasiparticle excitations in the bulk are anyons. We will not attempt to give a precise definition in this thesis, instead we will discuss several different phases of matter that can be characterized by some topological invariant and investigate what their properties are. In chapters 3 and 4 we will treat noninteracting systems, whereas chapters 5 and 6 deal with the interacting case.

It is important to mention one of the major features of topological phases at this point. Some of these phases can carry quasiparticles which could serve as robust fundamental building blocks for the future hardware of a decoherence-free quantum computer [13]. Information can be stored in the nonlocal nature of these particles and the qubits are manipulated by exchanging the particles in space. An example of such a phase is the Moore-Read state which is discussed in chapter 6.

After this short general introduction in topological phases of matter we will dedicate the next section to the quantum Hall effect, with a focus on its connection to topology.

1.2 Quantum Hall physics and topology

Although it was not immediately clear at the time when von Klitzing conducted his famous experiment leading to the discovery of the *quantum Hall effect* [1], it is now considered to be the first example of a topological phase of matter. He discovered that under certain extreme conditions a two-dimensional electron gas in a perpendicular strong magnetic field has an off-diagonal resistance that does not depend linearly on the strength of the magnetic field. Instead, for certain ranges it develops a plateau, i.e. it becomes quantized and the Hall conductance can be expressed as $\sigma_H = n \frac{e^2}{h}$, with n a positive integer. This result was totally unexpected, because it implied that in a complicated medium such as a Hall conductor, a physical quantity could be quantized exactly in terms of the ratio of two fundamental constants of nature.

The scientific community has not been standing by idly since then. Much progress has been made and a lot has been written on this subject. Therefore, we will select a few topics within the broad field of quantum Hall physics to present in this part of the introduction, since these are related most to our results in chapters 3 and 4. We limit ourselves to discussing topological aspects of the one-particle problems that underly quantum Hall phases, and postpone the treatment of the fractional quantum Hall effect until chapter 2. There is also extensive literature about the integer quantum Hall effect (IQHE), including reviews to which we refer the reader for a more detailed account [35–38].

1.2.1 Landau problem

A basic starting point for understanding the IQHE is the Landau problem [39]. It describes a particle of charge q and mass m in \mathbb{R}^2 subject to a perpendicular constant magnetic field $\mathbf{B} = B\hat{z}$. The corresponding Hamiltonian can be exactly solved and is given by

$$H = \frac{1}{2m} (\mathbf{p} - q\mathbf{A})^2, \quad (1.5)$$

with \mathbf{A} the vector potential for which $\mathbf{B} = \nabla \times \mathbf{A}$. There are several ways one can solve this system and in chapter 3 we will solve it explicitly by identifying its spectrum generating algebra, but for now we merely give some results. Its spectrum is

$$E_n = \hbar\omega_c(n + \frac{1}{2}), \quad n = 0, 1, \dots, \quad (1.6)$$

where every integer n labels a so-called Landau level and $\omega_c = \frac{qB}{m}$ is the cyclotron frequency associated with the orbit of a classical particle. Choosing the symmetric gauge $\mathbf{A}(\mathbf{r}) = \frac{1}{2}\mathbf{B} \times \mathbf{r}$, the normalized eigenstates of the lowest Landau level (LLL) in polar

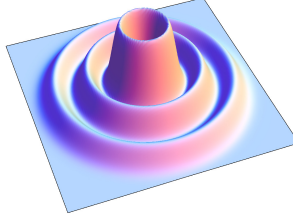


Figure 1.2: Density profiles of a few orbitals in the LLL, namely $k = 2, 12$ and 30 . The rotational symmetry, stemming from the symmetric gauge, is clearly visible.

coordinates are

$$\psi_{n=0,k}(\mathbf{r}) = \frac{1}{\sqrt{2\pi}} \frac{r^k e^{ik\phi}}{\sqrt{2^k k!}} \exp(-r^2/4\ell^2). \quad (1.7)$$

These states are rotationally symmetric and are localized around $r \sim \ell\sqrt{2k}$, where k is the eigenvalue of the angular momentum operator $L_z = -i\partial_\phi$. The density profiles of three of these eigenstates are plotted in fig. 1.2.

The quantum problem has a characteristic length scale $\ell^2 = \frac{\hbar}{qB}$, called the *magnetic length*, which dictates the area occupied by a particle as can be seen from the Gaussian factor in (1.7). In an infinite sample each Landau level (LL) is infinitely degenerate, since the energy does not depend on k , but for a finite sample of area A there are $N_\phi = \frac{BA}{\phi_0}$ states available, where $\phi_0 = h/q$ is a flux quantum. The number of filled orbitals N_e divided by the number of available states is the *filling fraction* $\nu = \frac{N_e}{N_\phi}$. The Hall conductance can be expressed in terms of the filling fraction as $\sigma_H = \nu \frac{e^2}{h}$. When the system is at one of the plateaus, i.e. the conductance does not change as a function of magnetic field, the filling fraction is exactly an integer. This phenomenon can not be explained from the Landau problem alone, and one needs to incorporate a confining potential and random impurities, as is the case in real experiments. The next topic we address is Laughlin's argument for the quantization of the Hall conductance.

1.2.2 Laughlin argument

The exact quantization of the Hall conductance $\sigma_H = n \frac{e^2}{h}$ strongly suggests that there must be some underlying topological invariant. The first attempt to explain this quantization was made by Laughlin [2], nowadays known as the *Laughlin argument*, in which he uses gauge invariance to show that the conductance must be quantized.

Consider a ribbon of length L with periodic boundary conditions along the x -direction. It has a constant magnetic field perpendicular to its surface and a potential difference V between the two edges of the ribbon. Imagine that a flux is switched on which pierces through the hole of the ribbon. The changing flux corresponds to a term $\delta A_x(t)$ in the Hamiltonian.

For a clean system the density of states consists of sharp delta functions at every Landau level, but when there is disorder in the system, the peaks broaden into extended states close to the Landau energy with tails of localized states. If all states were localized, the addition of δA_x would only result in multiplying the one-particle wave functions by a phase $\exp(ie\delta A_x x/\hbar)$, but when there are extended states we must have $\delta A_x = n' \frac{\hbar}{eL} = n' \phi_0/L$, with $n' \in \mathbb{Z}$ for the states to be single-valued. The effect of δA_x is that the energy of a single-particle state increases linearly and the position around which it is centered also shifts linearly.

After adding one flux quantum to the system, it is a gauge transformation away from the situation without flux so the increase of energy has to come from the charge transfer of one edge of the ribbon to the other. The current is given by $I = n \frac{e^2}{h} V = \sigma_H V$, where n is the number of filled LLs. Note that this quantization occurs whenever the Fermi energy lies in a mobility gap, meaning that only localized states can be excited at this energy. Whenever we sweep the chemical potential away from the mobility gap, σ_h is no longer quantized and we are at a transition between two plateaus.

A number of questions can be raised considering Laughlin's argument, for instance: how does the particular geometry influence the results? What happens in the presence of large disorder? To fully understand the quantization of the Hall conductance we need heavier machinery, which is presented in the following paragraphs. Still, Laughlin's argument has proved useful in many different situations, since the response of a system to the insertion of flux can give you much insight into the topology of the phase. This tool is encountered again in chapter 4, where we use it to show the emergence of excitations with a nontrivial spin-texture after inserting 'non-Abelian' flux.

To show how the quantized Hall conductance can be linked to a topological invariant we first need to introduce several notions: the Berry phase, parallel transport, and Chern numbers. A review on this can be found in [37]. For a review on Berry phases related to electronic properties we recommend [40].

1.2.3 Berry phase

In 1984 Berry showed, in a beautifully written paper, that an energy eigenstate of a quantum system described by a Hamiltonian $H(\mathbf{R})$ picks up a phase when the set of parameters \mathbf{R} on which the Hamiltonian depends is varied adiabatically from an initial value \mathbf{R}_i to some final value \mathbf{R}_f [41]. The phase factor consists of two parts: the dynamical phase and the geometric phase, where the latter is now widely known as the *Berry phase*. Let us follow his derivation in some detail.

Consider a Hamiltonian $H(\mathbf{R})$, which depends on a set of parameters $\mathbf{R} = (R_1, R_2, \dots)$. Imagine that the parameters $\mathbf{R}(t)$ are varied between times $t = 0$ and $t = T$, where we will consider a closed loop \mathcal{C} in parameter space, meaning $\mathbf{R}(0) = \mathbf{R}(T)$. The Hamiltonian can be diagonalized at each point \mathbf{R} and we choose an orthonormal set of eigenstates

$$H(\mathbf{R})|n(\mathbf{R})\rangle = E_n(\mathbf{R})|n(\mathbf{R})\rangle. \quad (1.8)$$

Now assume that the ground state at every point in parameter space has a gap to the excited states. We want to follow its adiabatic evolution under the change of \mathbf{R} and since it starts out as an eigenstate of H it must stay an eigenstate, but there is freedom in the phase it picks up. The ground state $|\psi(t)\rangle$ must obey the Schrödinger equation at any point in parameter space

$$H(\mathbf{R}(t))|\psi(t)\rangle = i\hbar \frac{d}{dt}|\psi(t)\rangle, \quad (1.9)$$

which we may employ to find the phase of the eigenstate. Denoting the initial state as $|\psi(0)\rangle$, and adiabatically following the loop \mathcal{C} , the final state is

$$|\psi(T)\rangle = \exp\left(\frac{-i}{\hbar} \int_0^T dt E_n(\mathbf{R}(t))\right) \exp(i\gamma_n(\mathcal{C}))|\psi(0)\rangle, \quad (1.10)$$

where the Berry phase can be expressed as

$$\gamma_n(\mathcal{C}) = i \int_{\mathcal{C}} \langle n(\mathbf{R}) | \nabla_{\mathbf{R}} n(\mathbf{R}) \rangle \cdot d\mathbf{R}. \quad (1.11)$$

A beautiful aspect of the Berry phase is its analogy to gauge theories. For instance, the Aharonov-Bohm effect of a charged particle traveling around a flux tube, can be understood in terms of the Berry phase. In that case the Berry phase is equal to the flux enclosed by the loop and the quantity $\mathbf{A} = i \langle n(\mathbf{R}) | \nabla_{\mathbf{R}} n(\mathbf{R}) \rangle$ which is known as the *Berry connection*, is equal to the electromagnetic vector potential. Its connection to gauge theory can also be seen by noting that under a $U(1)$ transformation $|n\rangle \rightarrow e^{if(\mathbf{R})}|n\rangle$, the Berry connection transforms as a $U(1)$ gauge field $\mathbf{A} \rightarrow \mathbf{A} - \nabla_{\mathbf{R}} f(\mathbf{R})$. Obviously, this makes the Berry phase a gauge invariant object as is the case for magnetic flux in electrodynamics: $\oint \mathbf{A}_{\text{ED}} \cdot d\mathbf{l} = \Phi$.

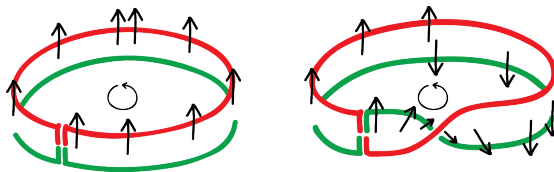


Figure 1.3: Parallel transport of a vector around the finite cylinder and the Möbius strip. In the latter case one sees that parallel transport leads to a nontrivial holonomy corresponding to an angle π , indicating that the Möbius strip has a nontrivial topology. This holonomy does not depend on the vector chosen and in quantum theory it corresponds to an observable because it is gauge invariant.

1.2.4 Parallel transport

It was Simon who pointed out to Berry that his geometric phase factor can be associated to the notion of parallel transport, where the Berry phase is the *holonomy* of the connection \mathbf{A} [5]. We will explain this terminology in more detail, because it will ultimately give us a topological interpretation of the quantized Hall conductance.

In flat space we can easily determine if two vectors are parallel to each other, but to compare two vectors at different points in a curved space we need the notion of *parallel transport* of a vector along a certain path. In order to use parallel transport, a connection \mathbf{A} needs to be defined on that space. If we now parallel transport a vector (for instance a quantum state) around a closed loop with a given connection it may happen that the vector ends up pointing in a different direction compared to the initial vector. If this is the case we speak of a nontrivial holonomy, which usually signals the presence of a curvature or a nonvanishing field strength \mathbf{B} somewhere inside the loop. Two examples are graphically depicted in fig. 1.3.

It should be clear how this notion relates to the Berry phase. The Berry connection \mathbf{A} allows us to parallel transport an energy eigenstate along a path in parameter space. The Berry phase $\gamma(\mathcal{C})$ gives the mismatch between the initial state and the final state obtained after transportation around the loop \mathcal{C} , and therefore is associated to the holonomy.

1.2.5 Chern numbers

A well-known relation between geometry and topology is the Gauss-Bonnet theorem. For a surface without a boundary it is given by

$$\frac{1}{2\pi} \int_{\mathcal{S}} K dA = 2(1 - g), \quad (1.12)$$

where the integral of the local curvature K is taken over the surface \mathcal{S} and g is the number of handles of \mathcal{S} , which is the invariant characterizing its topology. This was generalized

by Chern to apply also to eigenstates parametrized by two periodic variables forming a torus.

The quantization of the Hall conductance can be understood most easily from a minimally coupled Hamiltonian with a periodic potential. For a description in terms of a random potential we refer to refs. [42, 43]. Thouless et al. were the first to show that the quantization of the Hall conductance could be obtained from the bulk properties instead of using edges, as was the case for the Laughlin argument [3]. The invariant they obtained is now widely known as the TKNN number and the connection with topology was made by a number of authors [4–6].

In a periodic potential and a perpendicular uniform magnetic field we can define a two-dimensional magnetic Brouillon zone, which is equivalent to a torus T^2 . The Hall conductance can be expressed as

$$\sigma_H = \frac{e^2}{h} \frac{1}{2\pi i} \int_{T^2} (\nabla_{\mathbf{k}} \times \mathbf{A}(\mathbf{k})) \cdot d\mathbf{k}, \quad (1.13)$$

where $\mathbf{A}(\mathbf{k})$ is the Berry connection in terms of Bloch states. This results in zero conductance if the Berry connection is smooth and single-valued through the entire Brouillon zone. Imagine there is a point in the Brouillon zone for which \mathbf{A} is singular. We can perform a gauge transformation and define a new connection \mathbf{A}' which has its singularity at a different point. Now split the torus into two parts T and T' , where \mathbf{A} is single-valued in T and \mathbf{A}' is single-valued in T' , and the connections are related by a gauge transformation $\mathbf{A}' = \mathbf{A} - \nabla_{\mathbf{k}} f(k)$. Stokes' theorem can be applied to rewrite the surface integral in (1.13) to a line integral

$$\sigma_H = \frac{e^2}{h} \frac{1}{2\pi} \int_{\mathcal{C}} (\mathbf{A} - \mathbf{A}') \cdot d\mathbf{l} = \frac{e^2}{h} \frac{1}{2\pi} \int_{\mathcal{C}} \nabla_{\mathbf{k}} f(k) \cdot d\mathbf{l} = n \frac{e^2}{h}. \quad (1.14)$$

The origin of this integer n can be understood by noticing that the phase $e^{if(k)}$ should be single-valued along the contour \mathcal{C} , but that it can have nontrivial winding. For the IQHE the number of filled LLs n is associated with the number of flux quanta piercing a unit cell. Thus somewhere in such a unit cell there has to be a vortex of vorticity n . This is the singularity that causes the nontrivial winding number and as a result the quantized Hall conductance.

After this introduction to the topology behind the IQHE, we would like to shift our attention to a different branch of physics: ultracold atoms. At first sight it may seem unrelated to quantum Hall physics, but we will see shortly how the two are connected through the concept of artificial gauge fields.

1.3 Artificial gauge fields

In both chapters 3 and 4 we will encounter physical models that are generalizations of the IQHE, but are somewhat exotic from a condensed matter point of view. Studying a theoretical model is interesting in its own right, but in our case we can find a realization in the realm of ultracold atoms. These systems are often used to mimic all sorts of physical settings, because they can be controlled with such great precision. For instance, the dimensionality of the system can be controlled, which opens the door to investigate all sorts of one- or two-dimensional phenomena. Also, the atoms can be loaded into optical lattices making it possible to probe all kinds of lattice models which are of theoretical interest. Using Feshbach resonance, the interaction between the atoms can be set to any type: strongly attractive, strongly repulsive, noninteracting. The power of ultracold atoms not only lies in mimicking certain systems in, for instance, condensed matter theory or high energy physics, but they can even generalize those systems.

In chapters 3 and 4 we will encounter a generalization of the magnetic field, which is responsible for the formation of LLs. These generalized gauge fields can be created in a cloud of neutral cold atoms and are called *artificial gauge fields*. We emphasize that these artificial gauge fields are external, their configuration is fixed by the choice of the external control parameters and they do not have any dynamics themselves.

In the remainder of this section we will focus on three different setups that are used to generate artificial gauge fields. For more information on ultracold atoms in general, we refer the reader to a review article of Bloch et al. and the references therein [44].

1.3.1 Rotating cold atoms

Rotating ultracold atomic gases are the first example of a system in which an artificial gauge field can be realized. It is well known that a type II superconductor subject to a uniform magnetic field is characterized by the formation of a vortex lattice. An image of such a lattice is shown in fig. 1.4a. Of course, a superconductor consists of charged electrons and they are subject to a real magnetic field, not an artificial field. In 2000 the group of Dalibard conducted an experiment on a rotating cloud of neutral ultracold atoms [45]. Their data, depicted in fig. 1.4b, clearly shows the formation of vortices. This rotating gas of neutral atoms behaves as though it consists of charged particles in a magnetic field.

Let us sketch why a rotating gas of neutral particles behaves like a system with charged particles coupled to a magnetic field. Following [46], the Hamiltonian of a noninteracting gas of N identical particles confined to a cylindrically symmetric trap is

$$H = \sum_{i=1}^N \left(\frac{\mathbf{p}_i^2}{2m} + \frac{1}{2} m \omega_{\perp}^2 (x_i^2 + y_i^2) + \frac{1}{2} m \omega_{\parallel}^2 z_i^2 \right), \quad (1.15)$$

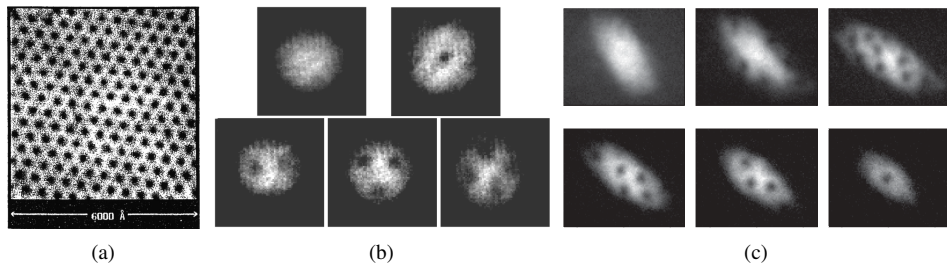


Figure 1.4: A vortex lattice can emerge in different physical systems. In fig. (a) we see a lattice in a type II superconductor subject to a perpendicular magnetic field [47]. Fig. (b) shows a lattice in a rotating gas of neutral atoms [45]. The lattice in fig. (c) was realized in a gas of neutral atoms which are coupled to laser fields [48].

with ω_{\perp} and ω_{\parallel} the trapping frequencies. Now imagine that the gas is rotating around the \hat{z} -axis so the angular momentum L_z is conserved. When we switch to a rotating reference frame, with angular momentum $\mathbf{\Omega} = \Omega \hat{z}$, the Hamiltonian in the rotating frame H_{rot} for one particle can be expressed as

$$\begin{aligned} H_{\text{rot}} &= H^{(1)} - \mathbf{\Omega} \cdot \mathbf{L} \\ &= \frac{1}{2m} (\mathbf{p} - q^* \mathbf{A}^*)^2 + \frac{1}{2} m (\omega_{\perp}^2 - \Omega^2) (x^2 + y^2) + \frac{1}{2} m \omega_{\parallel}^2 z^2. \end{aligned} \quad (1.16)$$

The first term is recognized as the kinetic term of a particle with charge q^* minimally coupled to an effective gauge field $\mathbf{A}^* = \frac{m}{q^*} \mathbf{\Omega} \times \mathbf{r}$, which corresponds to a magnetic field $\mathbf{B}^* = \frac{2m}{q^*} \mathbf{\Omega}$.

Even though we were considering neutral particles, in the rotating frame they are mathematically equivalent to a charged particle confined in a harmonic trap and subject to a uniform magnetic field pointing in the \hat{z} -direction. For rotations of order $\Omega \sim \omega_{\perp}$, the system is uniform in the plane perpendicular to \hat{z} , which leads to the Hamiltonian of the Landau problem in (1.5) plus a confining potential in the \hat{z} -direction. In the limit where the chemical potential is much smaller than $\hbar\omega_{\perp}$ and $\hbar\omega_{\parallel}$, the system is in a quasi two-dimensional LLL regime. This regime has been reached in experiments, see for instance [49].

1.3.2 Atom-laser coupling

The next setup in which artificial gauge fields can be realized, is an ultracold atomic cloud with atom-laser coupling. The main idea behind this scheme is that a neutral atom which is coupled through its internal degrees of freedom to a well-designed laser field, may pick up a Berry phase after traveling around a closed loop [50, 51]. As we saw in section 1.2 this phase is similar to the Aharonov-Bohm phase that a charged particle picks up when moving in a background magnetic field. So the Berry connection associated to such a setup can be thought of as an artificial (or geometric) gauge field.

Following ref. [51] we present a simple two-level system in which an artificial gauge field can be implemented. The atom of our toy model has two internal degrees of freedom which we will denote by $|g\rangle$ and $|e\rangle$. A general Hamiltonian can be written as

$$H = \left(\frac{\mathbf{p}^2}{2m} + V \right) \mathbb{I} + U, \quad (1.17)$$

where the first part is diagonal in $\{|g\rangle, |e\rangle\}$ and the mixing term can be expressed as

$$U = \frac{\hbar\Omega}{2} \begin{pmatrix} \cos\theta & e^{-i\phi} \sin\theta \\ e^{i\phi} \sin\theta & -\cos\theta \end{pmatrix}. \quad (1.18)$$

This term lifts the degeneracy of the system and can be realized by coupling the atom to a spatially dependent laser, where Ω gives the strength of the coupling, θ is the mixing angle and ϕ is the phase angle. The eigenstates of U are called *dressed states* and we denote them by $|\chi_1(\mathbf{r})\rangle$ and $|\chi_2(\mathbf{r})\rangle$ with eigenvalues $\pm \frac{\hbar\Omega}{2}$.

Imagine we start out in $|\chi_1(\mathbf{r})\rangle$ and the atom moves adiabatically under influence of the laser. It will stay in the same eigenstate and after completing an entire loop the Berry phase it picks up is given by

$$\gamma(\mathcal{C}) = i \oint_{\mathcal{C}} \langle \chi_1 | \nabla \chi_1 \rangle \cdot \mathbf{r}. \quad (1.19)$$

The artificial gauge potential that can be associated to this Berry phase is

$$\mathbf{A} = i \langle \chi_1 | \nabla \chi_1 \rangle = \frac{1}{2} (\cos\theta - 1) \nabla\phi, \quad (1.20)$$

and the magnetic field can be expressed as

$$\mathbf{B} = -\frac{1}{2} \sin \theta \nabla \theta \times \nabla \phi. \quad (1.21)$$

Note that we have set the ‘charge’ q to unity. This field configuration is nontrivial as long as θ and ϕ are spatially dependent.

In an experiment performed by the Spielman group, atoms with more than two internal degrees of freedom were used [48]. They managed to produce an artificial gauge potential $\mathbf{A} = By\hat{x}$, which corresponds to a uniform magnetic field pointing in the \hat{z} -direction. Images of vortex lattices in their atomic cloud are displayed in fig. 1.4c.

1.3.3 Optical lattices

The atom-laser configuration we just discussed is a continuum model, but ultracold atoms also allow for a discrete setting. With optical lattices the periodic ionic potential of real materials can be mimicked. The authors of ref. [52] proposed a two-dimensional lattice setup for neutral atoms with an artificial magnetic field. When the atoms hop around a unit cell of the lattice, they pick up a phase, again in the same way as a charged particle on a lattice does in a real magnetic field. Let us briefly illustrate how such a setup can be accomplished.

A three-dimensional periodic potential can be created by standing wave laser fields. It results in a potential

$$V(\mathbf{r}) = V_x \sin^2(kx) + V_y \sin^2(ky) + V_z \sin^2(kz), \quad (1.22)$$

where the wave vector of the light is $k = 2\pi/\lambda$. Assume the lattice traps atoms with two different internal degrees of freedom $\{|g\rangle, |e\rangle\}$ and that V_x and V_z are so large that hopping in those directions can be neglected. In the \hat{x} -direction the polarization is adjusted in such a way that the minima which trap the different internal states of the atoms are shifted by $\Delta x = \lambda/4$. Applying a static electric field in the \hat{x} -direction creates an offset of Δ between two adjacent minima. This is schematically shown in fig. 1.5.

Hopping along the \hat{x} -direction can be controlled by two Raman lasers $\Omega_{1,2} = \Omega e^{\pm i q y}$ which drive transitions between the two internal states of the atom and along the \hat{y} -direction by the depth of the potential. Taking all contributions into account, the total Hamiltonian can be expressed as

$$H = J \sum_{n,m} \left(e^{2\pi i \alpha m} a_{n,m}^\dagger a_{n+1,m} + a_{n,m}^\dagger a_{n,m+1} + \text{h.c.} \right), \quad (1.23)$$

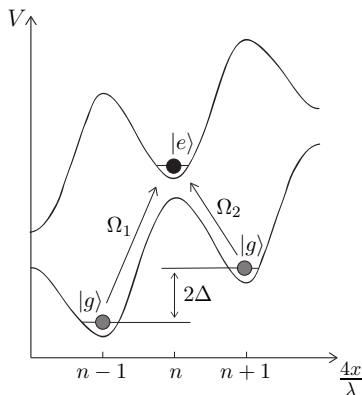


Figure 1.5: Potential landscape in the \hat{x} -direction. The local minima of the potential lie at $x_n = n\lambda/4$, where they alternate between an internal state denoted by $|g\rangle$ and $|e\rangle$. Hopping in this direction is accomplished by coupling to two Raman lasers $\Omega_{1,2}$.

where n and m label the minima of the potential at $x_n = n\lambda/4$ and $y_m = m\lambda/2$, and $\alpha = \frac{q\lambda}{4\pi}$ is the artificial flux through a unit cell. This Hamiltonian is the same studied by Hofstadter in ref. [53], which has the famous fractal spectrum nowadays called the *Hofstadter butterfly*. The flux through a unit cell depends on the strength of the magnetic field times the area of the cell, therefore it is difficult to reach high values of the flux in real metals as the unit cell is very small. When producing artificial gauge fields much higher values can be reached.

As mentioned before, not only can ultracold atomic settings be used to mimic certain condensed matter systems such as the IQHE and its lattice version, they also allow for certain generalizations. Non-Abelian gauge fields are one of these generalizations and the topic of the next section.

1.4 Non-Abelian gauge fields

Non-Abelian gauge fields give a proper description of interactions between elementary particles in high-energy physics, but in other fields of physics their presence is less obvious. After Berry's publication and Simon's interpretation of the geometric phase, Wilczek and Zee generalized their idea to a quantum system with a degenerate ground state manifold [54]. Before we introduce the non-Abelian geometric potential and show how this can be realized in ultracold atomic systems, we briefly mention some characteristics of non-Abelian gauge fields. In this introduction the main focus lies on their differences with $U(1)$ gauge fields.

1.4.1 Basic features of non-Abelian gauge fields

We are interested in the quantum problem of a particle coupled to an external non-Abelian gauge field A_μ , so we will not focus on the dynamics of the gauge fields themselves. Note that we use Greek indices to indicate the components of $(3 + 1)$ -dimensional space-time, whereas a boldface character represents spatial components.

The Hamiltonian for a nonrelativistic particle of mass m in an external magnetic field is

$$H = \frac{1}{2m}(\mathbf{p} - \mathbf{A})^2, \quad (1.24)$$

where the charge is set to $q = 1$. In the non-Abelian setup we generalize the framework to multicomponent wave functions, meaning that the vector potential or connection becomes Lie algebra valued, i.e. matrix valued. The non-Abelian cases we discuss have a two-component wave function, therefore the gauge group is $SU(2)$ and a local gauge transformation acts on the states as

$$\psi(x) \rightarrow \psi'(x) = U(x)\psi(x), \quad (1.25)$$

where x is a space-time coordinate. The gauge potential takes values in the Lie algebra corresponding to $SU(2)$ and can be decomposed into the Pauli matrices $A_\mu = A_\mu^a \sigma^a$, which generate this algebra. Introducing the covariant derivative

$$D_\mu = \partial_\mu - \frac{i}{\hbar}A_\mu, \quad (1.26)$$

and demanding that it transforms covariantly, i.e. $D'_\mu = U(x)D_\mu U^\dagger(x)$, imposes that the gauge potential has to transform as a connection

$$A_\mu \rightarrow A'_\mu = U(x)A_\mu U^\dagger(x) + i\hbar U(x)\partial_\mu U^\dagger(x). \quad (1.27)$$

This guarantees that the Hamiltonian in (1.24) transforms covariantly under the non-Abelian gauge group $SU(2)$.

Having defined the gauge potentials the non-Abelian version of the magnetic field or curvature can be introduced. It is also matrix valued like the gauge potential, and we want it to be a covariant quantity. This leads to the unique expression

$$\mathbf{B} = \nabla \times \mathbf{A} - \frac{i}{\hbar} \mathbf{A} \times \mathbf{A}. \quad (1.28)$$

The first term is the usual curl, while the second term $\mathbf{A} \times \mathbf{A}$ vanishes identically for Abelian gauge fields. In contrast to the Abelian case, even a uniform potential can produce a nonzero magnetic field. Another important difference is that in the Abelian case, two field configurations \mathbf{A} yielding the same magnetic field are necessarily equivalent up to a gauge transformation (on a simply connected space), but this is not the situation for non-Abelian gauge groups. Let us consider a specific example to make this statement explicit.

It is known from ref. [55] that there are two gauge-inequivalent kinds of non-Abelian vector potentials which produce a uniform magnetic field. This uniformity is defined in such a way that the gauge field at any two points in space is related by a gauge transformation. When this condition is met, a gauge can be chosen such that all the components of the corresponding curvature are constant. In this particular context we choose a magnetic field of the form $\mathbf{B} = 2\sigma_z \hat{z}$. The first option is an Abelian gauge field, which depends linearly on position

$$\mathbf{A}^{(1)} = \frac{1}{2}\mathbf{B} \times \mathbf{r} = \sigma_z \begin{pmatrix} -y \\ x \\ 0 \end{pmatrix}, \quad (1.29)$$

for which only $\nabla \times \mathbf{A}$ contributes to the field strength. The second possibility can be expressed as a non-Abelian gauge field that is spatially independent

$$\mathbf{A}^{(2)} = \begin{pmatrix} -\sigma_y \\ \sigma_x \\ 0 \end{pmatrix}, \quad (1.30)$$

such that $\mathbf{B} = -\frac{i}{\hbar}\mathbf{A} \times \mathbf{A}$. Although these two kinds of potentials give rise to the same magnetic field, they lead to completely different physical properties, as is to be expected due to their gauge inequivalency. While the first kind has a discrete Landau level spectrum for a particle in a background of such a gauge potential, the second one has a continuous spectrum. Part of the two different spectra are sketched in fig. 1.6.

1.4.2 Berry matrix

After introducing some basic features of non-Abelian gauge fields we turn to generalizing the Berry phase. In section 1.2 it was shown how the Berry connection could be interpreted as an (Abelian) gauge field. The topic we address next is how to generalize this to a non-Abelian gauge field.

Although parallel transport in the non-Abelian gauge theory setting was considered in detail before, for example in ref. [56], Wilczek and Zee generalized the Berry phase to a

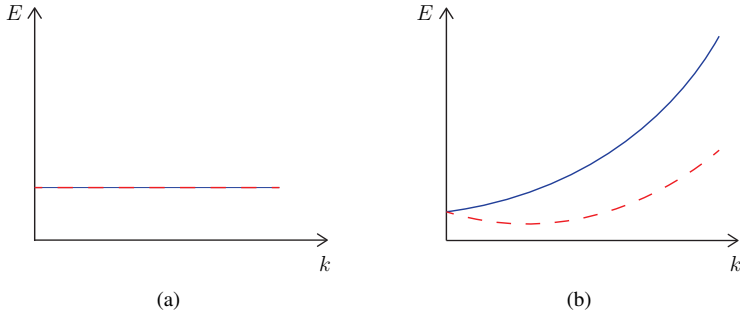


Figure 1.6: Lowest energy bands of a spin- $\frac{1}{2}$ particle minimally coupled to an $SU(2)$ gauge field, corresponding to $\mathbf{B} = 2\sigma_z \hat{z}$. There are two gauge inequivalent choices for the vector potential. The spectrum in fig. (a) results from an Abelian spatially dependent gauge field and the continuous spectrum in fig. (b) follows from a uniform non-Abelian configuration.

non-Abelian setting [54]. They consider a quantum system with a ground state degeneracy and they investigate a Hamiltonian $H(\mathbf{R})$ that depends on parameters \mathbf{R} . Similarly to the derivation presented in section 1.2, at each point \mathbf{R} in parameter space we may choose a basis of states $\{|n(\mathbf{R})\rangle\}$, but now we assume that there is a ground state degeneracy. Let us denote the basis that spans the N -dimensional ground state manifold as $|g_i(\mathbf{R})\rangle$ with $i = 1, \dots, N$. Starting in some ground state $|\psi(0)\rangle$ and adiabatically following a closed loop through parameter space, without closing the energy gap between the ground state manifold and the excited states, the final state $|\psi(T)\rangle$ can be expressed as

$$|\psi(T)\rangle = \exp\left(\frac{-i}{\hbar} \int_0^T dt E_n(\mathbf{R}(t))\right) U_B(\mathcal{C}) |\psi(0)\rangle, \quad (1.31)$$

where the Berry phase has been replaced by the *Berry matrix*

$$U_B(\mathcal{C}) = \mathcal{P} \exp\left(i \oint_{\mathcal{C}} \mathbf{A} \cdot d\mathbf{R}\right), \quad (1.32)$$

which is a path-ordered exponential of the Berry connection $\mathbf{A}_{ij} \equiv i\langle g_i(\mathbf{R}) | \nabla_{\mathbf{R}} g_j(\mathbf{R}) \rangle$. Upon a basis transformation $U_{ij}(\mathbf{R}) |g_j(\mathbf{R})\rangle$, the Berry connection transforms as a non-Abelian gauge field as in (1.27). The Berry matrix will be encountered in more detail in chapter 4.

1.4.3 Cold atoms

In 2005 two groups proposed an experimental setup to realize non-Abelian gauge fields in ultracold atoms. Both are based on the interpretation of the Berry matrix as an artificial non-Abelian gauge field.

Atom-laser coupling The group of Fleischhauer proposed a system based on atom-laser coupling [57]. Neutral multilevel atoms that move adiabatically in spatially dependent laser fields can have multiple degenerate dressed states. When a particle that is prepared in one of these dressed states moves adiabatically along a closed path in a background of the laser fields it can pick up a nontrivial Berry matrix. Thus it behaves as a charged particle coupled to a non-Abelian magnetic field.

Optical lattices The group of Lewenstein use the approach with an optical lattice [58]. Their strategy is very similar to the setup presented in ref. [52], except it is applied to atoms with k degenerate ground states and excited states $\{|g_i\rangle, |e_i\rangle\}$ with $i = 1, \dots, k$. Returning to fig. 1.5, the laser assisted tunneling is now a matrix that mixes the different states. To obtain a truly non-Abelian configuration the hopping in the \hat{y} -direction also has to be laser assisted, since at least two components of the gauge potential should not commute. The Hofstadter butterfly spectrum is generalized to what they call the *Hofstadter moth*.

This ends our digression into ultracold atomic systems. The last section of this chapter is devoted to topological phases in condensed matter physics. We will briefly mention some key notions involving a new class of phases, called topological insulators.

1.5 Topological insulators

In section 1.2 we have focused on the integer quantum Hall (IQH) phase and it has long been thought that these were the only noninteracting topological phases in condensed matter physics. Over the past decade different types have been predicted in band insulators and some have even been observed [34, 59, 60]. It is now understood that these phases, including the IQH phase fall into a framework called *topological insulators* [17–19]. It is a classification of noninteracting fermions with a bulk energy gap.

The different phases are determined by the number of spatial dimensions and the symmetries of the Hamiltonian and can be characterized by a topological invariant. For instance, in the IQHE time-reversal symmetry (TRS) is broken due to the presence of the magnetic field, whereas the two-dimensional quantum spin Hall effect (QSHE) preserves TRS. The QSHE was predicted in graphene [14], in strained semiconductors [15] and in HgTe quantum wells [61]. The latter led to the discovery of this effect in an experiment performed by the group of Molenkamp [16]. The QSHE belongs to the class of two-dimensional topological insulators with TRS and we will discuss it in the following

subsections.

1.5.1 2D time-reversal invariant topological insulator

The Hall conductivity is odd under time-reversal (TR), therefore it has to be zero for such a TR invariant topological insulator. How does a topological invariant arise for this type of insulator? A nice intuitive argument is given in ref. [33] for spin- $\frac{1}{2}$ band insulators in two spatial dimensions. The TR operator for spin- $\frac{1}{2}$ particles can be represented by $\Theta = \exp(i\pi\sigma_y/2\hbar)K$, where K denotes complex conjugation and the operator obeys $\Theta^2 = -1$. If the system is TR invariant the Bloch Hamiltonian $H_B(\mathbf{k})$ has the property

$$\Theta H_B(\mathbf{k}) \Theta^{-1} = H_B(-\mathbf{k}). \quad (1.33)$$

It follows that all states labeled by \mathbf{k} have a degenerate partner at $-\mathbf{k}$. Focusing on the edge states, there are two TR invariant points in the Brillouin zone, $k_x = 0$ and $k_x = \pi$, with x the coordinate along the edge and the lattice constant set to unity. These points have to be at least twofold degenerate, which follows from Kramers' theorem. The proof of this goes as follows. Assume there is a nondegenerate state $|\psi\rangle$. As Θ is a symmetry of the system, acting on the state would result in $\Theta|\psi\rangle = c|\psi\rangle$, with c a constant. Acting twice gives $\Theta^2|\psi\rangle = |c|^2|\psi\rangle$, but we also had $\Theta^2 = -1$ which leads to an inconsistency since $|c|^2 \neq -1$.

Two situations can occur and they are schematically depicted in fig. 1.7. Note that only half of the Brillouin zone is illustrated in these figures and all states have a TR invariant partner as a mirror image in the other half. In both figures Kramers degenerate pairs are located at the TR invariant points of the Brillouin zone and the Fermi energy lies between the valence band and the conduction band. In fig. 1.7a an even number of edge states crosses the Fermi energy. By modifying the Hamiltonian near the edge, the dispersion can be changed and this configuration can be continuously deformed into a state with no crossings, i.e. it is topologically equivalent to a trivial insulator. In fig. 1.7b there is an odd number of edge states crossing the Fermi energy, which makes it impossible to remove all edge states without closing the energy gap of the system or breaking TRS. In subsection 1.2.5 we saw how the IQHE could be labeled by a Chern number \mathbb{Z} , now we see that the TR invariant topological insulators in two dimensions are labeled by a \mathbb{Z}_2 invariant.

One particular model for a two-dimensional TR invariant topological insulator was proposed by Bernevig and Zhang [15]. Even though it has not been experimentally realized it gives a nice connection between several topics we have encountered in this introduction. The Hamiltonian they study describes a spin- $\frac{1}{2}$ particle in \mathbb{R}^2 and is given

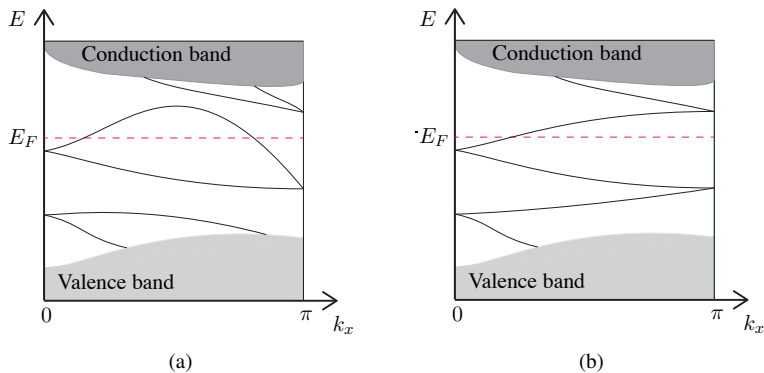


Figure 1.7: \mathbb{Z}_2 invariant for a TR invariant topological insulator is shown in a schematic way. Half of the Brillouin zone is shown as the other half is a mirror image. At the TR invariant points of the Brillouin zone, Kramers degenerate pairs must occur. The edge state crosses the Fermi energy an even or odd number of times, resulting in a trivial or nontrivial topological insulator.

by

$$H = \frac{\mathbf{p}^2}{2m} - L_z \sigma_z, \quad (1.34)$$

where the angular momentum in the perpendicular direction is coupled to the spin state. There are several different physical systems that obey the same mathematics.

1. When considering the nonrelativistic limit of a particle in electromagnetic fields, the spin-orbit coupling (SOC) term naturally arises as $(\mathbf{p} \times \mathbf{E}) \cdot \boldsymbol{\sigma}$. Consequently, the Hamiltonian in (1.34) corresponds to a charged particle in the interior of a uniformly charged cylinder.
2. It can also be described by a charged particle minimally coupled to a ‘non-Abelian’ gauge field $\mathbf{A} = \frac{1}{2} \mathbf{B} \times \mathbf{r}$, with $\mathbf{B} = B \sigma_z \hat{z}$ the magnetic field, which we encountered in (1.29) before. Of course this is not really a non-Abelian gauge field, since the components of the gauge field commute. This model effectively describes two layers of IQH states, where the two particle species feel an opposite magnetic field. Even though there is a magnetic field, TRS is not broken, since the field averages to zero. Methods for implementing these gauge fields in the cold atomic gases have been proposed in [62, 63].
3. The authors of [15] propose a zinc-blende semiconductor with shear strain gradients as most realistic model. The off-diagonal terms of the strain tensor can be chosen in such a

way that it results in the Hamiltonian in (1.34).

The model in (1.34) will reappear in chapters 3 and 4 as it is closely related to the models we discuss there.

1.5.2 Majorana fermions

Topological insulators come in many different flavors depending on their dimensionality and symmetries. This field of research is developing rapidly, and many of these classes of topological insulators have been realized experimentally, effective field theories have been written down and they have been generalized to interacting systems. However, probably the most exciting direction of research is the possible emergence of *Majorana fermions* γ [64, 65], spin- $\frac{1}{2}$ particles that were predicted in 1937 by Ettore Majorana [23]. As these particles are their own antiparticle, i.e. $\gamma = \gamma^\dagger$, they do not carry any charge or energy and it is very difficult to create let alone detect them.

Since the Majorana particles do not carry charge one of the obvious places to search for them is in superconductors as these systems do not require charge conservation. But the ordinary s -wave superconductors have Cooper pairs with electrons of opposite spin, and this pairing makes it impossible to build a Majorana fermion from these fundamental particles. Even though it is a far more exotic phase, Majorana particles do emerge as zero-modes in spinless superconductors, the so-called p -wave paired [20] and $(p + ip)$ -paired superconductors [21, 22] in one and two dimensions, respectively. It is now understood that these two systems fall into the classification of topological insulators and superconductors.

Two of these Majorana modes make up one conventional fermion $f = \frac{1}{2}(\gamma_1 + i\gamma_2)$, but the Majorana's can have positions that are arbitrarily far apart making f a highly nonlocal object. Moreover there is a degeneracy between f and f^\dagger , which results in non-Abelian statistics when Majorana modes are exchanged. We will return to a discussion of non-Abelian statistics in chapter 2.

It is challenging to create Majorana fermions in real experiments, but Fu and Kane led the way by realizing that the proximity effect between an s -wave superconductor and the surface states of a topological insulator could result in an effective $(p + ip)$ -superconductor [66]. In 2010 a proposal by two independent groups was made, where a one-dimensional wire with spin-orbit coupling subject to an external magnetic field, is placed on top of a conventional s -wave superconductor [67, 68]. This eventually led to an experiment conducted by the Kouwenhoven group, in which they observed very strong signatures of emerging Majorana zero-modes at the end points of such a wire [24]. This is a very exciting result and even though the observations are not yet conclusive, many other groups have obtained similar results [25–29]. It does seem like the condensed matter physicists have managed to be the first to create and detect a Majorana fermion since their theoretical prediction in 1937.

In this first chapter we introduced several topics all closely related to noninteracting topological phases of matter. The IQHE was discussed from a topological point of view, which enabled us to introduce topics like the Berry phase, parallel transport and Chern numbers. The Berry connection behaves as a gauge field and this correspondence is used to show how artificial gauge fields can be created in ultracold atomic clouds. These systems allow for a generalization to non-Abelian gauge fields by considering the Berry matrix. We showed some important differences between Abelian and non-Abelian gauge fields and commented on explicit realizations in ultracold atoms. We concluded the chapter with a discussion on topological insulators, which is a classification of noninteracting fermionic topological phases based on their symmetries and dimensionality. The IQHE fits in this classification and we treated an example of a two-dimensional insulator with TRS. Moreover, it was mentioned that Majorana fermions emerge in some of these topological phases.

The next chapter is an introduction to interacting topological phases. We will mainly focus on the quasiparticles of such phases and show how transitions between different topological phases come about.

CHAPTER 2

Topological symmetry breaking and fractional quantum Hall states

In the previous chapter we focused mostly on single-particle physics. Topological phases of matter that arise from an underlying strongly correlated theory are the topic of the present chapter. We do not treat the interactions explicitly, but rather use effective descriptions to capture the principal physical aspects of the collective behavior of such interacting systems. Unlike the traditional many-body field theories, different topological phases cannot be described by Landau's symmetry breaking principle. Instead, many topologically different phases may have the same symmetry and therefore have to be characterized by something else which is called topological order [69]. This can for instance be done by their ground state degeneracy on the torus [70], by their quasiparticle statistics [71, 72] or their edge states [73, 74].

The following discussion will set the stage for the content of chapters 5 and 6 without presenting any new results here. We start with a short introduction to $(2 + 1)$ -dimensional topological quantum field theory in section 2.1, where the main focus lies on the topological excitations carried by such phases and the interactions they have. In section 2.2 we present topological symmetry breaking, which is a concept that describes how transitions between different topological phases can take place, and is a main pillar on which chapters 5 and 6 are built. Section 2.3 serves to show how the excitations of fractional quantum Hall (FQH) states can be formulated in a Chern-Simons approach developed by Wen and a conformal field theory approach developed by Moore and Read.

2.1 Topological excitations in $(2 + 1)$ dimensions

If we wish to understand a condensed matter many-body problem we are forced to find other ways than by simply solving the Schrödinger equation. We cannot solve for all the particles that make up the system. Instead we need to find some *effective* low-energy field theory which describes experimental observations of the particular system well enough. The effective theories that describe phases with topological order such as the FQH phases are topological quantum field theories (TQFTs) [69]. These are theories that do not depend on the metric, they are invariant under diffeomorphisms. TQFT will not be discussed at length in this thesis, instead we are mainly interested in the excitations which can be carried by such topological phases and especially their interactions.

For an ordinary (non-topological) field theory, the excitations fall into representations

of a symmetry group, which corresponds to the symmetry of the Lagrangian or Hamiltonian of the system. When there is a ground state degeneracy, the different states can be related by the action of such a symmetry operator. Moreover, when there are different phases, these are characterized by the expectation value of some local order parameter, and transitions between different phases are induced by Landau's symmetry breaking. These are all well-known concepts within the framework of quantum field theory, but topological phases do not follow such a description. There is often no local order parameter and the Lagrangian (if there is one) does not have a symmetry in the manner described above. Still as it turns out, topological excitations can be labeled by representations of some underlying quantum group. The definition of a quantum group differs in the literature, but the precise mathematical structure is beyond the scope of this thesis. For a thorough treatment of the definitions that apply to our results we would like to refer the reader to the Ph.D. thesis of Slingerland [75].

The point of departure we take is that we view the set of topological excitations as a given 'anyonic model' [76, 77]. To clarify this, compare it to conformal field theory (CFT). One can start from a Lagrangian that is conformally invariant and find the algebra that correspond to that particular model. But there are many CFTs that do not have an effective Lagrangian description and still we can study their representation theory.

Starting from an anyonic model describing the excitations of some underlying topological phase, we label these quasiparticles by a finite set of topological charges a, b, c, \dots . They carry topological quantum numbers associated with the interactions between them. The types of interaction for a $(2 + 1)$ -dimensional TQFT are fusion and braiding, which are discussed in the following.

2.1.1 Fusion and splitting

The *fusion* of two particle types labeled by a and b is denoted by

$$a \times b = \sum_c N_{ab}^c c, \quad (2.1)$$

where $N_{ab}^c \in \mathbb{Z}_{\geq 0}$ gives the number of independent ways that a and b can fuse to c . These fusion rules are symmetric under interchange of a and b , i.e. $N_{ab}^c = N_{ba}^c$. For the fusion rules to make sense in any physical system, there has to be a unique sector representing the vacuum, for now denoted by \mathbb{I} , which means no particle at all. Also, we need to demand that for every particle a there is an antiparticle \bar{a} , in the sense that when these sectors fuse, they must have the vacuum sector in one of their fusion channels

$$a \times \bar{a} = \mathbb{I} + \sum_c N_{a\bar{a}}^c c. \quad (2.2)$$

In other words, $N_{a\bar{a}}^{\mathbb{I}} = 1$ for all sectors in the theory. To make the discussion more tangible let us consider the Ising model, which has three sectors labeled by $\{\mathbb{I}, \psi, \sigma\}$. Their fusion rules are given by

$$\mathbb{I} \times \mathbb{I} = \mathbb{I} \qquad \psi \times \mathbb{I} = \psi \qquad \sigma \times \mathbb{I} = \sigma \qquad (2.3)$$

$$\mathbb{I} \times \psi = \psi \qquad \psi \times \psi = \mathbb{I} \qquad \sigma \times \psi = \sigma \qquad (2.4)$$

$$\mathbb{I} \times \sigma = \sigma \qquad \psi \times \sigma = \sigma \qquad \sigma \times \sigma = \mathbb{I} + \psi . \qquad (2.5)$$

One can easily verify that this set of fusion rules satisfies the conditions just listed.

Quite naturally, when there is fusion the reverse can also be defined, which we call *splitting*. This just means that if $N_{ab}^c \neq 0$, then the particle labeled by c can split into the particles a and b . The fusion of three (or more) sectors needs to be associative ($a \times b) \times c = a \times (b \times c)$). This highly restricts such an anyon model and is related to the so-called pentagon equations of the theory, which are just the consistency conditions to assure associativity. For a derivation of the pentagon equations we refer the reader to the literature [76, 77].

The fusion of two or more particles $\{a_1, \dots, a_n\}$ to a sector b , spans a Hilbert space with dimension equal to the number of ways they can fuse to b . When a sector labeled by a is fused N times with itself the asymptotic growth of available fusion channels is given by $(d_a)^N$, where the positive real number d_a is called the *quantum dimension* of a . This quantum number is preserved under fusion which means that for sectors which have fusion rules as in (2.1), their quantum dimensions obey

$$d_a d_b = \sum_c N_{ab}^c d_c . \qquad (2.6)$$

For Abelian models, the quantum dimensions are all equal to unity. Clearly, the Ising model presented above is a non-Abelian model, since the σ particle has more than one fusion channel. The quantum dimensions of the three sectors are $d_{\mathbb{I}} = d_{\psi} = 1$ and $d_{\sigma} = \sqrt{2}$.

2.1.2 Braiding and topological spin

The statistics of particles is governed by two important principles: (i) particles of the same type are indistinguishable and (ii) they may exclude each other from being in the same state. We may think of particles as points in space, and we may interchange two particles twice which is equivalent to moving one particle around the other. Such an operation is called a *monodromy* and it may introduce a nontrivial phase factor in the two-particle wave function.

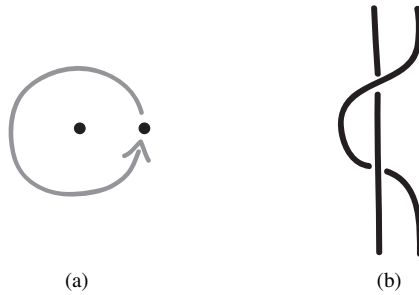


Figure 2.1: Exchanging two indistinguishable particles twice is equivalent to bringing one particle around the other. In fig. (a) a top view of this process is shown. A side view is depicted in fig. (b) where time flows upwards. Exchanging these point particles results in a nontrivial braid in $(2 + 1)$ -dimensional space-time.

In three or more spatial dimensions all such paths can be contracted to a point and therefore belong to the same topological class, meaning that such a monodromy always produces a trivial phase. If the particles are identical one could also consider a single interchange of the particles leading to the same indistinguishable configuration and corresponding to the square root of the monodromy. This implies that in three or more dimensions it could generate a phase equal to ± 1 on the state. It is this phase difference which underlies the fundamental distinction we make between bosons and fermions. The interchange of N identical particles is governed by the permutation group S_N , which only has one-dimensional representations.

This changes dramatically in two spatial dimensions, the case of our interest. When we have only two spatial dimensions at our disposal, the world lines of particles cannot cross, meaning that exchanging two indistinguishable particles twice does not yield the same configuration as the initial one. The braids of world lines encode the precise phase evolution of a multi-particle state, which is the origin of the existence of so-called *anyons* exhibiting fractional spin and statistics properties. The interchanges are now generated by elements of the braid group B_N , which acts on N strands. But it can get even more exotic than that. The braid group has nontrivial higher dimensional representations, meaning that the system can pick up a matrix instead of just a phase. Particles for which this is the case are called *non-Abelian anyons*. The adjective ‘non-Abelian’ indicates that it matters in which order they are interchanged, as opposed to Abelian anyons which only pick up a phase. These non-Abelian anyons are of high interest for the implementation of fault-tolerant quantum computation [13].

Braiding can be understood in terms of the Aharonov-Bohm effect that was encoun-

tered in the previous chapter, where a charged particle which is brought around a flux picks up a nontrivial phase factor. In an anyonic model the particles carry both ‘charge’ and ‘flux’, thus moving them around each other may have a nontrivial effect. Like the pentagon equations, there is another set of consistency conditions on the anyonic model associated to the order of braiding and fusing particles, which is called the hexagon equations.

Another important quantum number that we will use extensively is associated to a rotation of a particle of type a over a 2π angle, which we call the *topological spin* h_a . Under such a rotation, the wave function picks up a phase $\theta_a = e^{2\pi i h_a}$. The monodromy of anyons can also be expressed in terms of the spin. Assume that two particles a and b fuse to a specific channel c . Then the monodromy is given by

$$M_{ab}^c = h_c - h_a - h_b. \quad (2.7)$$

Let us once more return to the Ising model. The different sectors have spin $h_{\mathbb{1}} = 0$, $h_{\psi} = \frac{1}{2}$ and $h_{\sigma} = \frac{1}{16}$, from which we can calculate the monodromy.¹

After this brief introduction into anyonic models, where we presented the interactions between anyons and their quantum numbers, the next section is dedicated to transitions between different topological phases, i.e. phases carrying a different set of anyons.

2.2 Topological symmetry breaking

The transitions between different topological phases that we will study, are induced by the condensation of bosonic quasiparticles, very similar to what happens in a superconductor. In that case the electrons form Cooper pairs, which allows them to condense into a collective ground state, breaking the $U(1)$ gauge symmetry of electromagnetism. The transition between topological phases is called topological symmetry breaking, a formalism which has been developed in a series of papers [79–81] and successfully applied to many phase transitions between topological phases [82–87]. A more mathematical treatment can be found in [88, 89]. This formalism is the main building block for the results obtained in chapters 5 and 6. In the following, the different steps are presented in quite some detail.

Unbroken phase \mathcal{A}

As mentioned before we consider some topological phase without dealing with the exact underlying Lagrangian or Hamiltonian of the system. Rather, we start from a set of

¹We wish to remark that an anyonic model with sectors which are labeled by the three Wess-Zumino-Witten primary fields of the $SO(n)_1$ model, have exactly the same fusion rules as the Ising model [78]. For $n = 1$ the spins are also identical and we are dealing with the same anyonic model, but for $n = 2r + 1$ the non-Abelian sector has spin $h = \frac{2r+1}{16}$. Even though the fusion rules are still the same, these are different models.

quasiparticles which comprise an anyonic model. They interact with one another through fusion, splitting and braiding and we denote the phase carrying these topological excitations by \mathcal{A} .

A transition to a new phase can be driven by the formation of some nontrivial condensate. First, we should ask ourselves what the characteristics of the particles forming a condensate should be. The particles that may form a condensate have to be bosonic. Now, we have to be careful about what exactly we mean by this, since we are in two spatial dimensions. The two properties a bosonic sector labeled by b should have are

1. Trivial spin: $\theta_b = e^{2\pi i h_b} \Leftrightarrow h_b \in \mathbb{Z}$.
2. Partially trivial self-monodromy: When fusing with itself there has to be at least one fusion channel with trivial spin, i.e. for $b \times b = \sum_{a \in \mathcal{A}} N_{bb}^a a$ there is a sector $\tilde{a} \in \mathcal{A}$ with $N_{bb}^{\tilde{a}} \neq 0$ and $\theta_{\tilde{a}} = 1$.

When such a bosonic sector is present in the topological phase denoted by \mathcal{A} , we can apply the formalism of topological symmetry breaking (TSB) to induce a phase transition to a broken phase labeled by \mathcal{U} . Before we reach this broken phase there is an intermediate step in the formalism, which we will describe below.

Intermediate phase \mathcal{T}

Imagine that some parameters of the underlying microscopic system change in such a way that a condensate of bosonic quasiparticles forms. In chapter 5 we will go into more detail about the formation of a condensate, but for now we consider it as given.

When a condensate forms it breaks the initial symmetry denoted by \mathcal{A} down to a different residual symmetry which we call \mathcal{T} . Again compare this to a superconductor. After condensation of the Cooper pairs, electric charge is conserved modulo $2e$, and pairs of electrons can be created and annihilated for free. When a condensate of topological quasiparticles forms, the topological charge is defined modulo the charge of b . For instance, when one of the original fusion rules of \mathcal{A} is $a_1 \times b = a_2$, after the formation of a condensate it is impossible to distinguish between a_1 and a_2 , and they become *identified* with each other. This immediately implies that the bosonic particle forming the condensate becomes identified with the vacuum of the initial phase \mathcal{A} : $b \sim \mathbb{I}$.²

There is another situation that could (and often does) occur for some of the sectors in a non-Abelian theory. Consider the following fusion rule of a sector $a \in \mathcal{A}$

$$a \times a = \mathbb{I} + b + \dots \quad (2.8)$$

²When b is a non-Abelian particle, it has to split up into several particles in the broken phase \mathcal{T} and one of these particle is identified with the vacuum, while the others are excitations in \mathcal{T} . However, in this thesis we will not encounter such a bosonic particle.

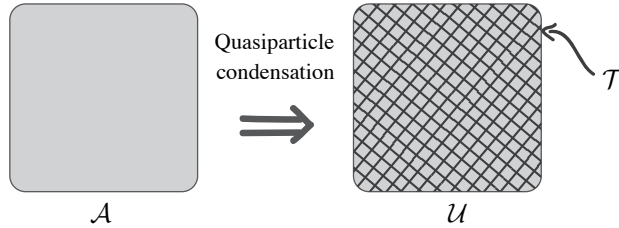


Figure 2.2: The topological phase on the left of the diagram is the original unbroken phase \mathcal{A} which contains a nontrivial bosonic sector b . When a condensate of these bosonic sectors forms, the system is driven through a phase transition, ultimately resulting in a broken unconfined phase \mathcal{U} . The confined particles are expelled from the bulk of \mathcal{U} and reside at the boundary of the system. This boundary contains all the sectors of \mathcal{U} plus the confined particles and therefore is given by \mathcal{T} .

To bring our point across we do not have to indicate the terms that could follow after the first two. The sector b is the boson that forms the condensate and should be trivial in the intermediate phase \mathcal{T} , i.e. it becomes identified with the vacuum sector \mathbb{I} of \mathcal{A} . Therefore, the particle denoted by a has two different ways of fusing to the ‘vacuum’ when we are in the phase \mathcal{T} , which should not be possible in a physically consistent phase. Therefore such a sector should *split* into two or more sectors in the intermediate phase. This is quite similar to ordinary group theory. For instance, when we have a three-dimensional representation of $SU(3)$ it is not irreducible under the subgroup $SU(2)$, it decomposes as $3 \rightarrow 1 + 2$. The splitting and identification of sectors can be summarized in the *branching rules*

$$a \rightarrow \sum_t n_a^t t, \quad (2.9)$$

where $a \in \mathcal{A}$, $t \in \mathcal{T}$ and n_a^t is a positive integer. For future reference, we call the sectors $a \in \mathcal{A}$ that branch to the same sector $t \in \mathcal{T}$ the *lifts* of t .

Branching and fusion should commute, which severely restricts the branching rules and implies that quantum dimensions are preserved under branching, i.e. $d_a = \sum_t n_a^t d_t$. In general, it is a very nontrivial task to determine a new consistent set of fusion rules for the intermediate phase \mathcal{T} . Fortunately, the phases we will consider in this thesis have a fairly simple structure.

Broken unconfined phase \mathcal{U}

Once the sectors of \mathcal{T} and their fusion rules have been determined, there is one last step we should take. When different sectors of the initial phase \mathcal{A} become identified with each other in the intermediate phase, it does not imply that they have well-defined braiding

interactions in \mathcal{T} . To illustrate this, consider two sectors $a_1, a_2 \in \mathcal{A}$ which become identified with each other, i.e. $a_1 \times b = a_2$, where b is a bosonic sector that condenses and drives the transition to \mathcal{T} . Now imagine we bring a_1 around b in the condensed phase \mathcal{T} . Since b represents the vacuum in \mathcal{T} there should not be any nontrivial interaction between a_1 and b , and to ensure this we have to demand that the monodromy of any sector in the new phase with the condensate is trivial, i.e. $\theta_{a_2} \theta_{a_1}^{-1} \theta_b^{-1} = 1$. As b is a bosonic sector this boils down to $h_{a_2} - h_{a_1} \in \mathbb{Z}$. The sectors of \mathcal{T} that do not have trivial braiding with the new vacuum, have to be expelled from the bulk, because they would cause a domain wall of finite energy in the condensate. In chapter 5 we will go into more detail regarding the interpretation of these confined particles.

After following all the steps presented above, we are left with a broken unconfined phase \mathcal{U} which carries topological excitations with well-defined fusion and braiding relations. The boundary of \mathcal{U} with a trivial phase, for instance the vacuum, is not simply described by \mathcal{U} , as would have been the case had we started from a phase \mathcal{U} without applying TSB to an initial phase \mathcal{A} . The boundary must also contain the confined sectors that were expelled from the bulk. The correct description of the boundary is therefore given by the intermediate phase \mathcal{T} . In chapter 6 we will consider a boundary between \mathcal{U} and another nontrivial topological phase. A schematic overview of the phase transition is depicted in fig. 2.2.

Now that we have explained the formalism of TSB we turn to the specific anyonic models that we will treat in chapters 5 and 6. These are the topological excitations of certain FQH phases. Therefore, the next section will be devoted to the effective theory describing these phases and in particular to the quantum numbers of the topological excitations.

2.3 Effective theory FQH states

After the discovery of the IQHE, yet another, even more far reaching observation was made. In 1982 Tsui et al. reported on an experiment where they observed a plateau in the Hall conductance at a fractional value $\sigma_H = \frac{1}{3}e^2/h$ [7]. This is now known as the fractional quantum Hall effect (FQHE) and has been observed at several other fractions as well. The FQHE cannot be understood from a noninteracting perspective, as the Coulomb interaction between the electrons needs to be incorporated to understand this fractional effect. Laughlin was the first to write down a trial wave function for the $\nu = 1/3$ effect [8] and to recognize that the excitations over the ground state should have fractional charge, after which Halperin showed that these quasiparticles obey fractional statistics [71, 72].

In the previous section we set the stage for TSB in a general topological phase. In this section we want to present the quantum numbers associated with the excitations of certain FQH states. These will cover the states on which we apply TSB in chapters 5 and 6. We first show how the FQH states are related to Chern-Simons (CS) theory and later

we present its connection to CFT. These descriptions allow us to extract the quantum numbers of the topological excitations and give a useful interpretation in terms of vertex operators. There is much more that can be said about FQH states, but that is beyond the scope of this thesis.

2.3.1 K matrix formalism

A powerful tool to describe highly correlated systems is writing down an effective low-energy field theory. For the FQHE these are Ginzburg-Landau or CS Lagrangians [90–92]. In this thesis we will use the description in terms of CS theory and follow the logic presented in ref. [32]. The Lagrange density can be written as

$$\mathcal{L} = \frac{1}{4\pi} \epsilon^{\mu\nu\lambda} \left(a_{i,\mu} K_{ij} \partial_\nu a_{j,\lambda} + 2e A_\mu \partial_\nu t_i a_{i,\lambda} \right), \quad (2.10)$$

where $a_{i,\mu}$, with $i = 1, \dots, N$, are N $U(1)$ gauge fields and A_μ is the external electromagnetic field. The specific topological state is characterized by an integer valued coupling matrix K_{ij} and an integer valued N -dimensional charge vector t_i . The filling fraction of the quantum Hall phase can be expressed in terms of this K matrix and the charge vector as

$$\nu = t_i K_{ij}^{-1} t_j. \quad (2.11)$$

A generic quasiparticle is characterized by an N -dimensional integer vector \mathbf{l} and its charge $Q_{\mathbf{l}}$ is given by

$$Q_{\mathbf{l}} = e t_i K_{ij}^{-1} l_j. \quad (2.12)$$

The monodromy of two particles labeled by \mathbf{l} and \mathbf{m} can be expressed as

$$M_{\mathbf{l},\mathbf{m}} = l_i K_{ij}^{-1} l_j, \quad (2.13)$$

where the topological spin is given by $h_{\mathbf{l}} = \frac{1}{2} M_{\mathbf{l},\mathbf{l}}$. These quantities are all invariant under a $SL(N, \mathbb{Z})$ transformation, therefore phases with different K matrices and charge vectors belong to the same universality class whenever they are related by an $SL(N, \mathbb{Z})$ transformation.

The simplest examples are the Laughlin states, for which the K matrix is an odd integer $K = M$ and the charge vector has only one component $t = 1$. This gives a filling fraction of $\nu = 1/M$, the fundamental quasiparticle $l = \pm 1$ has self-monodromy (statistics) $M_{\pm 1} = \pi/M$ and charge $Q_{\pm 1} = \pm e/M$. The Laughlin states can be viewed as a state in which the electrons form a collective ground state, with fundamental excitations

of charge e/M . But this picture can be extended by assuming that these quasiparticles can again form a new collective state with new quasiparticles as excitations. This construction is called the Haldane-Halperin (HH) hierarchy [71, 93] and is one of the main topics of chapter 6. The K matrix and charge vector of the HH hierarchy are

$$K_{ij} = p_i \delta_{ij} - \delta_{i,j-1} \text{sgn}(p_{i+1}) - \delta_{i,j+1} \text{sgn}(p_i), \quad t_i = \delta_{1i}, \quad (2.14)$$

with no summation over the repeated indices, and p_0 is an odd integer and $p_{i>0}$ are even integers.

We will use this notation in chapter 6 extensively, however in the next subsection we would like to introduce a different description of FQH states, in terms of CFTs. We do this because it has been quite an important development in the understanding of FQH states, especially on the level of wave functions, and we feel that this gives a better sense of the quantum numbers involved.

2.3.2 CFT description

In 1984 Witten proposed and proved a deep connection between $(2 + 1)$ -dimensional CS theory and $(1 + 1)$ -dimensional CFT [94]. In the following we briefly discuss this connection in relation to the wave functions describing the bulk of FQH states and the edge states of a finite quantum Hall (QH) system.

Bulk wave functions In a seminal paper written by Moore and Read, a connection was established between CFT correlators and QH wave functions [11]. The main idea is that the ground state wave function of a FQH state can be described by a correlator of CFT vertex operators $V_e(z_i)$ at N electron position z_i , $i = 1, \dots, N$. This correlator can be decomposed into conformal blocks. When the correlator is evaluated a background charge needs to be inserted by hand in order to get a nontrivial result. Quasiparticles can be incorporated into this scheme by inserting suitable vertex operators $V_{qp}(w_i)$ at position w_i . Moore and Read show how the Laughlin wave functions can be derived from a $U(1)$ CFT: the compactified chiral boson. Then they generalize this to more complicated CFTs, where they show the emergence of non-Abelian quasiparticles. The state they propose derives from an Ising CFT and is now widely known as the Moore-Read (MR) state, which is a leading candidate for the plateau observed at filling fraction $\nu = 5/2$ [95, 96]. An insightful review of the connection between CFT and QH wave functions can be found in [97].

From the CFT point of view fusion of quasiparticles can be understood by taking the operator product expansion of the fields which represent these quasiparticles. Determining the statistics of quasiparticles is a very nontrivial task. Once the wave function is obtained from the above description (taking the CFT correlator), adiabatically braiding one quasiparticle around another results in a Berry holonomy and the explicit monodromy

where the physical observable is the combination of the two [98]. To find the true monodromy one can use the plasma analogy. For the Laughlin states this was done in ref. [72] and for the MR state in refs. [99, 100].

CFTs usually describe critical phenomena, but bear in mind that the description of the FQH bulk states in terms of CFT correlators does not imply that the FQH state is a critical theory. As we have mentioned before, it is a theory with a bulk gap and the quasiparticles are massive localized topological excitations.

Next we consider the edge of a FQH state and see that it is described by a critical theory, which is the same CFT from which the bulk states are built.

Edge states In an experimental setup the FQH sample will always have an edge. In 1982, Halperin argued that the current is carried along the edges because the confining potential lifts the Landau levels at the edge of the sample [73]. Around a decade later, Wen showed that the edge states can be understood from an effective field theory perspective [74, 101, 102], which can be argued from gauge invariance. The CS term is no longer gauge invariant when the manifold has an edge, but when we include a term in the action defined on the edge of the system, which exactly cancels the boundary term of the bulk after a gauge transformation, the total system $S = S_{\text{bulk}} + S_{\text{boundary}}$ is gauge invariant. Wen showed that for the $U(1)$ CS gauge fields, this boundary term corresponds to a chiral Luttinger liquid [103, 104]

$$S_{\text{boundary}} = \frac{1}{4\pi} \int dx dt \left((\partial_t \phi)^2 - v^2 (\partial_x \phi)^2 \right), \quad (2.15)$$

where x is the coordinate along the boundary and the field ϕ is subject to the chiral constraint $\partial_t \phi = v \partial_x \phi$. The conserved current of this theory is $J_\mu = \epsilon_{\mu\nu} \partial^\nu \phi$ and its modes form a $U(1)$ Kac Moody algebra. The action in (2.15) is a CFT with central charge $c = 1$. In chapter 5 we will go into more detail about this CFT and consider specific boundary conditions which lead to a compactified chiral boson.

Quasiparticles are now represented by inserting the appropriate conformal operators at either the edge or in the bulk. In chapters 5 and 6 we apply TSB to several FQH states, where in the former chapter we will mainly use the CFT description and in the latter we will mostly use the K matrix notation.

Let us conclude this last introductory chapter with a short recap of the topics that we encountered. No new results were presented, instead we set the stage and fixed notations for chapters 5 and 6. This chapter commenced with an introduction to particle-like excitations that are carried by a topological phase. These particles interact with one another

through fusion and braiding, and such a set of topological particles together with their specific interactions is called an anyonic model.

We proceeded by explaining the formalism called topological symmetry breaking, which is a way of describing phase transitions between different topological phases. A transition via this formalism takes place when a condensate of bosonic excitations forms.

The last section focused on the fractional quantum Hall phases. The effective low-energy description of most FQH states are Chern-Simons theories which are indeed topological field theories. The excitations of these phases form an anyonic model and it was shown how the quantum numbers of these particles can be obtained from the K matrix formalism. We ended by pointing out the connection between the FQH phases and conformal field theory, which describes the bulk wave functions as well as the gapless edge excitations.

CHAPTER 3

Noncompact dynamical symmetry of a spin-orbit coupled oscillator

This chapter is based on the following publication:

S.M. Haaker, F.A. Bais, and K. Schoutens, NONCOMPACT DYNAMICAL SYMMETRY OF A SPIN-ORBIT-COUPLED OSCILLATOR, *Phys. Rev. A* **89**, 032105 (2014).

It is the rich structure revealed by topological phases of matter which inspires the investigation of model systems where such phases can be realized. In chapter 1 we discussed an example, the IQH phase, and briefly touched upon a larger class of such phases called topological insulators. We introduced the Landau problem which describes a charged particle confined to two dimensions and subject to a perpendicular magnetic field. This system is characterized by its highly degenerate spectrum, the levels of which are called the Landau levels. Even though it is a simple single-particle problem, much of the IQHE can be understood from this basic picture.

In the present chapter we study a three-dimensional analog of the Landau problem, which was proposed by Li and Wu as a continuum model for TR invariant topological insulators in three dimensions [105]. They study a particular model (which we will introduce in more detail below) for spin- $\frac{1}{2}$ fermions in the background of a non-Abelian gauge potential, tuned in such a way that a flat dispersion is achieved. The authors argue that this model has helical Dirac surface modes if open boundary conditions are imposed. These modes are protected by TRS and are indicative of a nontrivial three-dimensional topological insulator phase.

The authors focus on the construction of the eigenfunctions of the model, revealing some remarkable properties such as a form of quaternionic analyticity. In this chapter we present a complementary algebraic approach to the problem. A particular goal is to understand the degeneracies in the spectrum from an underlying symmetry algebra point of view. In general, compact symmetry algebras lead to finite degeneracies, whereas non-compact symmetries give rise to infinite degeneracies.¹ In our work we are confronted with a mixture of finite and infinite degeneracies in the spectrum, posing a puzzle as to

¹This is true for the unitary representations we are interested in, it does not hold for the nonunitary ones.

the nature of the underlying symmetry algebra. This problem was studied in [106] as well, where the authors conclude that an accidental degeneracy does not always imply an underlying symmetry, precisely because of the mixture of infinite and finite degeneracies in this model. We will show that there is a finite number of operators commuting with the Hamiltonian which forms a nonlinear algebra, which we recognize as a ‘deformed’ $SO(3, 2)$ symmetry. These generators include the spin- $\frac{1}{2}$ generalization of a pair of symmetry vectors that are reminiscent of the Runge-Lenz vector of the Kepler problem. After a simple rescaling of the operators we obtain the linear noncompact Lie algebra $SO(3, 2)$, which generates the corresponding Anti de Sitter group. The so-called *singleton* representation of this algebra plays a key role in explaining both the infinite and finite degeneracies that feature in the spectrum.

We remark that, quite generally, an insight into the symmetry algebra underlying a quantum problem is quite useful. On the one hand, the representation theory provides a catalogue of possible families of quantum states; on the other hand an algebraic structure may contain clues to an underlying geometric picture. An example featuring both these aspects is the $\mathcal{W}_{1+\infty}$ symmetry of quantum Hall phases [107, 108]. This symmetry reflects the incompressibility of the quantum Hall liquids and it enables an algebraic organization of edge excitations of these same liquids.

This chapter is organized as follows. In section 3.1 we present the Hamiltonian of interest, and discuss its spectrum and its degeneracies. Section 3.2 is devoted to the symmetry algebra of the system. We write down all the symmetry operators in a coordinate independent form and show that they form a nonlinear algebra. Moreover, we show that a simple rescaling of the operators results in a linear algebra and give the representations of this Lie algebra. In section 3.3 we present the operators that allow us to connect states of different energies, the so-called spectrum generating algebra.

3.1 Spin-orbit coupled harmonic oscillator

The model proposed in [105], to describe a continuous three-dimensional topological insulator, is a spin- $\frac{1}{2}$ fermion in a three-dimensional harmonic potential with a SOC term of fixed strength. The Hamiltonian reads

$$H = \frac{\mathbf{p}^2}{2m} + \frac{1}{2}m\omega^2\mathbf{r}^2 - \omega\mathbf{L} \cdot \boldsymbol{\sigma}, \quad (3.1)$$

where L_i is the usual orbital angular momentum and σ_i are the Pauli matrices. The model is mathematically equivalent to a spin- $\frac{1}{2}$ particle minimally coupled to a static external

$SU(2)$ gauge field plus a particular scalar potential

$$H = \frac{1}{2m} (\mathbf{p} - q\mathbf{A})^2 + V(r). \quad (3.2)$$

The components of the vector potential are $A_i = \frac{1}{2}\omega\epsilon_{ijk}\sigma_j r_k$ and the harmonic potential is given by $V(r) = -\frac{1}{2}m\omega^2 r^2$. Note that the components of \mathbf{A} are 2×2 matrices. Since these components do not commute with each other, this is a so-called non-Abelian gauge field, which we encountered in section 1.4.

The field strength associated to this gauge field points in the radial direction and grows with r . This gauge potential can be seen as the three-dimensional version of two different two-dimensional ones. For fixed radius $r = 1$, this is a spin- $\frac{1}{2}$ particle confined to S^2 in a perpendicular magnetic field, resulting in non-Abelian Landau levels on the sphere, which we will encounter in chapter 4. In \mathbb{R}^2 it describes two decoupled layers of quantum Hall states where the two types of particles feel an opposite perpendicular magnetic field. We came across this configuration in chapter 1 and it serves as a toy model for the QSHE [15].

In the remainder of this chapter we use the notation in the form of the three-dimensional spin-orbit coupled harmonic oscillator given in (3.1) and work in units where $m = 1/2$, $\omega = 1$, $\hbar = 1$.

Since this is a single-particle radial problem there are several ways of solving the system. As we are interested in the algebraic approach we will look for operators that commute with the Hamiltonian. First of all, H commutes with the total angular momentum operators $\mathbf{J} = \mathbf{L} + \frac{1}{2}\boldsymbol{\sigma}$. The Hilbert space arranges into $SU(2)$ multiplets, where every irreducible representation may be labeled by its \mathbf{J}^2 eigenvalue $j_{\pm}(j_{\pm} + 1)$. Here $j_{\pm} = l \pm \frac{1}{2}$, and $l = 0, 1, \dots$ is associated with the orbital angular momentum \mathbf{L}^2 , which also commutes with the Hamiltonian. We can diagonalize in \mathbf{J}^2 and J_3 as is standard in the $SU(2)$ case, but we will choose a slightly different convention. Instead, we first define $A_3 \equiv \mathbf{L} \cdot \boldsymbol{\sigma} + 1$. This operator commutes with H and with \mathbf{J}^2 and its eigenvalue can be easily obtained from the relation $A_3 = \mathbf{J}^2 - \mathbf{L}^2 + \frac{1}{4}$. We will label the eigenstates of H by their A_3 and J_3 eigenvalues

$$A_3 \psi_{n,l',m} = l' \psi_{n,l',m}, \quad J_3 \psi_{n,l',m} = m \psi_{n,l',m}, \quad (3.3)$$

where $l' = \pm 1, \pm 2, \dots$ and $-(|l'| - \frac{1}{2}) \leq m \leq |l'| - \frac{1}{2}$. The eigenvalues of \mathbf{J}^2 in terms of l' follow from the relation $\mathbf{J}^2 = A_3^2 - \frac{1}{4}$.

In section 3.3 we will derive the spectrum by constructing energy ladder operators, but at this point we simply solve the Schrödinger equation, giving us the spectrum and the energy eigenstates. Switching to spherical coordinates and using separation of variables,

the angular part is found to be a linear combination of spherical harmonics $Y_{lm}(\hat{\Omega})$

$$\chi_{lm}^+ = \sqrt{\frac{l+m+1}{2l+1}} Y_{lm} \begin{pmatrix} 1 \\ 0 \end{pmatrix} + \sqrt{\frac{l-m}{2l+1}} Y_{l,m+1} \begin{pmatrix} 0 \\ 1 \end{pmatrix} \quad (3.4)$$

$$\chi_{lm}^- = \sqrt{\frac{l-m}{2l+1}} Y_{lm} \begin{pmatrix} 1 \\ 0 \end{pmatrix} - \sqrt{\frac{l+m+1}{2l+1}} Y_{l,m+1} \begin{pmatrix} 0 \\ 1 \end{pmatrix}, \quad (3.5)$$

where the spin states are diagonal in σ_z . Note that we momentarily switched to labeling the states by l and \pm , where $\mathbf{L}^2 \chi_{lm}^\pm = l(l+1) \chi_{lm}^\pm$. The (unnormalized) radial part of the eigenstates is the same for both \pm states

$$R_{kl}(r) = r^l e^{-r^2/4} \mathbf{L}(-2k, 2l + \frac{5}{2}, r^2/2). \quad (3.6)$$

The generalized Laguerre polynomial \mathbf{L} , has a finite number of terms for these particular values. The spectrum is given by

$$E = \begin{cases} 2k + \frac{3}{2} & l' > 0 \\ 2k - 2l' + \frac{5}{2} & l' < 0 \end{cases}, \quad (3.7)$$

where $k = 0, 1, \dots$. The energy does not depend on m , which reflects the conservation of total angular momentum \mathbf{J} , but there is a bigger (accidental) degeneracy in the system. For the +branch, the energy does not depend on l' , resulting in an infinite degeneracy at every energy level. On the other hand, the -branch also has a degeneracy in l' , but it is finite. We can express the energy in terms of a new quantum number n as

$$E = n + \frac{3}{2}, \quad \begin{cases} l' > 0 : & n = 0, 2, \dots \\ l' < 0 : & n = 3, 5, \dots \end{cases}. \quad (3.8)$$

For n even, the energy levels have an infinite degeneracy, and for n odd, the allowed values of l' are $l' = -1, \dots, \frac{1}{2}(1-n)$. The spectrum is depicted in fig. 3.1. We want to stress that the infinite degeneracy of the +branch is only present when the strength of the SOC term in the Hamiltonian is exactly $\pm\omega$.²

²If the strength is $+\omega$, there is an infinite degeneracy in the -branch.

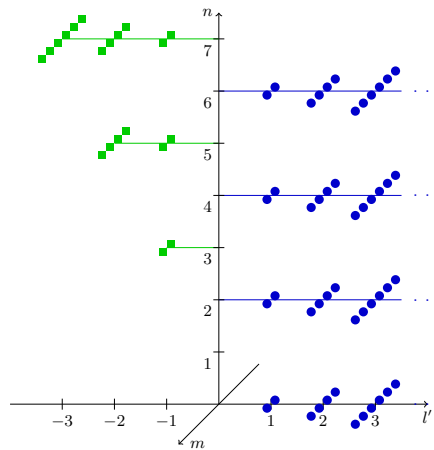


Figure 3.1: The spectrum of the spin-orbit coupled harmonic oscillator. The blue dots represent the states of the +branch. At each energy level they are infinitely degenerate with only a lower bound at $l' = 1$. The green squares represent states of the finitely degenerate -branch. In both cases, for every value of l' there is at most one $SU(2)$ multiplet.

3.2 Symmetry algebra

The aim of the present chapter is to understand the degeneracies in the spectrum from an underlying symmetry algebra. The authors of ref. [106] raised the following question: does an accidental degeneracy always imply a symmetry algebra? They investigated the degeneracies of the Hamiltonian in (3.1) and concluded that there is no such algebra. Their conclusions were mainly based on the fact that a Lie algebra has either finite dimensional nontrivial irreducible representations or only infinite dimensional ones, depending on whether it is a compact or a noncompact algebra, respectively. As background material, we work out the representation theory of $SO(3)$ and its noncompact form $SO(2, 1)$ in appendix 3.A, where we explicitly show the differences in dimensionality of their representations. Clearly, the spectrum of H contains both finite and infinite dimensional representations, which is indeed puzzling. Moreover, the authors of ref. [106] constructed operators that connect different $SU(2)$ multiplets within one energy level by mapping $SU(2)$ highest weight states onto each other, but these operators do not commute with the Hamiltonian. We will show that it is possible to construct operators that commute with H and couple the different $SU(2)$ multiplets, and that these operators have an underlying noncompact Lie algebra structure.

Consider the following two Hermitian vector operators

$$\widetilde{M}_i = \frac{1}{4}(r_i A_3 + A_3 r_i) + \frac{1}{2}((\mathbf{p} \times \mathbf{J})_i - (\mathbf{J} \times \mathbf{p})_i) \quad (3.9)$$

$$\widetilde{N}_i = \frac{1}{2}(p_i A_3 + A_3 p_i) - \frac{1}{4}((\mathbf{r} \times \mathbf{J})_i - (\mathbf{J} \times \mathbf{r})_i) . \quad (3.10)$$

One may explicitly show that $\widetilde{\mathbf{M}}$ and $\widetilde{\mathbf{N}}$ both transform as vectors under \mathbf{J} and that they commute with the Hamiltonian. Moreover they connect different $SU(2)$ irreducible representations with each other, so they are exactly the operators that we were looking for. These operators are spin- $\frac{1}{2}$ generalizations of the well-known Runge-Lenz (RL) vector present in the Kepler problem.

We wish to determine the algebra $\widetilde{\mathbf{M}}$ and $\widetilde{\mathbf{N}}$ form together with \mathbf{J} and A_3 , which are the other symmetry operators. When computing the commutation relations of these operators we run into terms nonlinear in H and A_3 . The explicit commutation relations are given in appendix 3.B. The nonlinearity encountered here is very similar to what happens in the Kepler problem. In that case the RL vector \mathbf{A}^{RL} transforms as a vector under orbital angular momentum \mathbf{L} , but the different components commute as $[A_i^{\text{RL}}, A_j^{\text{RL}}] = -i\epsilon_{ijk} 2H^K A_k^{\text{RL}}$, where H^K is the Hamiltonian of the Kepler problem. The RL vector needs to be rescaled by $(-2H^K)^{-\frac{1}{2}}$ in order to obtain the well-known $SO(4)$ commutation relations.³

3.2.1 Rescaled operators

With this in mind we set out to find an appropriate rescaling factor, which would enable us to get a grip on the problem. The easiest way to find the correct rescaling is by looking at the action of the symmetry operators on an energy eigenstate $\psi_{n,\nu,m}$. In order to do so we write the operators in a Cartan basis. First we redefine

$$\widetilde{M}_\pm = \frac{1}{\sqrt{2}}(\widetilde{M}_x \pm i\widetilde{M}_y) \quad (3.11)$$

$$\widetilde{N}_\pm = \frac{1}{\sqrt{2}}(\widetilde{N}_x \pm i\widetilde{N}_y) . \quad (3.12)$$

As Cartan subalgebra we choose $\{J_3, A_3\}$ and the operators corresponding to the root vectors are

$$J_\pm = \frac{1}{\sqrt{2}}(J_x \pm iJ_y) \quad (3.13)$$

³For positive energy eigenstates, they form an $SO(3, 1)$ algebra.

$$\tilde{A}_+ = \frac{1}{\sqrt{2}}(\tilde{M}_z - i\tilde{N}_z) \quad (3.14)$$

$$\tilde{A}_- = \frac{1}{\sqrt{2}}(\tilde{M}_z + i\tilde{N}_z) \quad (3.15)$$

$$\tilde{B}_+ = -\frac{1}{\sqrt{2}}(\tilde{M}_+ - i\tilde{N}_+) \quad (3.16)$$

$$\tilde{B}_- = -\frac{1}{\sqrt{2}}(\tilde{M}_- + i\tilde{N}_-) \quad (3.17)$$

$$\tilde{C}_+ = \frac{1}{\sqrt{2}}(\tilde{M}_- - i\tilde{N}_-) \quad (3.18)$$

$$\tilde{C}_- = \frac{1}{\sqrt{2}}(\tilde{M}_+ + i\tilde{N}_+) . \quad (3.19)$$

The action of these operators on an energy eigenstate is

$$J_{\pm}\psi_{n,l',m} = \sqrt{\frac{1}{2}(l' - m \mp \frac{1}{2})(l' + m \pm \frac{1}{2})} \psi_{n,l',m \pm 1} \quad (3.20)$$

$$\tilde{A}_{\pm}\psi_{n,l',m} = \sqrt{\frac{1}{2}(l' - m \pm \frac{1}{2})(l' + m \pm \frac{1}{2})(n + 2l' \pm 1)} \psi_{n,l' \pm 1,m} \quad (3.21)$$

$$\tilde{B}_{\pm}\psi_{n,l',m} = \frac{l'}{2|l'|} \sqrt{(l' + m \pm \frac{1}{2})(l' + m \pm \frac{3}{2})(n + 2l' \pm 1)} \psi_{n,l' \pm 1,m \pm 1} \quad (3.22)$$

$$\tilde{C}_{\pm}\psi_{n,l',m} = \frac{l'}{2|l'|} \sqrt{(l' - m \pm \frac{1}{2})(l' - m \pm \frac{3}{2})(n + 2l' \pm 1)} \psi_{n,l' \pm 1,m \mp 1} . \quad (3.23)$$

Now it is straightforward to find the appropriate rescaling operator. Consider the operator $F = H + 2A_3 - \frac{5}{2}$, which commutes with H , A_3 and J_i and has the following eigenvalues

$$F\psi_{n,l',m} = (n + 2l' - 1)\psi_{n,l',m} . \quad (3.24)$$

The operators in eqs. (3.14-3.19) commute with F as $[F, \tilde{A}_{\pm}] = \pm 2\tilde{A}_{\pm}$, and similarly for \tilde{B}_{\pm} and \tilde{C}_{\pm} . Now rescale them as

$$A_+ = \frac{1}{\sqrt{F}}\tilde{A}_+ , \quad A_- = \tilde{A}_- \frac{1}{\sqrt{F}} , \quad (3.25)$$

and again similarly for \tilde{B}_{\pm} and \tilde{C}_{\pm} . Note that the order of the operators is important to ensure that $A_+^\dagger = A_-$ and that the right factor is obtained when acting on an energy

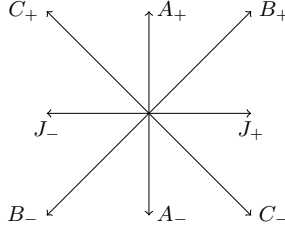


Figure 3.2: Root diagram of the rescaled algebra corresponding to $SO(3, 2)$. It is of rank 2, where we choose as Cartan subalgebra $\{J_3, A_3\}$.

eigenstate. For the scaling operator F to be well defined we need to make sure that $F > 0$ for all states in the Hilbert space. This condition is met for the states of the +branch, but the -branch includes states for which $F = 0$. We will address this point after discussing the representations of $SO(3, 2)$.

From the definitions of J_i, A_3, A_\pm, B_\pm and C_\pm we can explicitly compute the commutation relations of the rescaled symmetry operators, by acting on an energy eigenstate. They form a ten dimensional (linear) Lie algebra of rank 2, corresponding to the noncompact algebra $SO(3, 2)$. The corresponding group consists of transformations that leave the quadratic form $x_1^2 + x_2^2 + x_3^2 - x_4^2 - x_5^2$ invariant. The two generators of the Cartan subalgebra $\{J_3, A_3\}$ are compact generators, leading to the root diagram shown in fig. 3.2. The nonzero commutators are

$$\begin{aligned}
 [A_3, A_\pm] &= \pm A_\pm & [J_3, J_\pm] &= \pm J_\pm \\
 [A_3, B_\pm] &= \pm B_\pm & [J_3, B_\pm] &= \pm B_\pm \\
 [A_3, C_\pm] &= \pm C_\pm & [J_3, C_\pm] &= \mp C_\pm \\
 [J_\pm, A_\pm] &= \pm B_\pm & [J_\mp, B_\pm] &= \pm A_\pm \\
 [J_\mp, A_\pm] &= \pm C_\pm & [J_\pm, C_\pm] &= \pm A_\pm \\
 [A_\mp, B_\pm] &= \pm J_\pm & [A_\pm, C_\mp] &= \mp J_\pm \\
 [J_+, J_-] &= J_3 & [B_+, B_-] &= -(A_3 + J_3) \\
 [A_+, A_-] &= -A_3 & [C_+, C_-] &= -(A_3 - J_3).
 \end{aligned} \tag{3.26}$$

Since the symmetry operators $\{J_i, A_3, \widetilde{M}_i, \widetilde{N}_i\}$ and the rescaling operator F are Hermitian, we need to study the unitary representations of $SO(3, 2)$, in order to describe the spectrum in fig. 3.1. As we mentioned before, it is well known that the nontrivial uni-

tary irreducible representations of a noncompact group are all infinite dimensional. The unitary representations of the covering group of $SO(3, 2)$ have been studied by a number of authors [109, 110], and were completely classified by Evans [111]. One of the reasons why they attracted a lot of attention is because $SO(3, 2)$ and $SO(4, 1)$ are the only simple Lie groups which can be contracted to the Poincaré group.

3.2.2 $SO(3, 2)$ representation theory

Following Evan's notation, a representation can be labeled by its *extremal weight* (q, s) in the same way that one usually labels a representation of a compact group by its highest weight. The lower bound of A_3 is indicated by q and the lowest $SU(2)$ multiplet of the irreducible representation is labeled by s . The representation that forms the +branch has $q = 1$ and $s = \frac{1}{2}$. This representation was first found by Ehrman [109] and later Dirac wrote an explicit form of this representation [110], which is known as the *Dirac singleton* of spin- $\frac{1}{2}$. It is one of the singleton representations, because all its weights have unit multiplicity. While representations of compact groups are uniquely labeled by the value of the Casimir operators, noncompact groups might allow more than one inequivalent representation, which is the case for the representation that we are considering.

For completeness we give the action of the rescaled $SO(3, 2)$ operators on the eigenstates of H , which is indeed in exact agreement with the singleton representation

$$J_{\pm} \psi_{n, l', m} = \sqrt{\frac{1}{2}(l' - m \mp \frac{1}{2})(l' + m \pm \frac{1}{2})} \psi_{n, l', m \pm 1} \quad (3.27)$$

$$A_{\pm} \psi_{n, l', m} = \sqrt{\frac{1}{2}(l' - m \pm \frac{1}{2})(l' + m \pm \frac{1}{2})} \psi_{n, l' \pm 1, m} \quad (3.28)$$

$$B_{\pm} \psi_{n, l', m} = \frac{l'}{2|l'|} \sqrt{(l' + m \pm \frac{1}{2})(l' + m \pm \frac{3}{2})} \psi_{n, l' \pm 1, m \pm 1} \quad (3.29)$$

$$C_{\pm} \psi_{n, l', m} = \frac{l'}{2|l'|} \sqrt{(l' - m \pm \frac{1}{2})(l' - m \pm \frac{3}{2})} \psi_{n, l' \pm 1, m \mp 1} . \quad (3.30)$$

The structure and weight multiplicities of the representations can be well described by studying the decompositions under the various maximal subalgebras of $SO(3, 2)$. The following are the regular subalgebras that share the same Cartan subalgebra:

- (a) $SO(2) \times SO(3)$ generated by A_3 and J_i ,
- (b) $SO(2, 1) \times SO(2)$ generated by A_3, A_{\pm} and J_3 ,
- (c) $SO(2, 1) \times SO(2, 1) = SO(2, 2)$ generated by B_{\pm}, C_{\pm} and $A_3 \pm J_3$.

The weight decomposition under these subalgebras is shown in fig. 3.3 for the represen-

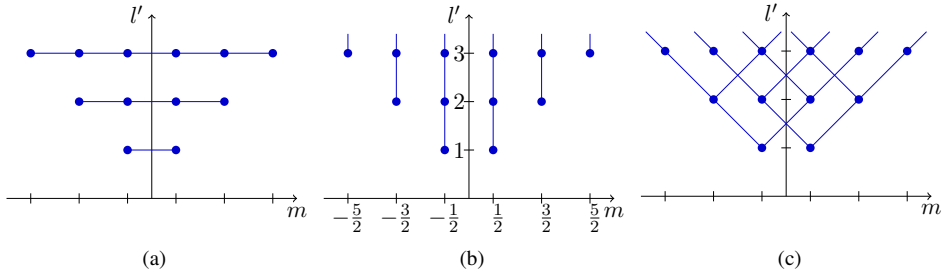


Figure 3.3: The three decompositions of the singleton under the subalgebras (a)-(c). The drawn lines connect the weights corresponding to the irreducible representations of these subalgebras. The figure shows the representation with $l' > 0$. The inequivalent representation with $l' < 0$ can be obtained by reflection in the m -axis.

tation with $l' > 0$. The weight diagram of the inequivalent representation with $l' < 0$ is obtained by reflection in the m -axis.

It turns out that there is one more regular maximal subalgebra of interest in this problem. Clearly the $SO(3, 2)$ does not only have the $SO(2, 2)$ we just discussed, but also the conformal $SO(3, 1)$ subalgebra which is maximal. It is generated by the J_i operators where we add the rescaled \widetilde{M}_i operators, denoted by M_i (picking \widetilde{N}_i instead of \widetilde{M}_i gives an equivalent representation). The M_i operators can be expressed in terms of the $SO(3, 2)$ roots as follows

$$M_z = \frac{1}{\sqrt{2}}(A_+ + A_-), \quad M_{\pm} = \frac{1}{\sqrt{2}}(C_{\mp} - B_{\pm}). \quad (3.31)$$

Note that we cannot choose the same Cartan subalgebra since A_3 is not part of this subalgebra. When acting on the eigenstates of the Hamiltonian, we obtain exactly the same coefficients and multiplicities as described by Harish-Chandra in ref. [112], where he constructs the unitary infinite dimensional representations of $SO(3, 1)$ in terms of the irreducible representations of the $SO(3)$ subalgebra. From this we may conclude that the degeneracies in the spectrum also form an irreducible representation (principal series) under the $(3 + 1)$ -dimensional Lorentz algebra. Bearing in mind the inclusions $SO(3, 2) \supset SO(3, 1) \supset SO(3)$, it is not so surprising that the singleton remains irreducible under $SO(3, 1)$, in contrast with the situation for $SO(2, 2)$ depicted in fig. 3.3c. However, the largest symmetry in our problem remains the $SO(3, 2)$ algebra.

3.2.3 Representations of the physical operators

Now let us return to the physical unrescaled operators

$$\begin{aligned}\tilde{A}_+ &= \sqrt{F}A_+ = \frac{1}{\sqrt{2}}(\tilde{M}_z - i\tilde{N}_z) \\ \tilde{A}_- &= A_- \sqrt{F} = \frac{1}{\sqrt{2}}(\tilde{M}_z + i\tilde{N}_z),\end{aligned}\tag{3.32}$$

where $\tilde{B}_\pm, \tilde{C}_\pm$ are defined in the same fashion. We want to determine what the influence is of the rescaling factor F on the singleton representation. In other words, knowing the $SO(3, 2)$ representation, how do we obtain the spectrum of the physical system? First note that the $SU(2)$ multiplets are not affected by the rescaling factor since \mathbf{J} has not been rescaled and commutes with F . So we need to figure out which $SU(2)$ representations are present in the physical spectrum.

As was mentioned before $F > 0$ for all the states of the +branch, meaning that the coefficients of the physical unrescaled operators will be altered by this factor, but we will still be left with an infinite dimensional representation characterized by the same lower bound $l' = 1$ and with the same multiplicities. The -branch, the states with negative A_3 eigenvalue, also form an infinite representation under $SO(3, 2)$ in this case with an upper bound $l' = -1$, but the physical lowering operators annihilate the states for $l' = \frac{1}{2}(1-n)$. This creates a lower bound depending on the energy level, resulting in a finite dimensional truncation of the representation. This all perfectly agrees with the spectrum in fig. 3.1.

We remark that the operator-dependent scale transformations in (3.32) are very similar to the so-called Holstein-Primakoff transformations [113]. The latter relate bosonic oscillators $\{a, a^\dagger\}$ to $SU(2)$ spin operators $\{S_\pm, S_z\}$ through

$$\begin{aligned}S_+ &= \sqrt{(2s - a^\dagger a)} a, \quad S_- = a^\dagger \sqrt{(2s - a^\dagger a)}, \\ S_z &= (s - a^\dagger a).\end{aligned}\tag{3.33}$$

The bosonic operators have infinite dimensional representations, but in this form they become finite dimensional. For instance, when we act with S_- on a state with S_z eigenvalue $-s$ it annihilates this state because $a^\dagger a = 2s$ and the coefficient vanishes. A transformation very similar to (3.33) relates the symmetry operators for two-dimensional Landau levels on the plane to those pertaining to finite-dimensional Landau levels in a spherical geometry [93], as we will also see in chapter 4.

3.3 Spectrum generating algebra

After determining the symmetry algebra and explaining why there are both finite and infinite degeneracies present in this system, we will now describe operators that connect different energy levels, the so-called spectrum generating algebra (SGA).⁴ Two operators that commute with J_3 and A_3 are

$$\begin{aligned} K_+ &= -\frac{1}{2}b_i^\dagger b_i^\dagger \\ K_- &= -\frac{1}{2}b_i b_i, \end{aligned} \quad (3.34)$$

where the b_i^\dagger and b_i are the usual bosonic raising and lowering operators

$$\begin{aligned} b_i^\dagger &= r_i/2 - ip_i \\ b_i &= r_i/2 + ip_i \\ [b_i, b_j^\dagger] &= \delta_{ij}, \quad [b_i, b_j] = [b_i^\dagger, b_j^\dagger] = 0, \end{aligned} \quad (3.35)$$

in terms of which the harmonic oscillator part of the Hamiltonian can be expressed as $H_{\text{HO}} = b_i^\dagger b_i + \frac{3}{2}$. The operators K_\pm raise or lower the energy by steps of two as can be seen from their commutator

$$\begin{aligned} [H, K_\pm] &= \pm 2K_\pm \\ [K_+, K_-] &= -(H + A_3 - 1). \end{aligned} \quad (3.36)$$

It is evident that they form an $SO(2,1)$ algebra when we define $K_3 = H + A_3 - 1$. The representation theory of this algebra is well known [114] and again the unitary irreducible representations are all infinite dimensional, reflecting the fact that the energy is not bounded from above.

The coefficients of these operators, when acting on an energy eigenstate, are

$$K_\pm \psi_{n,\nu',m} = \frac{1}{2} \sqrt{(n+1 \pm 1)(n+2\nu' \pm 1)} \psi_{n \pm 2, \nu', m}. \quad (3.37)$$

⁴The authors of [105] also construct operators that connect different energy levels, but they use the radial symmetry of the system and only consider one-dimensional radial operators. Our construction is coordinate independent.

Unitary irreducible representations of $SO(2, 1)$ have either a lower or an upper bound and can be uniquely defined by this bound. For every value of l' and m there is an infinite tower of states, corresponding to one such representation. From the coefficients of K_{\pm} , we see that for the +-branch all representations have a lower bound $n = 0$ and the representations of the -branch have a lower bound $n = -2l' + 1$, in perfect agreement with the physical spectrum.

Note that the algebra $SO(2, 1) \times SO(3)$ spanned by K_i and J_i is associated with the radial symmetry of the system, allowing us to write the wave function as a product of a radial and an angular function, see for example [115]. We would like to mention that when we rescale K_{\pm} by a factor of $\sqrt{(H - \frac{1}{2})/F}$, these operators commute with the entire symmetry algebra, resulting in a dynamical algebra $SO(2, 1) \times SO(3, 2)$.

We can also construct operators that move between the two branches. Consider

$$T_+ = \sum_i b_i^\dagger \sigma_i, \quad T_- = \sum_i b_i \sigma_i, \quad (3.38)$$

in terms of which the Hamiltonian can be expressed as $H = T_+ T_- + \frac{3}{2}$.⁵ These operators anticommute with A_3 and map +-branch states onto -branch states and vice versa: the action on an energy eigenstate is

$$\begin{aligned} T_+ \psi_{n,l',m} &= \sqrt{n + 2l' + 1} \psi_{n+2l'+1, -l', m} \\ T_- \psi_{n,l',m} &= \sqrt{n} \psi_{n+2l'-1, -l', m}. \end{aligned} \quad (3.39)$$

We have not yet succeeded in extending the $SO(3, 2)$ symmetry algebra to a complete spectrum generating (super) algebra including both the K_{\pm} and T_{\pm} operators.

Let us end this chapter by summarizing the main results that have been presented. We have explicitly constructed the symmetry algebra of a spin-orbit coupled harmonic oscillator given in (3.1). Besides the $SU(2)$ symmetry coming from conservation of total angular momentum we have identified six other operators that commute with H , and which are a spin-generalized version of the Runge-Lenz vector. Commuting these symmetry operators results in nonlinear commutation relations, which were expected since there are finite and infinite degeneracies in this model. We showed that a simple rescaling

⁵This structure clearly shows the supersymmetry of this model. H has a supersymmetric partner given by $H_- = T_- T_+ + \frac{3}{2}$. For more details see [116].

of the operators leads to linear commutation relations which we recognize as an $SO(3, 2)$ algebra. The infinite degenerate branches of the spectrum are the singleton representation of $SO(3, 2)$ and the finite degenerate levels are a truncated version of the singleton. We also identify four operators that connect different energy levels with each other, forming the spectrum generating algebra.

Appendix

3.A Representation theory $SO(3)$ versus $SO(2, 1)$

In this appendix we classify all unitary representations of $SO(3)$ and its noncompact variant $SO(2, 1)$. We do not present any new results, but rather show some features of noncompact groups, which are often a less common topic in physics books than compact groups. Moreover, both groups are subgroups of $SO(3, 2)$, which was the symmetry group that we studied in this chapter.

The algebra of the groups have three generators and their commutation relations are

$$[J_1, J_2] = ig_{33}J_3, \quad [J_2, J_3] = iJ_1, \quad [J_3, J_1] = iJ_2, \quad (3.40)$$

where $g_{33} = 1$ corresponds to $SO(3)$ and $g_{33} = -1$ to $SO(2, 1)$. All operators commute with the Casimir operator defined by

$$J^2 = J_1^2 + J_2^2 + g_{33}J_3^2. \quad (3.41)$$

We choose to diagonalize in J^2 and J_3 , which is the compact $SO(2)$ subgroup in both cases

$$J^2|Xa\rangle = X|Xa\rangle, \quad X \in \mathbb{R} \quad (3.42)$$

$$J_3|Xa\rangle = a|Xa\rangle, \quad a \in \mathbb{R}. \quad (3.43)$$

For the compact group it does not matter in which generator we choose to diagonalize, but this is not true for $SO(2, 1)$. Diagonalizing in one of the noncompact operators $J_{1,2}$, which generates an $SO(1, 1)$ algebra, we are forced to choose a continuous basis rather than a discrete one. For more details on this choice we refer to the literature [117, 118]. Here we continue with a discrete basis diagonal in the compact generator J_3 .

We can define raising and lowering operators $J_{\pm} = \frac{1}{\sqrt{2}}(J_1 \pm iJ_2)$, which commute as

$$[J_+, J_-] = g_{33}J_3, \quad [J_3, J_{\pm}] = \pm J_{\pm}, \quad (3.44)$$

$$J^2 = g_{33}J_3^2 + 2J_{\pm}J_{\mp} \mp g_{33}J_3. \quad (3.45)$$

Rewriting the Casimir operator in terms of these ladder operators we find the coefficients

$$J_{\pm}|Xa\rangle = \frac{1}{\sqrt{2}}\sqrt{X - g_{33}a(a \pm 1)}|Xa \pm 1\rangle. \quad (3.46)$$

We see that the unitary representation must have

$$X - g_{33}a(a \pm 1) \geq 0, \quad (3.47)$$

and we know from $[J_3, J_{\pm}] = \pm J_{\pm}$ that the value of a takes steps of unity. From this point on let us consider the compact and noncompact cases separately.

Compact $SO(3)$ We know from (3.41) that $X \geq 0$ and it is easy to see that $a(a \pm 1) \geq -\frac{1}{4}$, which means that the representations must have an upper and lower bound. Writing

$$X = a_{\max}(a_{\max} + 1) = a_{\min}(a_{\min} - 1), \quad (3.48)$$

implies that $a_{\min} = -a_{\max}$ and a must be an integer or half integer. With $a_{\max} = j$ and $a = m$, we obtain

$$J^2|jm\rangle = j(j+1)|jm\rangle, \quad j = 0, \frac{1}{2}, 1, \dots \quad (3.49)$$

$$J_3|jm\rangle = m|jm\rangle, \quad -j \leq m \leq j \quad (3.50)$$

$$J_{\pm}|jm\rangle = \frac{1}{\sqrt{2}}\sqrt{j(j+1) - m(m \pm 1)}|jm \pm 1\rangle. \quad (3.51)$$

Note that these coefficients are invariant under

$$j \rightarrow -j - 1 \quad (3.52)$$

$$m \rightarrow m, \quad (3.53)$$

which would map to an equivalent representation. The multiplets of this compact group are depicted in fig. 3.4, where we also indicated the equivalent irreps.

Noncompact $SO(2, 1)$ Because of the minus sign in (3.41), $X \in \mathbb{R}$ can be negative and the representations do not have to have two bounds, which implies the emergence of infinite dimensional multiplets. Another difference is that this noncompact group has con-

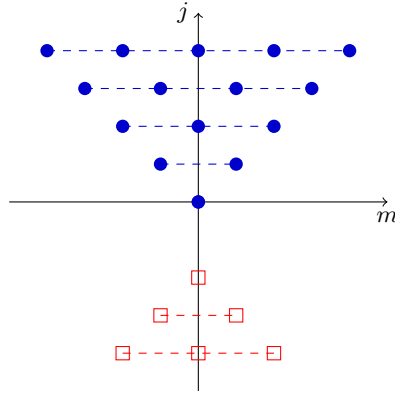


Figure 3.4: The irreducible unitary representations of $SO(3)$. The states belonging to the same multiplet are connected by dashed lines. Note that all multiplets are finite dimensional. The blue solid circles and the red open squares are equivalent ways of labeling the irreps.

tinuous and discrete representations. The former has no bounds and the latter has either an upper or a lower bound. Here we are only interested in the discrete representations, i.e. the half-infinite ones.

Assume there is a lower bound $X = -a_{\min}(a_{\min} - 1)$ or an upper bound $X = -a_{\max}(a_{\max} + 1)$. Again it follows that $a_{\min} = -a_{\max}$, but we must conclude that $a_{\min} \geq 0$ and $a_{\max} \leq 0$, so we get two infinite representations labeled by the same J^2 eigenvalue. Writing $a_{\min} = k \geq 0$ we get

$$J^2|k a\rangle = k(1 - k)|k a\rangle, \quad k = \frac{1}{2}, 1, \frac{3}{2}, \dots \quad (3.54)$$

$$J_3|k a\rangle = a|k a\rangle, \quad a = \pm k, \pm(k + 1), \dots \quad (3.55)$$

$$J_{\pm}|k a\rangle = \frac{1}{\sqrt{2}} \sqrt{k(1 - k) + a(a \pm 1)} |k a \pm 1\rangle. \quad (3.56)$$

The only finite dimensional representation is the trivial one labeled by $k = 0$. The representations are shown in fig. 3.5 by blue solid circles. Note that the value of the Casimir

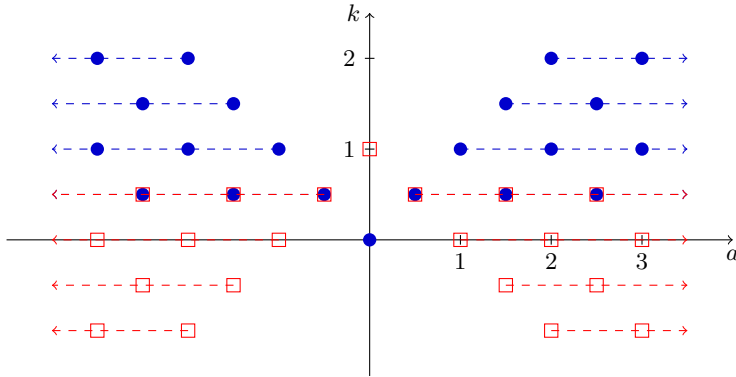


Figure 3.5: The blue solid circles indicate the irreps of the covering group of $SO(2, 1)$. States belonging to the same multiplets are connected by dashed lines. The eigenvalue of the Casimir operator does not determine the representation, there are two inequivalent irreps corresponding to the same value k . An equivalent set of representations is depicted by the open red squares.

operator no longer uniquely labels an irrep. These coefficients are invariant under

$$k \rightarrow -k + 1 \tag{3.57}$$

$$a \rightarrow a, \tag{3.58}$$

implying the existence of an equivalent set of representations, which is depicted in fig. 3.5 by red open squares.

3.B Commutation relations physical operators

As mentioned in section 3.2 the commutation relations of the unrescaled symmetry operators contain nonlinear terms. We will explicitly give the nonzero commutation relations here. The following five commutation relations are linear and are the same as those of $SO(3, 2)$

$$\begin{aligned}
 [J_i, J_j] &= i\epsilon_{ijk}J_k \\
 [J_i, \widetilde{M}_j] &= i\epsilon_{ijk}\widetilde{M}_k \\
 [J_i, \widetilde{N}_j] &= i\epsilon_{ijk}\widetilde{N}_k \\
 [A_3, \widetilde{M}_i] &= -i\widetilde{N}_i \\
 [A_3, \widetilde{N}_i] &= i\widetilde{M}_i .
 \end{aligned} \tag{3.59}$$

The next three nonzero commutation relations are nonlinear and therefore are not similar to those of $SO(3, 2)$

$$\begin{aligned}
 [\widetilde{M}_i, \widetilde{M}_j] &= -i\epsilon_{ijk}J_k(H + 3A_3 - \frac{3}{2}) \\
 [\widetilde{N}_i, \widetilde{N}_j] &= -i\epsilon_{ijk}J_k(H + 3A_3 - \frac{3}{2}) \\
 [\widetilde{M}_i, \widetilde{N}_j] &= i\delta_{ij}A_0(H + 3A_3 - \frac{3}{2}) + \frac{1}{4}i\delta_{ij} - \frac{i}{2}(J_iJ_j + J_jJ_i) .
 \end{aligned} \tag{3.60}$$

CHAPTER 4

Non-Abelian gauge potentials: Landau problem and non-Abelian flux

This chapter is based on the following publication:

B. Estienne, S.M. Haaker, and K. Schoutens, PARTICLES IN NON-ABELIAN GAUGE POTENTIALS: LANDAU PROBLEM AND INSERTION OF NON-ABELIAN FLUX, *New J. Phys.* **13**, 045012 (2011).

In the previous chapter we considered a generalization of the two-dimensional Landau levels to a three-dimensional system, where a non-Abelian background gauge field resulted in a flat spectrum. We focused on understanding the degeneracy from the construction of a symmetry algebra. In the present chapter we will yet again investigate a system with degenerate Landau levels. We return to two dimensions and analyze noninteracting spin- $\frac{1}{2}$ particles in an external non-Abelian field. The spectrum on a compact manifold is found and the response to insertion of non-Abelian flux is investigated. Inspired by the usual Abelian setting we will reflect on some of the fundamental differences with our non-Abelian setup. This chapter can be divided into two main parts.

In section 4.1 we analyze and solve the Landau level problem in spherical geometry, highlighting the fundamental role of the total angular momentum $\mathbf{J} = \mathbf{L} + \mathbf{S}$, which commutes with the Hamiltonian. In this setup, the non-Abelian field penetrating the sphere agrees with the asymptotic (large radius) limit of the non-Abelian magnetic monopoles first discussed by 't Hooft and Polyakov [119, 120]. One reason to focus on spherical geometry is that this context is known to be particularly useful for the purpose of a numerical study of many-body states arising upon adding interactions to the Landau level problem [93].

In section 4.2 we proceed to the process in which a non-Abelian flux is inserted in a background of otherwise Abelian flux. Thought experiments involving insertion of (Abelian) flux are often invoked as a probe of the characteristics of the quantum phase of a many-body system. One well-known example is the argument by Laughlin that we encountered in section 1.2. It originally showed that the Hall conductance must be quantized, but it has another consequence. The insertion of a unit flux through a gapped

medium with fractional Hall conductance $\sigma_H = \nu e^2/h$ leads to the nucleation of an excitation with fractional electron charge $e^* = \nu e$ at the edge of the sample. Another example is the case of the quantum spin Hall state, where insertion of flux leads to spin-full excitations at the edge [14]. A motivation for the present study has been the desire to extend these considerations to non-Abelian flux.

The first case we will consider is such that $J_z = L_z + S_z$ remains a good quantum number during the flux insertion. This suggests a prominent role for transitions where particles flip their spin while at the same time changing their L_z quantum number by (plus or minus) one unit, i.e. they jump to an adjacent Landau level orbital of the Abelian problem. The resulting state is a spin-texture of unit electric and topological charge, which is easily identified as a quantum Hall skyrmion. More general external fields lead to more intricate textures as we will also show.

The appendices contain further details and background material. In appendix 4.A we recall the main results of the Landau problem on the plane, and in appendix 4.B we treat the S^2 case. In appendix 4.C we present more details on the derivation of the spectrum on the sphere in a non-Abelian background, and in appendix 4.D a detailed derivation of non-Abelian flux insertion is given.

4.1 The non-Abelian Landau problem

In the present chapter we focus on the simplest case of non-Abelian gauge fields, where the gauge field \mathbf{A} and the field strength \mathbf{B} are 2×2 Hermitian matrices. For the basics on non-Abelian gauge fields and how they are realized we refer the reader to section 1.4. The gauge group we focus on here is $U(2) = U(1) \times SU(2)$ and it decomposes into an Abelian $U(1)$ part, namely the fields proportional to the identity matrix \mathbb{I} , and a non-Abelian $SU(2)$ component, whose fields are linear combinations of the Pauli matrices σ_i .

The $U(2)$ case is a natural choice as it is the simplest one allowing non-Abelian gauge fields. However there is a deeper reason to focus on $U(2)$ gauge fields. The physics corresponding to a particle coupled minimally to such a non-Abelian gauge field is mathematically equivalent to the physics arising in a two-dimensional electron gas when taking into account relativistic corrections in the Pauli-Schrödinger equation, such as the Thomas term

$$H_T = -\frac{q\hbar}{4m^2c^2} \boldsymbol{\sigma} \cdot (\mathbf{E} \times \mathbf{p}) . \quad (4.1)$$

This SOC term mimics the effect of a non-Abelian gauge potential

$$\mathbf{A} \sim \mathbf{E} \times \boldsymbol{\sigma} . \quad (4.2)$$

In this section we study the quantum problem of a nonrelativistic particle confined to a two-dimensional manifold in the background of a uniform perpendicular $U(2)$ magnetic field. We present the spectra for two different geometries: the plane and the sphere. It turns out that this Hamiltonian can be mapped exactly to that of an electron in two dimensions in a perpendicular $U(1)$ magnetic field, when the Thomas term is present and an additional perpendicular $U(1)$ electric field \mathbf{E} is applied.

4.1.1 On the plane

In order to set this problem on the plane, we consider a perpendicular, uniform magnetic field $\mathbf{B} = B_z \hat{z}$, where B_z is a 2×2 Hermitian matrix. A basis can be chosen such that the matrix B_z is diagonal

$$B_z = B\mathbb{I} + \frac{2}{\hbar}\beta'^2\sigma_z = B(\mathbb{I} + 2\beta^2\sigma_z) , \quad (4.3)$$

where we introduced the pure number $\beta = \frac{\beta'}{\ell B}$ involving the magnetic length $\ell = \sqrt{\frac{\hbar}{B}}$ (for $B > 0$). We will set $\hbar = 1$ in the following. The magnetic field is a $U(2)$ matrix, and is a superposition of a $U(1)$ field B and a $SU(2)$ field $2\beta^2 B\sigma_z$.

Since the magnetic field is no longer gauge invariant, as was discussed in section 1.4, one has to specify the non-Abelian part of the potential \mathbf{A} . The first kind of potential $\mathbf{A} = \frac{1}{2}\mathbf{B} \times \mathbf{r}$ boils down to an Abelian $U(1) \times U(1)$ gauge group, and the physics is simply that of two noninteracting species of particles coupled to different Abelian magnetic fields, like we encountered in the context of the QSHE. The second kind however, a constant and noncommutative potential given by

$$\mathbf{A} = \frac{B}{2} \begin{pmatrix} -y\mathbb{I} \\ x\mathbb{I} \\ 0 \end{pmatrix} + \beta' \begin{pmatrix} -a\sigma_y \\ a^{-1}\sigma_x \\ 0 \end{pmatrix} , \quad (4.4)$$

is much more interesting and leads to new physics [121–124]. The Hamiltonian describing a particle confined to a plane in this non-Abelian background is

$$H = \frac{1}{2m}(\mathbf{p} - \mathbf{A})^2 . \quad (4.5)$$

It turns out that this problem can be mapped exactly to the Hamiltonian of a two-dimensional electron in the presence of both Rashba and Dresselhaus spin-orbit interactions, and it was first solved in this context by Zhang [125].

The system in (4.5) enjoys the translation symmetry of the plane. The magnetic translation operators are insensitive to the non-Abelian part of \mathbf{A} since it is uniform, and have the usual expressions

$$T_x = \left(-i\partial_x - \frac{y}{2\ell^2} \right), \quad T_y = \left(-i\partial_y + \frac{x}{2\ell^2} \right), \quad (4.6)$$

which implies the following commutation relations

$$[\mathbf{a} \cdot \mathbf{T}, \mathbf{b} \cdot \mathbf{T}] = -i \frac{(\mathbf{a} \times \mathbf{b}) \cdot \hat{z}}{\ell^2} \mathbb{I}. \quad (4.7)$$

The r.h.s. is simply the flux of the Abelian part of the magnetic field $B\mathbb{I}$ through the parallelogram delimited by the vectors \mathbf{a} and \mathbf{b} , and the (Abelian) magnetic length scale is ℓ . Only the Abelian part of the magnetic field is quantized, and the number of states in a given Landau level will therefore depend on the Abelian field strength B .

In the next section we will solve this problem on the sphere. With this in mind, we demand rotational symmetry around the \hat{z} -axis, and focus on the symmetric gauge

$$\mathbf{A} = \frac{B}{2} \begin{pmatrix} -y\mathbb{I} \\ x\mathbb{I} \\ 0 \end{pmatrix} + \beta' \begin{pmatrix} -\sigma_y \\ \sigma_x \\ 0 \end{pmatrix}. \quad (4.8)$$

This gauge choice corresponds to the absence of Dresselhaus interaction, and the Hamiltonian in (4.5) is much simpler to solve in this case. Moreover it can be mapped to a Thomas term in (4.1) in the presence of a perpendicular uniform electric field $\mathbf{E} \sim \beta' \hat{z}$.

The Hamiltonian can be expanded as

$$H = \omega_c \left(a^\dagger a + \sqrt{2}\beta(a^\dagger \sigma_+ + a\sigma_-) + \frac{1}{2}(1 + 2\beta^2) \right), \quad (4.9)$$

where a, a^\dagger are the usual annihilation and creation operators appearing in the Landau problem (see appendix 4.A). Up to a change of spin basis $U = \sigma_x$, eq. (4.9) is equal to the celebrated Jaynes-Cummings Hamiltonian, and it is a straightforward exercise to

obtain its spectrum

$$E_0 = \omega_c \left(\frac{1}{2} + \beta^2 \right), \quad (4.10)$$

$$E_n^\pm = \omega_c \left(n \pm \sqrt{2\beta^2 n + \frac{1}{4} + \beta^2} \right). \quad (4.11)$$

4.1.2 On the sphere

It can be rather instructive to solve such a problem on a sphere instead of the plane. Since the surface of the sphere is finite, the degeneracy of the Landau levels becomes finite too, which is very interesting for numerical studies. Moreover the translation invariance of the plane is promoted to the rotational symmetry of the sphere, and the spectrum decomposes into $SU(2)$ multiplets. In the Abelian case this geometry was first solved in [126, 127], and later used by Haldane [93] in the context of the QH effect. We refer the reader to appendix 4.B for more details on the Abelian problem on the sphere.

Field configuration

A uniform perpendicular magnetic field implies the presence of a magnetic monopole at the center of the sphere. In the Abelian case, as explained in section 1.1 and repeated in appendix 4.B, the corresponding potential \mathbf{A}_{Ab} must have a singularity (Dirac string) somewhere on the sphere, for instance at the south pole $\theta = \pi$

$$\mathbf{A}_{\text{Ab}} = \frac{N_\Phi}{2} \frac{1 - \cos(\theta)}{r \sin(\theta)} \hat{\phi}. \quad (4.12)$$

When Dirac's quantization condition $N_\Phi \in \mathbb{Z}$ is satisfied, this singularity has no physical consequence as it can be moved around through gauge transformations [31]. It implies the well-known quantization of the magnetic flux piercing the sphere, which must be equal to an integer number of flux quanta N_Φ

$$\int_S \mathbf{B} \cdot d\mathbf{S} = 2\pi N_\Phi \quad \Rightarrow \quad B_r = \frac{N_\Phi}{2r^2}. \quad (4.13)$$

To the $U(1)$ potential in (4.12) we add an $SU(2)$ component $\mathbf{A}(\alpha) = \mathbf{A}_{\text{Ab}} + \mathbf{A}_{\text{NA}}(\alpha)$, where

$$\mathbf{A}_{\text{NA}}(\alpha) = \alpha \frac{\mathbf{r} \times \boldsymbol{\sigma}}{r^2}. \quad (4.14)$$

Once again this corresponds to a Thomas term as in (4.1) with a radial uniform electric field $\mathbf{E} \sim \alpha \hat{r}$. As we will see below, this is the correct extension of the symmetric gauge on the plane in (4.8). The corresponding magnetic field is

$$B_r = \frac{N_\Phi}{2r^2} - 2\alpha(1 - \alpha) \frac{(\mathbf{r} \cdot \boldsymbol{\sigma})}{r^3}. \quad (4.15)$$

As the radial $U(1)$ field is created by a magnetic monopole, it is not very surprising that the $SU(2)$ counterpart involves a non-Abelian monopole. Indeed, the potential $\mathbf{A}_{\text{NA}} = \alpha \frac{\mathbf{r} \times \boldsymbol{\sigma}}{r^2}$ is the large distance asymptote of a true non-Abelian monopole [119, 120], and has no singularity on the sphere. Since we only consider external fields, \mathbf{A}_{NA} does not have to satisfy the field equations and α can be any real number.

Hamiltonian and spectrum

The details about the derivation of the spectrum of a particle confined to a sphere of radius r in this non-Abelian background can be found in appendix 4.C, while here we give the main results. The Hamiltonian is given by

$$H(\alpha) = \frac{1}{2mr^2} \left[\mathbf{r} \times (\mathbf{p} - \mathbf{A}(\alpha)) \right]^2, \quad (4.16)$$

which is a scalar under global rotations generated by $\mathbf{J} = \mathbf{L} + \mathbf{S}$, where \mathbf{L} generates magnetic angular momentum (see appendix 4.C) and $\mathbf{S} = \frac{1}{2}\boldsymbol{\sigma}$ is the spin operator. Its eigenstates form $SU(2)$ multiplets corresponding to the decomposition of the Hilbert space into irreducible representations of \mathbf{J}

$$\mathcal{H} = (j_0) \oplus 2(j_1) \oplus 2(j_2) \oplus \cdots \oplus 2(j_n) \oplus \cdots, \quad (4.17)$$

where $j_n = \frac{N_\Phi - 1}{2} + n$. The corresponding eigenvalues are

$$E_0(\alpha) = \frac{1}{2mr^2} \left(\frac{N_\Phi}{2} - 2\alpha(1 - \alpha) \right), \quad (4.18)$$

$$E_n^\pm(\alpha) = \frac{1}{2mr^2} \left(n(N_\Phi + n) - 2\alpha(1 - \alpha) \pm \sqrt{(2\alpha - 1)^2 n(N_\Phi + n) + \left(\frac{N_\Phi}{2}\right)^2} \right). \quad (4.19)$$

As can be seen in fig. 4.1, multiple level crossings occur. This also happens in the planar case [123], which can be recovered from the sphere in the limit of infinite radius as we

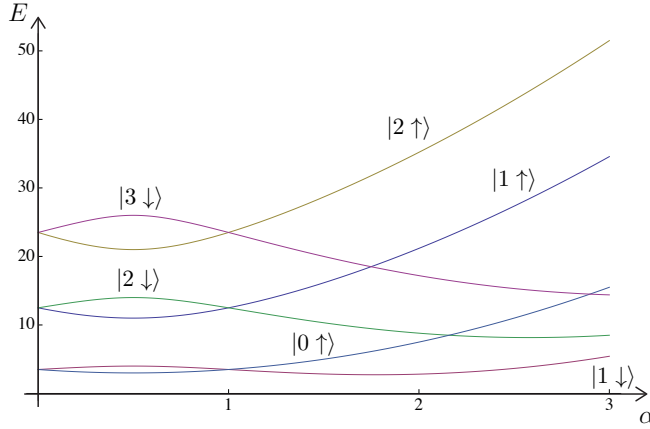


Figure 4.1: Band structure for the non-Abelian Landau problem on the sphere as a function of the non-Abelian field strength α . This case corresponds to $N_\Phi = 7$ Abelian flux quanta, and only the lowest part of the spectrum is shown.

will show now.

Recovering the plane

The non-Abelian field \mathbf{A}_{NA} we considered on the sphere, is indeed the correct extension of the planar symmetric gauge in (4.8). The planar problem is recovered by taking the sphere radius $r \rightarrow \infty$ while keeping constant the gauge field strength on the surface

$$\frac{N_\Phi}{2r^2} \sim B, \quad \frac{\alpha}{r} \sim \beta' = \frac{\beta}{\sqrt{B}}. \quad (4.20)$$

The vector potential and the magnetic field in this limit become

$$\mathbf{A} \rightarrow \frac{B}{2} \begin{pmatrix} -y\mathbb{I} \\ x\mathbb{I} \\ 0 \end{pmatrix} + \beta' \begin{pmatrix} -\sigma_y \\ \sigma_x \\ 0 \end{pmatrix}, \quad \mathbf{B} \rightarrow B (\mathbb{I} + 2\beta^2 \sigma_z) \hat{z}. \quad (4.21)$$

It is straightforward to check that the eigenvalues of the Hamiltonian $E_n^\pm(\alpha)$ behave in the planar limit as

$$E_0(\alpha) \rightarrow \omega_c \left(\frac{1}{2} + \beta^2 \right), \quad (4.22)$$

$$E_n^\pm(\alpha) \rightarrow \omega_c \left(n \pm \sqrt{2\beta^2 n + \frac{1}{4} + \beta^2} \right), \quad (4.23)$$

reproducing the planar spectrum. Moreover one can expand the Hamiltonian on the sphere in terms of \mathbf{L}

$$H = \frac{1}{2mr^2} \left[\mathbf{L}^2 - \left(\frac{N_\Phi}{2} \right)^2 + 2\alpha \left(\mathbf{L} + \frac{N_\Phi}{2} \frac{\mathbf{r}}{r} \right) \cdot \boldsymbol{\sigma} + 2\alpha^2 \right], \quad (4.24)$$

and using the Holstein-Primakoff representation

$$L_+ = b^\dagger \sqrt{N_\Phi + 2a^\dagger a - b^\dagger b}, \quad (4.25)$$

$$L_- = \sqrt{N_\Phi + 2a^\dagger a - b^\dagger b} b, \quad (4.26)$$

$$L_z = b^\dagger b - \frac{N_\Phi}{2} - a^\dagger a, \quad (4.27)$$

we recover the planar Hamiltonian

$$H \rightarrow \omega_c \left[\left(a^\dagger a + \frac{1}{2} \right) + \sqrt{2}\beta (a\sigma + a^\dagger \sigma_+) + \beta^2 \right]. \quad (4.28)$$

That we indeed recover the planar Hamiltonian is not surprising in view of the mapping of this problem consisting of a spin- $\frac{1}{2}$ electron under an effective non-Abelian potential, to the Thomas term with a perpendicular electric field. Indeed, the infinite radius limit of a sphere in a radial \mathbf{E} and \mathbf{B} field is clearly equal to the plane under perpendicular \mathbf{E} and \mathbf{B} fields (keeping the field strength constant).

In summary, in this section we analyzed the non-Abelian Landau problem on the sphere and obtained the spectrum. The degeneracy of Abelian Landau levels is preserved, and the number of states per area remains $1/\ell^2$, as we expected since the magnetic translation operators were not affected by the non-Abelian part of the field configuration. In the next part of this chapter we will focus on the response of an Abelian configuration on the plane

to the insertion of non-Abelian flux.

4.2 Adiabatic insertion of non-Abelian flux

We wish to consider the insertion of non-Abelian flux in an IQH fluid. In the Abelian case, the celebrated Laughlin argument shows that the insertion of a quantum of Abelian flux leads to the accumulation of electric charge $\pm\nu e$, with ν the filling fraction of the QH liquid. In section 1.2 we repeated the argument of Laughlin and showed how the adiabatic insertion of flux leads to a shift of the single-particle states. This argument is easily adjusted to a disc geometry, which we will use in the following.

The background magnetic field corresponds to a vector potential $A_\phi = Br/2$ and we adiabatically insert flux by adding $\delta A_\phi = \Phi(t)/\phi_0 r$ to the Hamiltonian. This does not result in a contribution to the magnetic field away from the origin. After inserting one unit of flux, the system can be mapped back to the original one and the LLL states labeled by their L_z quantum number shift like

$$|m\rangle \rightarrow |m+1\rangle. \quad (4.29)$$

For more details on these eigenstates see appendix 4.A.

In the present chapter we will start from an IQH system and insert a non-Abelian field configuration $\delta\mathbf{A}$ centered around the origin as done for the Abelian situation described above. We choose $\delta\mathbf{A}$ in such a way that

- (i) it generates no magnetic field away from the origin,
- (ii) it can be removed by a gauge transformation.

We start from a system where a nonrelativistic spin- $\frac{1}{2}$ particle confined to the plane is subject to an external perpendicular magnetic field, $B_z = B\mathbb{I}$. For the vector potential we choose the symmetric gauge and express it in cylindrical coordinates as

$$A_\phi = \frac{Br}{2}\mathbb{I}. \quad (4.30)$$

The Hamiltonian of the system $H = \frac{1}{2m}(\mathbf{p} - q\mathbf{A})^2\mathbb{I}$, acts identically on both spin states, i.e. the Landau levels are doubly degenerate. We only consider the LLL and write for the eigenstates $|m, \epsilon\rangle$ where $\epsilon \in \{\uparrow, \downarrow\}$ are the σ_z eigenstates.

In the main part of this section we will present two particular field configurations labeled by $M = 0$ and $M = -1$, and derive the effect of inserting such a field configuration into the system. A generic configuration, labeled by an integer M of which these two are specific cases, can be found in appendix 4.D. There we also give a more detailed deriva-

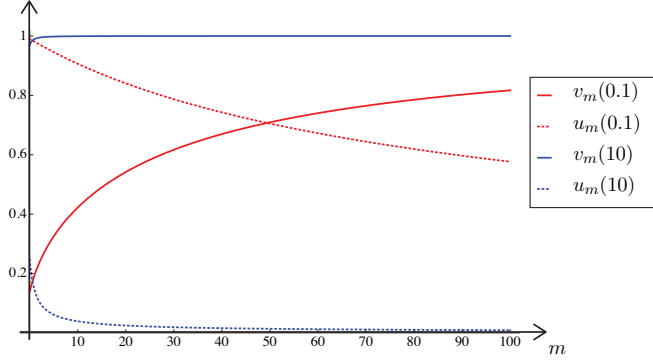


Figure 4.2: Mixing coefficients $u_m(\lambda)$ and $v_m(\lambda)$, for two different values of λ . Around $m \sim 1/(2\lambda^2)$, $u_m(\lambda)$ and $v_m(\lambda)$ are equal to each other.

tion, to avoid any cumbersome equations in the main body of this chapter, and we explain how the label M can be interpreted.

Mimicking the insertion of Abelian flux briefly mentioned at the start of this section, we will insert a gauge field in such a way that no additional magnetic field is created away from the origin. Furthermore, we choose a symmetric gauge and make the simplification $\partial_z(\delta\mathbf{A}) = \mathbf{0}$. The field can be expressed as a pure gauge

$$\delta\mathbf{A} = iU(\lambda)\nabla U^\dagger(\lambda), \quad (4.31)$$

for some unitary matrix $U(\lambda)$, which depends on a parameter λ controlling the adiabatic process. The evolved Hamiltonian is now easily found to be

$$H(\lambda) = \frac{1}{2m} ((\mathbf{p} - q\mathbf{A})\mathbb{I} - q\delta\mathbf{A})^2 = U(\lambda)H(0)U^\dagger(\lambda). \quad (4.32)$$

Since this is just a gauge transformation, we immediately see that the gap $\hbar\omega_c$ separating the subspace of ground states from excited states at every point in parameter space remains unchanged. Also, the eigenstates of the evolved Hamiltonian in (4.32) are simply $U(\lambda)|m, \epsilon\rangle$. To find the state we end up in after this adiabatic process, we need to include the Berry matrix as was explained in section 1.4. We now turn to explicit results for the gauge configurations with $M = 0$ and $M = -1$.

The case $M = 0$

The $M = 0$ non-Abelian field configuration is as follows

$$\begin{aligned}\delta A_r(\lambda) &= \frac{-\lambda}{1 + (\lambda r)^2} \sigma_\phi \\ \delta A_\phi(\lambda) &= \frac{-\lambda^2 r}{1 + (\lambda r)^2} \sigma_z + \frac{\lambda}{1 + (\lambda r)^2} \sigma_r,\end{aligned}\quad (4.33)$$

where we introduced the Pauli matrices in cylindrical coordinates, $\sigma_r = \boldsymbol{\sigma} \cdot \hat{r}$ and $\sigma_\phi = \boldsymbol{\sigma} \cdot \hat{\phi}$. The reason we label this field by $M = 0$ is stated in appendix 4.D and will become especially clear for the case $M = -1$. Note that for $r \gg 1/\lambda$ this field configuration does not depend on λ and behaves as

$$\delta A_\phi \sim -\frac{1}{r} \sigma_z + \mathcal{O}\left(\frac{1}{r^2}\right). \quad (4.34)$$

The field configuration in this limit corresponds to shifting the orbital of a spin- \uparrow (spin- \downarrow) particle by $+1$ (-1), precisely what would happen by inserting an Abelian flux quantum, where the sign depends on the spin of the particle. From this point onwards, we will refer to such a field as a σ_z -flux quantum, to explicitly distinguish it from an insertion of a spin independent Abelian flux quantum.

Our starting point is a fully polarized IQH state, represented as a product state $|\psi(0)\rangle = \bigotimes_{m=0}^{m_f} |m \uparrow\rangle$, which has the first $(m_f + 1)$ LLL orbitals filled with spin- \uparrow particles. We adiabatically insert the non-Abelian flux of (4.33) by slowly sweeping the parameter from $\lambda = 0$ to its final value. Precisely as in the Abelian case, the evolved state is gauged back to the initial situation so that the final state lives in the same Hilbert space as the initial one. The explicit calculation of the Berry matrix can be found in appendix 4.D, and here we merely give the final state

$$|\psi_0(\lambda)\rangle = \bigotimes_{m=0}^{m_f} \left(u_m(\lambda) |m \uparrow\rangle - v_m(\lambda) |m + 1 \downarrow\rangle \right). \quad (4.35)$$

The mixing coefficients $u_m(\lambda)$ and $v_m(\lambda)$ depend on both the orbital quantum number m and the adiabatic parameter λ . Their explicit form is given in (4.75) and they are plotted in fig. 4.2 as a function of m , for two values of λ . Around orbital number $m \sim 1/(2\lambda^2)$, $u_m(\lambda)$ and $v_m(\lambda)$ cross, resulting in a vanishing of the z -component of the spin. The asymptotic behavior of the mixing coefficients as $m \rightarrow \infty$ can be read off from (4.76).

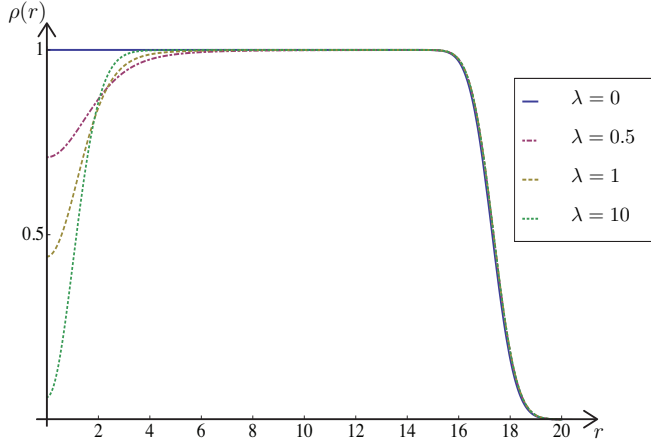


Figure 4.3: Density profile for different values of λ of a product state where the first 150 orbitals are filled with spin- \uparrow particles. Before flux insertion ($\lambda = 0$), there is a flat profile, but for finite values of λ , a quasi-hole of unit charge is created around the origin.

For large m , corresponding to a radius $r \gg 1/\lambda$, the adiabatic process boils down to a shift $|m \uparrow\rangle \rightarrow |m+1 \downarrow\rangle$. This follows directly from the Berry matrix calculation, but it can be understood simply from the conservation of $J_z = L_z + \frac{1}{2}\sigma_z$. At large distance the flux we insert is essentially a σ_z -flux quantum as in (4.34), and it induces a charge transfer $|m\rangle \rightarrow |m+1\rangle$, since all particles are spin- \uparrow , changing the angular momentum L_z by one unit. Then the only way to accommodate the conservation of J_z is through an accompanying spin flip $|\uparrow\rangle \rightarrow |\downarrow\rangle$.

We can analyze the effect of this adiabatic insertion on the product state by looking at the density and spin profile of the final state in (4.35). The density is given by

$$\rho(r; \lambda) = \sum_{m=0}^{m_f} \frac{r^{2m} e^{-r^2/2}}{2^m m! 2\pi} \left(u_m(\lambda)^2 + v_m(\lambda)^2 \frac{r^2}{2(m+1)} \right), \quad (4.36)$$

and is shown in fig. 4.3 for four different values of λ . The solid line is a flat profile and shows the droplet before insertion of the non-Abelian field configuration. Once the flux is inserted, charge is depleted from the origin and deposited at the edge of the droplet. This corresponds to exactly one unit of charge.

The expectation value of spin in the z -direction of these configurations is depicted in fig. 4.4. The state prior to flux insertion is the blue solid line, which has a trivial spin-

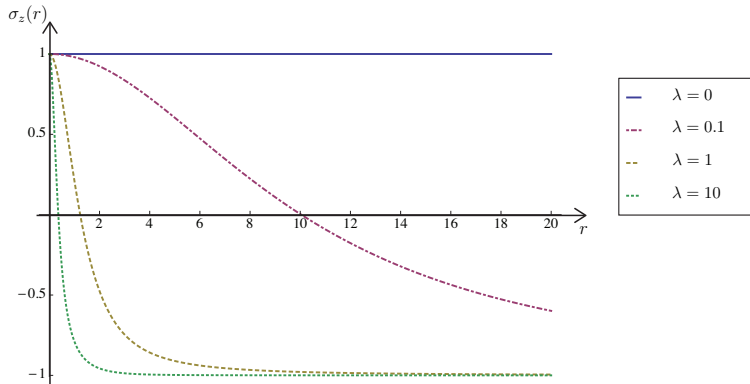


Figure 4.4: Expectation value of the z -component of the spin field in a product state where the initial state has its first 150 orbitals filled with spin- \uparrow particles. These profiles occur after insertion of non-Abelian flux, for different values of λ . An insertion of finite λ creates a nontrivial spin-texture. The radius at which the expectation value of σ_z equals zero is around $r \sim 1/\lambda$.

texture. Upon increasing λ , particles move one orbital out while flipping their spin. This motion starts at the outer edge of the sample and propagates towards the center. When the final value of λ has been reached, the particles constitute a spin-texture of size $1/\lambda$ with spin- \uparrow at the origin and spin- \downarrow at the edge of the droplet. Fig. 4.5a shows the spin field after inserting a flux parameterized by $\lambda = 1/3$. Fig. 4.5b displays the (x, y) -components of the spin field, showing that the spins have an in-plane winding number of 1.

The charged spin-texture created by the insertion of non-Abelian flux is recognized as a quantum Hall skyrmion of unit electric charge, $q = e$, and unit topological charge, $Q_{\text{top}} = 1$. The topological charge, given by the Pontryagin index Q_{top} , measures the winding of the spin vector around the system (see, for example, chapter 7 of ref. [128]). The plane can be mapped to a sphere by identifying the points at infinity with the south pole, resulting in a mapping of the spin field to the sphere characterized by the homotopy group $\pi_2(S^2) = \mathbb{Z}$.

The case $M = -1$

The second non-Abelian field configuration we will treat corresponds to the $M = -1$ case of the generic flux presented in appendix 4.D. We will insert the field adiabatically

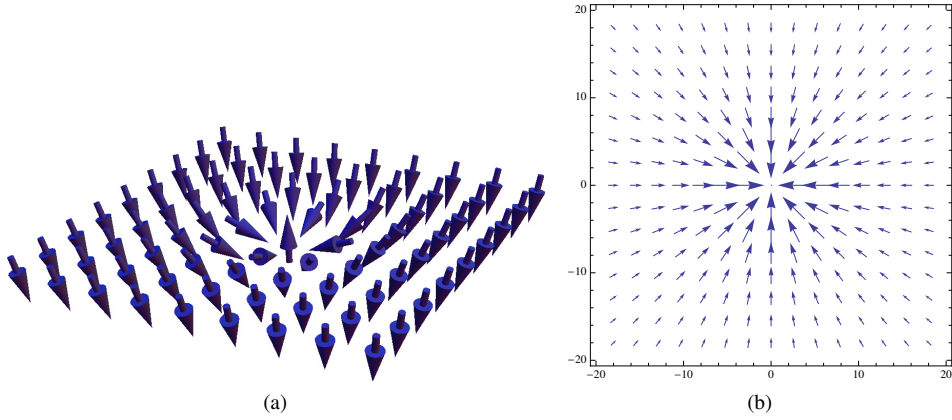


Figure 4.5: Spin-texture obtained after inserting non-Abelian flux with $\lambda = 1/3$. The three components of the spin field are shown in fig. (a). At the origin the spin points up and at the edge it points down. Fig. (b) depicts the x - and y -components of the spin field. These two figures clearly show that a skyrmion with in-plane winding 1 is created.

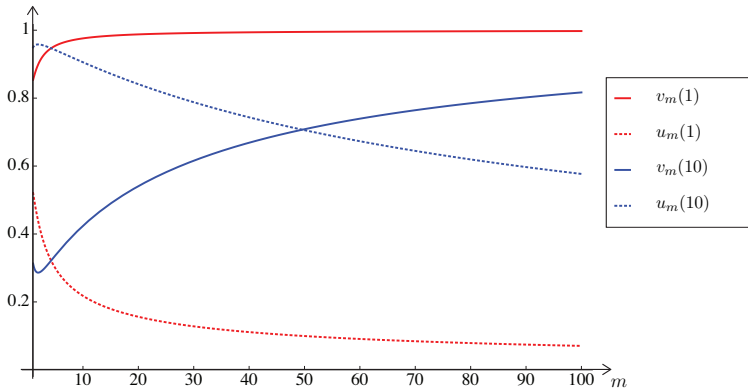


Figure 4.6: Mixing coefficients of (4.39) for two different values of the adiabatic parameter λ . The point where $u_m(\lambda) = v_m(\lambda)$ is around $m \sim \lambda^2/2$. The asymptotes of the coefficients are exactly opposite to the $M = 0$ case.

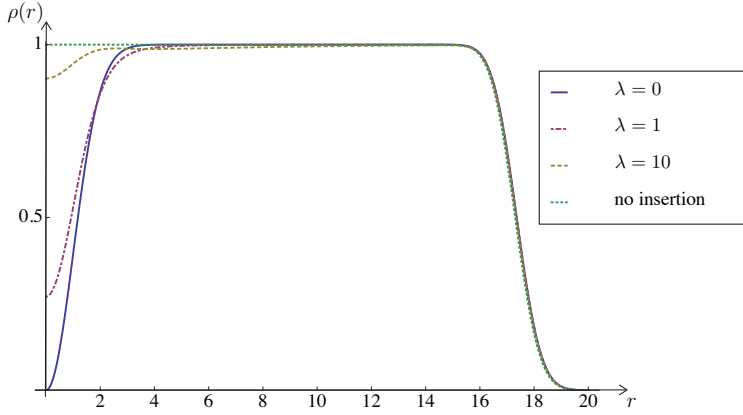


Figure 4.7: Density of a product state before and after flux insertion for different values of λ . The flat profile depicts the initial product state. For $\lambda = 0$ a σ_z -flux quantum is inserted creating a quasihole at the origin. At finite λ , there is still a density depletion around the origin, but it is less sharp.

into the initial setting of (4.30) and it is given by

$$\begin{aligned}\delta A_r(\lambda) &= \frac{\lambda}{\lambda^2 + r^2} \sigma_\phi \\ \delta A_\phi(\lambda) &= -\frac{r}{\lambda^2 + r^2} \sigma_z - \frac{\lambda}{\lambda^2 + r^2} \sigma_r.\end{aligned}\quad (4.37)$$

There is a subtlety which did not arise in the previously discussed configuration and which will shed light on why we label the different fields by an integer M . In this case $\delta A_\phi(0) = \frac{-1}{r} \sigma_z \neq 0$, which is the insertion of a σ_z -flux quantum, resulting in a shift of orbital number depending on the spin of the particle

$$|m \uparrow\rangle \rightarrow |m + 1 \uparrow\rangle, \quad |m \downarrow\rangle \rightarrow |m - 1 \downarrow\rangle. \quad (4.38)$$

The adiabatic process consists of two parts now. We start by adiabatically inserting a σ_z -flux quantum, leading to the configuration in (4.37) at $\lambda = 0$. After that we slowly sweep λ to its final value. Note that at every point of the adiabatic process we are able to find the eigenstates of the evolved Hamiltonian and therefore we know the Berry matrix. Again starting from a product state of spin- \uparrow particles and gauging back to the original

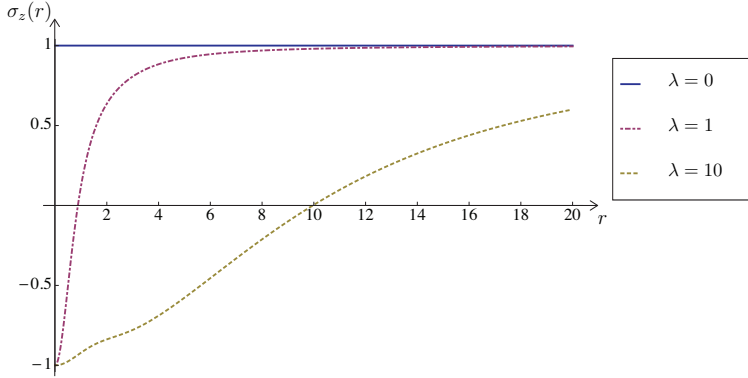


Figure 4.8: Expectation value of the z -component of the spin field, in a product state in (4.39) for different values of λ . The radius at which the state is unpolarized is around $r \sim \lambda$.

Hamiltonian after the adiabatic process we get a final state

$$|\psi_{-1}(\lambda)\rangle = \bigotimes_{m=0}^{m_f} \left(u_{m+1}(\lambda) |m+1 \uparrow\rangle - v_{m+1}(\lambda) |m \downarrow\rangle \right), \quad (4.39)$$

where the coefficients can be found in (4.75) and are plotted in fig. 4.6. The scale at which the spins are flipped is set by $r \sim \lambda$.

The density of the state in (4.39) is shown in fig. 4.7, before flux insertion, and for the values $\lambda = 0, 1, 10$. Again charge is depleted from the origin, but this time the depth of the hole is largest for $\lambda = 0$, i.e. after the insertion of a σ_z -flux quantum. Upon increasing λ , particles move inward while flipping their spin. This motion starts at the origin and moves out towards the edge of the sample. The resulting spin-texture is depicted in figs. 4.8 and 4.9. The electric charge $q = e$ is the same as for $M = 0$, but the topological charge $Q_{\text{top}} = -1$ has opposite sign.

Before we turn to the conclusions of this chapter, we would like to remark on the non-triviality of the final state after a flux insertion. At first sight it may seem that the system should stay trivial, as we are always a gauge transformation away from the original setup. Recall that a changing flux induces an electric field. So even though the magnetic field does not change due to the flux insertion and we are always a gauge transformation away from the initial state, there is an electric field that acts on the charges of the system, causing the nontrivial charged spin-texture.

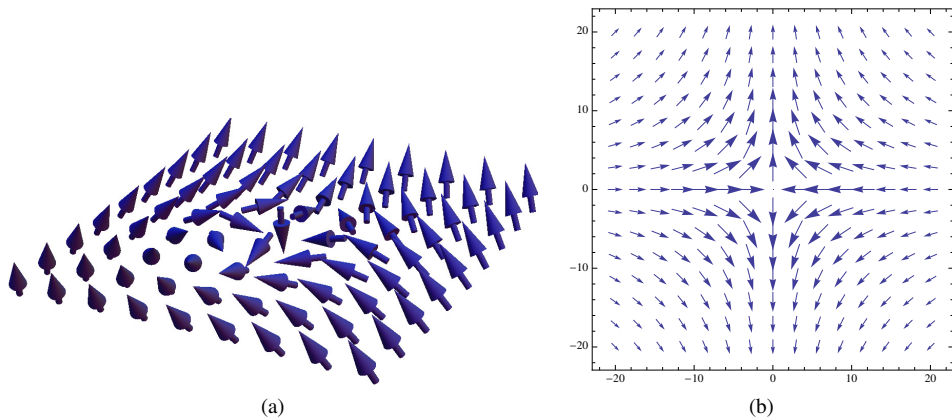


Figure 4.9: Fig. (a) shows the spin field for a final state labeled by $\lambda = 5$. At the origin the spin is pointing down, at the edge it points up. Fig. (b) shows the x - and y -components of the same spin field, from which we see that this flux insertion creates a skyrmion with in-plane winding number -1 .

In this chapter we solved the non-Abelian Landau problem on the sphere, and analyzed the charge and spin dynamics induced by the insertion of non-Abelian flux in an otherwise Abelian background. Let us end now with a few remarks.

In the usual (Abelian) QH setting, skyrmions arise due to a balance between the effects of the Zeeman energy, which favors single overturned spins, and the Coulomb interaction, which favors configurations with small spin-gradients [129]. It is quite remarkable that our procedure of driving the noninteracting polarized electron gas with non-Abelian external flux leads to the very same skyrmion configurations.

Repeating the non-Abelian flux insertion in a background of a $\nu = 2$ IQH state, with both the spin- \uparrow and spin- \downarrow LLLs completely filled, has a very different effect. In this case, the bulk state cannot accommodate any spin-flips and the effects of the flux insertion are limited to the edges. Inserting non-Abelian flux through the central hole in a Corbino disc leads to neutral $S_z = \pm 1$ excitations at both the inner and the outer edge. This situation is in many ways reminiscent of a thought experiment, where a minimal amount of Abelian flux inserted into a two-dimensional quantum spin Hall topological phase acts as a spin pump, resulting in neutral $S_z = \pm 1/2$ excitations at the edges [33].

The details of the charge and spin dynamics associated to the insertion of non-Abelian flux depend on the specific form of our gauge potentials and on the way these depend

on the sweep-parameter λ . One expects that many features, in particular the topological quantum numbers characterizing the resulting spin-textures, will be robust against changes in the detailed shape of the external gauge potentials.

Appendix

4.A Landau levels on the plane

For the purpose of being self-contained, and also in order to fix notations, we recall the main results of the Landau problem on the plane. Some aspects have been discussed in chapter 1 as well, but we will go into more detail here.

We consider a particle of charge q and mass m confined to a plane, under an external perpendicular magnetic field $\mathbf{B} = B\hat{z}$ (with $qB > 0$). We choose the symmetric gauge

$$\mathbf{A} = \frac{B}{2} \begin{pmatrix} -y \\ x \\ 0 \end{pmatrix} = \frac{Br}{2} \hat{\phi}, \quad (4.40)$$

which behaves as a vector under rotations around \hat{z} . The only scale of the classical problem is the cyclotron frequency ω_c

$$\omega_c = \frac{qB}{m}. \quad (4.41)$$

The quantum mechanical problem has an additional scale, the magnetic length ℓ

$$\ell = \sqrt{\frac{\hbar}{qB}}. \quad (4.42)$$

The Hamiltonian in the symmetric gauge reads

$$H = \frac{1}{2}\omega_c \left(\left(-i\ell\partial_x + \frac{y}{2\ell} \right)^2 + \left(-i\ell\partial_y - \frac{x}{2\ell} \right)^2 \right). \quad (4.43)$$

It is very convenient to go to complex coordinates (rescaled by the magnetic length), and to introduce two commuting families of creation and annihilation operators

$$a = \sqrt{2} \left(\bar{\partial} + \frac{z}{4} \right) \quad a^\dagger = \sqrt{2} \left(-\partial + \frac{\bar{z}}{4} \right) \quad (4.44)$$

$$b = \sqrt{2} \left(\partial + \frac{\bar{z}}{4} \right) \quad b^\dagger = \sqrt{2} \left(-\bar{\partial} + \frac{z}{4} \right), \quad (4.45)$$

where $\partial = \frac{\partial}{\partial z}$ and $\bar{\partial} = \frac{\partial}{\partial \bar{z}}$. In this notation the Hamiltonian and angular momentum take the following form

$$H = \omega_c \left(a^\dagger a + \frac{1}{2} \right), \quad L_z = b^\dagger b - a^\dagger a, \quad (4.46)$$

from which the spectrum $E_n = \omega_c(n + 1/2)$ follows immediately. Since b and b^\dagger commute with the Hamiltonian, states labeled by different eigenvalues of L_z are infinitely degenerate. The subspace of energy $E_n = \omega_c(n + 1/2)$ is called the n th LL.

Denoting by n and m the eigenvalues of $a^\dagger a$ and $b^\dagger b$ respectively, the Hilbert space is spanned by the states $|n, m\rangle$ for $n, m \geq 0$. The quantum number m is related to the value of the angular momentum as follows $L_z|n, m\rangle = (m - n)|n, m\rangle$. The explicit form of the wave functions is known and involves a special class of functions called Hermite polynomials. Here we focus on the LLL $n = 0$, which is obtained by acting with b^\dagger on the state $|0, 0\rangle$

$$|0, m\rangle = \frac{(b^\dagger)^m}{\sqrt{m!}} |0, 0\rangle \rightarrow \langle z|0, n\rangle = \frac{1}{\sqrt{2\pi}} \frac{z^m}{\sqrt{2^m m!}} \exp(-z\bar{z}/4). \quad (4.47)$$

4.B Landau levels on the sphere

In this section of the appendix we will state the main results of the Landau problem on the sphere, and set $q = \hbar = 1$.

Field configuration: magnetic monopole

On the sphere, a uniform perpendicular magnetic field $\mathbf{B}(\mathbf{r}) = \frac{N_\Phi}{2r^2} \hat{r}$ implies the presence of a magnetic monopole at the center of the sphere, and the potential $\mathbf{A}(\mathbf{r})$ must have a Dirac string, as we already encountered in section 1.1. The gauge where the singularity lies at the south pole

$$\mathbf{A} = \frac{N_\Phi}{2} \frac{1 - \cos(\theta)}{r \sin(\theta)} \hat{\phi}, \quad (4.48)$$

and the gauge where the singularity lies at the north pole

$$\mathbf{A} = -\frac{N_\Phi}{2} \frac{1 + \cos(\theta)}{r \sin(\theta)} \hat{\phi}, \quad (4.49)$$

are related by the unitary transformation $U = e^{iN_\Phi\phi}$, which implies that N_Φ has to be an integer.

Hamiltonian and spectrum

The Hamiltonian of a particle confined to the sphere of radius r in the background of such a magnetic monopole is

$$H = \frac{\mathbf{\Lambda}^2}{2mr^2}, \quad \text{with } \mathbf{\Lambda} = \mathbf{r} \times (\mathbf{p} - \mathbf{A}). \quad (4.50)$$

The operators Λ_a have the following (gauge invariant) commutation relations

$$[\Lambda_a, \Lambda_b] = i\epsilon_{abc}(\Lambda_c + (\mathbf{r} \cdot \mathbf{B})r_c), \quad (4.51)$$

and the generators of (magnetic) rotations have the form

$$\mathbf{L} = \mathbf{\Lambda} - (\mathbf{r} \cdot \mathbf{B})\mathbf{r} = \mathbf{\Lambda} - \frac{N_\Phi}{2}\hat{r}. \quad (4.52)$$

They generate an $SU(2)$ algebra

$$[L_a, L_b] = i\epsilon_{abc}L_c, \quad (4.53)$$

and the Hamiltonian can be expressed as a Casimir \mathbf{L}^2 . Indeed the relation

$$\mathbf{\Lambda}^2 = \mathbf{L}^2 - \left(\frac{N_\Phi}{2}\right)^2, \quad (4.54)$$

ensures that all L_a commute with the Hamiltonian and gives the spectrum of the Hamiltonian

$$E_l = \frac{1}{2mr^2} \left(l(l+1) - \left(\frac{N_\Phi}{2}\right)^2 \right). \quad (4.55)$$

The last statement simply comes from the $SU(2)$ algebra obeyed by L_a , which forces the eigenvalues of \mathbf{L}^2 to be of the form $l(l+1)$ where $l \in \frac{1}{2}\mathbb{N}$. However, not all the values of l are part of the physical spectrum. Using the explicit expression of \mathbf{L} , Wu and Yang [126,127] obtained the following decomposition of the Hilbert space into irreducible

representations of the $SU(2)$ algebra generated by \mathbf{L}

$$\mathcal{H} = \left(\frac{N_\Phi}{2}\right) \oplus \left(\frac{N_\Phi}{2} + 1\right) \oplus \cdots \oplus \left(\frac{N_\Phi}{2} + n\right) \oplus \cdots \quad (4.56)$$

and the (Abelian) spectrum on the sphere reads

$$E_n = \frac{1}{2mr^2} \left(n(N_\Phi + n + 1) + \frac{N_\Phi}{2} \right), \quad n \geq 0. \quad (4.57)$$

4.C Details about the non-Abelian field on the sphere

In this section of the appendix we derive the spectrum of the Hamiltonian

$$H(\alpha) = \frac{1}{2mr^2} \left[\mathbf{r} \times (\mathbf{p} - \mathbf{A}(\alpha)) \right]^2, \quad (4.58)$$

which describes a particle confined to a sphere of radius r in the non-Abelian background potential

$$\mathbf{A}(\alpha) = \mathbf{A}_{\text{Ab}} + \alpha \frac{\mathbf{r} \times \boldsymbol{\sigma}}{r^2}, \quad (4.59)$$

where \mathbf{A}_{Ab} is the $U(1)$ potential given in (4.48). Note that there is a gauge transformation mapping $\alpha \rightarrow 1 - \alpha$ implemented by the unitary transformation $U = \hat{r} \cdot \boldsymbol{\sigma} = \sigma_r$.

Rotational symmetry and decomposition of the Hilbert space

There are two sets of $SU(2)$ generators in this problem:

- (i) the usual (Abelian) action on the coordinates implemented by $\mathbf{L} = \mathbf{r} \times (\mathbf{p} - \mathbf{A}_{\text{Ab}}) - \frac{N_\Phi}{2} \hat{r}$ defined in (4.52),
- (ii) the rotations in spin space generated by $\mathbf{S} = \frac{1}{2} \boldsymbol{\sigma}$.

The Hamiltonian we are considering is not invariant under \mathbf{L} and \mathbf{S} separately. However, it is a scalar under global rotations generated by $\mathbf{J} = \mathbf{L} + \mathbf{S}$, as can be seen from the expansion in terms of \mathbf{J}

$$H(\alpha) = \frac{1}{2mr^2} \left[\mathbf{J}^2 + \frac{1}{4} - 2\alpha(1 - \alpha) + (2\alpha - 1) \left(\mathbf{J} \cdot \boldsymbol{\sigma} - \frac{1}{2} + \frac{N_\Phi}{2} U \right) + \frac{N_\Phi}{2} U \right]. \quad (4.60)$$

Therefore this Hamiltonian is block diagonal with respect to the decomposition of the Hilbert space into irreducible representations of \mathbf{J} . This decomposition follows directly

from the Abelian one in (4.56)

$$\mathcal{H} = \left(\frac{N_\Phi - 1}{2} \right) \oplus 2 \left(\frac{N_\Phi + 1}{2} \right) \oplus 2 \left(\frac{N_\Phi + 3}{2} \right) \oplus 2 \left(\frac{N_\Phi + 5}{2} \right) \oplus \dots \quad (4.61)$$

Spectrum

Working in the subspace $\mathbf{J}^2 = j(j+1)$, we simply need to diagonalize the term $X = (2\alpha - 1) (\mathbf{J} \cdot \boldsymbol{\sigma} - \frac{1}{2} + \frac{N_\Phi}{2} U) + \frac{N_\Phi}{2} U$. We first derive the following two relations

$$\{U, (\mathbf{J} \cdot \boldsymbol{\sigma} - \frac{1}{2} + \frac{N_\Phi}{2} U)\} = 0 \quad (4.62)$$

$$(\mathbf{J} \cdot \boldsymbol{\sigma} - \frac{1}{2})^2 = \mathbf{J}^2 + \frac{1}{4}. \quad (4.63)$$

The first one is a consequence of the gauge equivalence $UH(\alpha)U = H(1 - \alpha)$, and the second one can be checked using the explicit form of \mathbf{J} . From this we deduce that X^2 is a constant

$$X^2 = (2\alpha - 1)^2 (\mathbf{J}^2 + \frac{1}{4}) + \alpha(1 - \alpha)N_\Phi^2, \quad (4.64)$$

and we get the following spectrum for X

$$\lambda_{(j)}^\pm = \pm \sqrt{(2\alpha - 1)^2 \left((j + \frac{1}{2})^2 - (\frac{N_\Phi}{2})^2 \right) + (\frac{N_\Phi}{2})^2}. \quad (4.65)$$

As can be seen in (4.17), for $j \geq \frac{N_\Phi + 1}{2}$ there are two representations of spin- j . However there is a unique representation of spin $j = \frac{N_\Phi - 1}{2}$. Rewriting $j = n + \frac{N_\Phi - 1}{2}$, we get the following spectrum for the Hamiltonian

$$E_0(\alpha) = \frac{1}{2mr^2} \left(\frac{N_\Phi}{2} - 2\alpha(1 - \alpha) \right) \quad (4.66)$$

$$E_n^\pm(\alpha) = \frac{1}{2mr^2} \left(n(N_\Phi + n) - 2\alpha(1 - \alpha) \pm \sqrt{(2\alpha - 1)^2 n(N_\Phi + n) + (\frac{N_\Phi}{2})^2} \right). \quad (4.67)$$

4.D Generic non-Abelian field configuration

In this appendix, we give a detailed derivation of the final state obtained after an adiabatic insertion of non-Abelian flux into a background given in (4.30). This is done for the generic case of which two specific examples are discussed in section 4.2. The field configuration we insert is the following

$$\begin{aligned}\delta A_r(\lambda) &= - \left(M + \frac{1}{2} \right) \frac{2\lambda r^{2M}}{1 + \lambda^2 r^{2+4M}} \sigma_\phi \\ \delta A_\phi(\lambda) &= \left(M + \frac{1}{2} \right) \frac{1 - \lambda^2 r^{2+4M}}{1 + \lambda^2 r^{2+4M}} \frac{1}{r} \sigma_z + \left(M + \frac{1}{2} \right) \frac{2\lambda r^{2M}}{1 + \lambda^2 r^{2+4M}} \sigma_r - \frac{1}{2r} \sigma_z ,\end{aligned}\tag{4.68}$$

where M can be interpreted as the number of σ_z -flux quanta inserted, which will be explained below (4.70). When we insert this field the Hamiltonian can be expressed as $H_M(\lambda) = U_M(\lambda)H(0)U_M^\dagger(\lambda)$, where

$$U_M(\lambda) = \frac{1}{\sqrt{1 + \lambda^2 r^{2+4M}}} \begin{pmatrix} 1 & -\lambda \bar{z} r^{2M} \\ \lambda z r^{2M} & 1 \end{pmatrix} \exp(iM\phi\sigma_z) .\tag{4.69}$$

At every point of the adiabatic process we know the LLL eigenstates of the evolved Hamiltonian, and they are given by

$$|\alpha(\lambda)\rangle = U_M(\lambda)|m, \epsilon\rangle .\tag{4.70}$$

Before we proceed with calculating the Berry matrix an important subtlety needs to be considered. We wish to insert this field configuration into a background given in (4.30). But at $\lambda = 0$ and for $M \neq 0$ (4.68) is given by $\delta A_\phi(0) = (M/r)\sigma_z \neq 0$, which means we have to start by adiabatically inserting M σ_z -flux quanta, resulting in a shift of the orbitals depending on the spin of the particle

$$|m \uparrow\rangle \rightarrow |m - M \uparrow\rangle , \quad |m \downarrow\rangle \rightarrow |m + M \downarrow\rangle .\tag{4.71}$$

After the insertion of these σ_z -flux quanta, we slowly sweep λ from zero to some final value resulting in (4.68). Now we can use the eigenstates in (4.70) to compute the Berry

connection

$$\mathcal{A}_{\alpha,\beta} \equiv i\langle\alpha(\lambda)|\frac{d}{dt}|\beta(\lambda)\rangle = i\langle\alpha(0)|U_M^\dagger\dot{U}_M|\beta(0)\rangle, \quad (4.72)$$

where

$$iU_M^\dagger\dot{U}_M = \frac{i\dot{\lambda}}{1 + \lambda^2 r^{2+4M}} \begin{pmatrix} 0 & -\dot{z}^{2M+1} \\ z^{2M+1} & 0 \end{pmatrix}. \quad (4.73)$$

The Berry connection only has nonzero elements between states of the form $\{U_M(\lambda)|m \uparrow\rangle, U_M(\lambda)|m + 2M + 1 \downarrow\rangle\}$. Written in this basis, for every m the Berry matrix is a 2×2 matrix

$$U_B^m = \cos(\theta_m^{(M)}(\lambda))\mathbb{I} + i\sin(\theta_m^{(M)}(\lambda))\sigma_y, \quad (4.74)$$

where the angle is given by

$$\theta_m^{(M)}(\lambda) = \int_0^\infty dr \arctan(\lambda r^{1+2M}) \frac{r^{2+2M+2m} e^{-r^2/2}}{2^{m+M} \sqrt{2m!(m+2M+1)!}}. \quad (4.75)$$

This angle has interesting asymptotes in two different limits

$$\lim_{m \rightarrow \infty} \theta_m^{(M)} = \arctan(\lambda(2m)^{M+1/2}) \quad (4.76)$$

$$\lim_{\lambda \rightarrow \infty} \theta_m^{(M)} = \frac{\pi}{2} \frac{\Gamma(m+M+3/2)}{\sqrt{m!(m+2M+1)!}}. \quad (4.77)$$

After the adiabatic insertion of flux we gauge the system back to the initial one. This cycle has the following effect on a single particle state $|m \uparrow\rangle$

$$U_M^\dagger(\lambda)U_B^m(\lambda)U_M(\lambda)|m \uparrow\rangle = u_m^{(M)}(\lambda)|m \uparrow\rangle - v_m^{(M)}(\lambda)|m + 2M + 1 \downarrow\rangle, \quad (4.78)$$

where the mixing coefficients are expressed in terms of (4.75)

$$u_m^{(M)}(\lambda) \equiv \cos(\theta_m^{(M)}(\lambda)), \quad v_m^{(M)}(\lambda) \equiv \sin(\theta_m^{(M)}(\lambda)). \quad (4.79)$$

We can see that the equality in (4.78) holds by inserting unity

$$\mathbb{I} = \sum_{m', \epsilon} U_M(\lambda) |m', \epsilon\rangle \langle m', \epsilon| U_M^\dagger(\lambda), \quad (4.80)$$

between U_M^\dagger and U_B^m . After deducing the effect of the two stages of the adiabatic process, we can combine them to find the final state.

Before we give the final state, one last remark needs to be made. Since we want to stay in the LLL, we have to put the state on a Corbino disc, meaning that we fill the orbitals of the initial product state with spin- \uparrow particles starting from some initial orbital m_i up to a final orbital m_f . The two specific adiabatic flux insertions given in section 4.2 are actually the only two situations for which the Corbino disc is not a necessary geometry for staying in the LLL.

Starting from a product state on a Corbino disc where the orbitals are filled with spin- \uparrow particles, the final state after first adiabatically inserting M σ_z -flux quanta, then cranking up the value of λ in (4.68), and finally gauging back to the initial configuration, is given by

$$|\psi_M(\lambda)\rangle = \bigotimes_{m=m_i}^{m_f} \left(u_{m-M}^{(M)}(\lambda) |m - M \uparrow\rangle - v_{m-M}^{(M)}(\lambda) |m + 1 + M \downarrow\rangle \right). \quad (4.81)$$

CHAPTER 5

Topological symmetry breaking: Domain walls and an instability of chiral edges

This chapter is based on unpublished work:

F.A. Bais and S.M. Haaker, TOPOLOGICAL SYMMETRY BREAKING: DOMAIN WALLS AND PARTIAL INSTABILITY OF CHIRAL EDGES, arXiv:1407.5790.

After focusing on one-particle models in chapters 3 and 4, we now turn to the characteristics of the collective behavior of topological phases that result from underlying interactions between the basic degrees of freedom. In chapter 2 we gave an introduction to such phases where we showed how the topological excitations of these phases and their fusion and braiding interactions form an anyonic model. The FQH phases probably are the most studied of these and we showed how the Abelian states can be expressed in terms of Wen's K matrix stemming from a CS theory in the bulk. These states as well as many non-Abelian states allow for a CFT description, where the gapless edge modes correspond to CFT vertex operators and the bulk wave functions can be expressed as correlators of these same operators. This bulk-boundary correspondence strongly suggests that as long as the bulk is topologically ordered, no perturbations can destroy the chiral gapless edge theory. For nonchiral edges there is the possibility of counter-propagating edge modes gapping out, and a criterium for stable edges is given in terms of a Lagrange subgroup criterion [130, 131], which has recently also been formulated in terms of so-called symmetry enriched phases [132–135].

In the current chapter, we point out a particular incompleteness of this picture. We show that a careful treatment of the problem necessarily has to take into account the possibility of Bose condensation in the bulk corresponding to TSB. This formalism has been presented in section 2.2, and it describes phase transitions between different topologically ordered phases due to the condensation of bosonic quasiparticles breaking the quantum group symmetry. Here we will show how simple chiral models corresponding to specific Laughlin states may be unstable due to TSB and decay into a different topological phase.

The simplest of these are states describing QH fluids at filling fractions $\nu = 1/8$ and $\nu = 1/9$.

The second part of this chapter will be devoted to showing how a careful treatment of TSB gives rise to a degeneracy in vacuum states in the broken phase. This eventually results in a spontaneous breaking of the symmetry when the system chooses one of these vacua as its ground state. This picture allows for the possibility of different domains within one broken phase and we give a description of the domain walls between them. It turns out that the stability of such a wall is related to the presence of particles that are confined in the bulk and therefore expelled to the boundary. These particles are not confined at the boundary, but they do acquire a mass as solitons. This mechanism is interesting because it shows that gapping out by creating a conventional mass term and therefore breaking the chiral symmetry, is not the only way to create massive excitations.

5.1 Unstable chiral $U(1)$ states

As explained in section 2.3 many FQH states have a CFT description. In this chapter we focus on the Laughlin states, which describe Abelian FQH liquids at filling fraction $\nu = 1/M$, where M is a positive integer. For M even it is a bosonic system and for M odd fermionic. The Laughlin states have a description in terms of fairly simple chiral CFTs, namely the compactified boson. In appendix 5.A we will derive the spectrum of this CFT and show for which particular compactification radii the theory becomes rational, i.e. containing a finite number of primary fields under an extended algebra. Appendix 5.B will be devoted to the quantum numbers of the bosonic and fermionic Laughlin states and how they can be expressed in terms of this chiral CFT. In the present section we show which Laughlin states can be driven through a transition by applying TSB, treating the bosonic and fermionic cases separately.

5.1.1 Unstable bosonic Laughlin states

In appendix 5.B.1 we illustrate how the topological excitations of the bosonic Laughlin state at filling fraction $\nu = 1/M$ can be described by a $U(1)_{M/2}$ theory. We will now show that phases with filling fraction

$$\nu = \frac{1}{M} = \frac{1}{2l^2k}, \quad l = 2, 3, \dots, \quad k = 1, 2, \dots, \quad (5.1)$$

have at least one nontrivial boson that can drive a transition to a broken phase carrying less sectors.

The initial phase is $\mathcal{A} = U(1)_{l^2k}$, corresponding to a chiral boson compactified at

radius $R = l\sqrt{2k}$, which has $2l^2k$ sectors with spins

$$h_n = \frac{n^2}{4l^2k}, \quad n = 0, 1, \dots, 2l^2k - 1. \quad (5.2)$$

It contains a nontrivial bosonic sector $b = 2lk$, which has spin $h_b = k$. When this boson forms a condensate, the other sectors arrange in orbits of length l under fusion with the boson

$$n \sim n + 2lk \sim \dots \sim n + 2lk(l - 1), \quad (5.3)$$

which means that the sectors belonging to the same orbit get identified with each other as they are equal up to fusion with the condensate. This results in an intermediate phase \mathcal{T} which carries excitations with fusion rules \mathbb{Z}_{2lk} .

As we saw in section 2.2 these sectors in general do not have well-defined braiding interactions. To check which sectors become confined in the broken phase, we consider the monodromy of a sector n with the boson

$$M_{n,b} = h_{n+b} - h_n - h_b = \frac{n}{l}. \quad (5.4)$$

Clearly, the unconfined sectors can be expressed as $n = ml$, where $m = 0, 1, \dots, 2k - 1$ and we see that they have spin $h_m = \frac{m^2}{4k}$. This we recognize as the sectors of a compactified boson at radius $R = \sqrt{k}$, so the broken unconfined phase is $\mathcal{U} = U(1)_k$. Of course if this k is again of the form $k = l^2k'$ there will be other bosons left in the theory, which can also condense.

We observe that the highest unstable filling fractions occur at $\nu = 1/8, 1/16, 1/18, \dots$. We must conclude that even though they are chiral theories, i.e. protected from back-scattering, the edge current is not entirely protected since a condensate can form. Nevertheless, there are channels that are still protected, so there should still be a current along the edge.

Example $l = 2, k = 1$

We will work out one specific example of an unstable bosonic Laughlin state, which describes a QH liquid at filling fraction $\nu = 1/8$. The reason for this is twofold: it will shed some light on the general procedure described above, and we will use this particular state at length in the second part of this chapter.

We start from a phase with $\mathcal{A} = U(1)_4$, which corresponds to a compactified chiral boson at radius $R = 2\sqrt{2}$. There are eight sectors in the theory which are labeled by $n = 0, \dots, 7$. The conformal weights are $h_n = \frac{n^2}{16}$ and the sector $n = 4$ has spin $h_4 = 1$,

which is the only nontrivial boson in this theory. When it condenses the original sectors get identified in the following way

$$0 \sim 4 \tag{5.5}$$

$$1 \sim 5 \tag{5.6}$$

$$2 \sim 6 \tag{5.7}$$

$$3 \sim 7 . \tag{5.8}$$

The intermediate phase \mathcal{T} carries four sectors which have \mathbb{Z}_4 fusion rules. The only sector that is local with respect to the condensate is labeled by $n = 2$, therefore we end up with a broken unconfined phase described by $\mathcal{U} = U(1)_1$.

5.1.2 Unstable fermionic Laughlin states

The same analysis can be performed for the fermionic Laughlin states. In appendix 5.B.2 we show that a state at $\nu = 1/M$ for odd M , has sectors belonging to $U^+(1)_{2M}$. As we will demonstrate now for filling fraction

$$\nu = \frac{1}{M} = \frac{1}{l^2 k}, \quad l = 3, 5, \dots, \quad k = 1, 3, \dots, \tag{5.9}$$

a phase transition can occur.

Starting from $\mathcal{A} = U^+(1)_{2l^2 k}$ corresponding to a chiral boson compactified at radius $R = l\sqrt{k}$, there are $2l^2 k$ sectors with spins

$$h_n = \frac{n^2}{2l^2 k}, \quad n = 0, 1, \dots, 2l^2 k - 1 . \tag{5.10}$$

The charge e fermion is given by $f = l^2 k$ and has spin $h_f = l^2 k/2$. There is a nontrivial boson in this theory $b = 2lk$, which has spin $h_b = 2k$. When these particles form a condensate the original \mathcal{A} sectors rearrange into orbits of length l identical to (5.3). The broken intermediate phase has fusion rules $\mathcal{T} = \mathbb{Z}_{2lk}$ and the monodromy of these sectors with the bosonic particle is

$$M_{n,b} = \frac{2n}{l} . \tag{5.11}$$

The unconfined particles are those for which $n = ml$ with $m = 0, 1, \dots, 2k - 1$ and their spins are given by $h_m = \frac{m^2}{2k}$. They form a broken unconfined phase $\mathcal{U} = U^+(1)_{2k}$ at

radius $R = \sqrt{k}$, corresponding to a fermionic Laughlin state at filling fraction $\nu = 1/k$. The highest fractions at which this occurs are $\nu = 1/9, 1/25, 1/27, \dots$. For instance, the state at $\nu = 1/9$ breaks to a Laughlin state at $\nu = 1$, which is an IQH phase.

In this first section we showed that simple chiral models are not completely stable. Even though the edge modes are protected from backscattering, some of these models have a nontrivial bosonic sector in its spectrum, which may form a condensate. Topological charge is no longer conserved and certain sectors may disappear into the new vacuum or become confined.

5.2 Domain walls and confinement

In the previous section we applied TSB to drive a phase transition from a Laughlin state, which describes an Abelian FQH liquid at filling fraction $\nu = 1/M$, to another Laughlin state at larger filling fraction. In this section we wish to take a closer look at the nature of the confined particles. We know that they must be expelled from the bulk of a broken phase, but what happens at the boundary? Moreover, we will demonstrate that different domains can appear in the broken \mathcal{U} phase and show how the confined particles play a prominent role in the stability of the domain walls separating different domains.

5.2.1 Vertex operators and Wilson loops

To be definite and explicit we will consider the specific example of an unstable bosonic Laughlin state at $\nu = 1/8$. In subsection 5.2.5 we will comment on how to generalize this to other unstable Laughlin states presented in the previous section.

Instead of simply considering the distinct topological sectors and their quantum numbers, we will cast them in a more familiar CFT form. The bulk is described by a $U(1)$ CS field at level $k = 8$ and the edge has gapless edge modes corresponding to a chiral boson theory compactified at radius $R = \sqrt{8}$. In the bulk the CS field can be written as a pure gauge $a_i(z) = \partial_i \phi(z)$, but on the boundary there are dynamical degrees of freedom corresponding to $U(1)_4$. The mode expansion of $\phi(x)$ compactified on a radius $R = \sqrt{8}$ on a cylinder of circumference L is

$$\phi(x) = \frac{2\pi\hat{N}}{\sqrt{8}L} x + \sqrt{8} \hat{\chi} + \text{oscillator modes} , \quad (5.12)$$

where x is the spatial coordinate along the edge, and we will discard the oscillator modes as we are only interested in the distinct topological sectors. The conserved current $\partial_x \phi$ leads to a conserved charge $\frac{1}{2\pi R} \int_0^L \partial_x \phi dx = \hat{N}/R^2$. The charge operator and the zero mode have commutation relations $[\hat{\chi}, \hat{N}] = i$.

Let us define several operators that play a crucial role in our subsequent analysis.

The operators that create a localized topological charge are the normal ordered vertex operators

$$V_n(x) =: e^{i \frac{n}{\sqrt{8}} \phi(x)} : , \quad (5.13)$$

where we will omit writing the normal ordering symbol from now on. The vertex operators are invariant under $\phi(x) \rightarrow \phi(x) + 2\pi R$, have conformal weights $h_n = \frac{n^2}{16}$ and transform under the global symmetry $\phi(x) \rightarrow \phi(x) + f$ as irreps: $V_n \rightarrow e^{inf/R} V_n$. The operators that measure charge take the form of a Wilson loop, a nonlocal object defined as

$$W_q = \exp \left[\frac{iq}{\sqrt{8}} \int_{-L/2}^{L/2} a_x dx \right] = e^{2\pi i q \hat{N}/8} . \quad (5.14)$$

It is the exponentiated conserved global charge operator which is invariant under the global $U(1)$ symmetry. Note that this operator can be extended to the bulk where it becomes *locally* gauge invariant under the transformation $\phi(z) \rightarrow \phi(z) + f(z)$ for any value of q , and we will use it at various values of q to probe the phase structure of the theory later on.

It is also interesting to consider open Wilson line operators

$$W_q(x_1, x_2) = \exp \left[\frac{iq}{\sqrt{8}} \int_{x_1}^{x_2} \partial_x \phi(x) dx \right] , \quad (5.15)$$

which are still invariant under the global $U(1)$ symmetry, but if extended to the bulk are not invariant under the local $U(1)$. For our analysis, an interesting gauge invariant operator is obtained by attaching quasiparticles represented by vertex operators to these Wilson lines with an integer value $q = n$

$$V_n(z_1) W_n(z_1, z_2) V_n^\dagger(z_2) . \quad (5.16)$$

From this expression it follows naturally that a quasiparticle of charge n cannot exist alone. There is always an antiparticle present and they are connected by a Wilson line which in the present case is just a Dirac string, a gauge artifact that can be moved around without changing the physics. This reflects the bulk-boundary correspondence: if we want to insert a single quasiparticle in the bulk there has to be an antiparticle somewhere on the boundary too.¹

¹The bulk-boundary correspondence is usually motivated by demanding charge neutrality.

Let us return to the edge theory. We label the distinct topological charge sectors by $n = 0, \dots, 7$, which are the eigenvalues of \hat{N} and they can be created using the operators

$$\bar{V}_n = \exp \left[i \frac{n}{\sqrt{8}L} \int_{-L/2}^{L/2} \phi(x) dx \right] = e^{in\hat{x}}. \quad (5.17)$$

These are nonlocal operators that act on the vacuum state as $\bar{V}_n|0\rangle = |n\rangle$ and commute with the charge operators as $[\hat{N}, \bar{V}_n] = n\bar{V}_n$, so they act as ladder operators on the charge eigenstates

$$\bar{V}_n|n'\rangle = |n+n'\rangle \pmod{8}. \quad (5.18)$$

The eight topological sectors form irreps of a global \mathbb{Z}_8 group generated by $W_1 = e^{\frac{2\pi i}{8}\hat{N}}$ ($W_1^8 = 1$) and the ground state $|0\rangle$ is unique. The algebra of the operators that create a unit of charge and measure charge is

$$W_m V_n = V_n W_m e^{2\pi n m i/8}, \quad (5.19)$$

which holds for both \bar{V}_n and $V_n(x)$.

Now that we have presented the relevant operator content of the chiral compactified boson of the \mathcal{A} theory, we will move to a description of the formation of a condensate in this context.

5.2.2 Vacuum expectation value and ground state degeneracy

We are interested in which part of the topological structure of the bulk and boundary theory is preserved and what novel structures we may encounter if we assume that some nontrivial operator condenses. Phase transitions are usually accompanied by some order parameter obtaining a finite expectation value in the new phase, and the operators we have at our disposal are the vertex operators. Clearly, in the unbroken phase \mathcal{A} they all have vanishing vacuum expectation value, but in the broken phase we will assume that for some V_b we have

$$|\langle V_b \rangle|^2 \neq 0. \quad (5.20)$$

This implies that the ground state should be of the form

$$|n\rangle_b = \sum_t c_t |n+tb\rangle, \quad (5.21)$$

where t is an integer and c_t some coefficient, which should be chosen such that the states form an orthonormal set. In addition we require this new ground state to be invariant under rotations of 2π generated by $\hat{R} = e^{i2\pi\hat{N}^2/16}$, which acts on the states as

$$\hat{R} |n\rangle_b = \sum_t c_t e^{i2\pi(n+tb)^2/16} |n+tb\rangle. \quad (5.22)$$

From the first term with $t = 0$, we see that we should have $n = 0$ or $n = 4$. For both of these values of the charge we need to set $b = 4$, from which it follows that in this new phase there are two possible ground states given by

$$|0\rangle_{\pm} = \frac{1}{\sqrt{2}} (|0\rangle \pm |4\rangle). \quad (5.23)$$

The condition that the ground state is invariant under \hat{R} is equivalent to demanding integer spin which is a property a condensable sector should have. The difference with older work on TSB is that we recognize two different ground states instead of only $|0\rangle_+$, which may result in different domains due to spontaneous symmetry breaking as we will see below.

The operator V_4 has nonzero expectation value, which can be interpreted in the same fashion as creating Cooper pairs in a superconductor. In our case, we can freely create and annihilate particles of topological charge $n = 4$. The states rearrange themselves as eigenstates of V_4

$$|n\rangle_{\pm} = \frac{1}{\sqrt{2}} (|n\rangle \pm |n+4\rangle), \quad n = 0, \dots, 3. \quad (5.24)$$

They form an orthonormal and a complete set of representations of the group $G = \mathbb{Z}_4 \otimes \mathbb{Z}_2$, generated by $W_2 = e^{2\pi i\hat{N}/4}$ and V_4 . These two operators commute: $[W_2, V_4] = 0$, and the action on the states is

$$W_2 |n\rangle_{\pm} = e^{2\pi i n/4} |n\rangle_{\pm} \quad (5.25)$$

$$V_4 |n\rangle_{\pm} = \pm |n\rangle_{\pm}. \quad (5.26)$$

In the broken phase the ground state is twofold degenerate and the operator that maps these two states onto each other is W_1

$$W_1 |0\rangle_{\pm} = |0\rangle_{\mp}. \quad (5.27)$$

These states carry a \mathbb{Z}_2 charge generated by W_1 , but no \mathbb{Z}_4 charge under W_2 .

Due to the degeneracy the system eventually chooses a vacuum expectation value. This is similar to what happens in the Ising model on a square lattice in two dimensions without an external field. The ground state corresponds to either all spins pointing up $|\uparrow\rangle$ or all pointing down $|\downarrow\rangle$. The operator that flips all spins simultaneously commutes with the Hamiltonian and generates a global \mathbb{Z}_2 symmetry. The operator that measures which ground state we are in is $M = \frac{1}{N} \sum_i \sigma_i^z$. In our case W_1 maps the two ground states onto each other and V_4 measures which state we are in.

5.2.3 Domain walls

Since there is a twofold degenerate ground state in the broken phase, the system eventually chooses one of these states resulting in a spontaneous breaking of the \mathbb{Z}_2 symmetry. However, it could happen that part of the system is in the $+$ ground state and the other part in the $-$ state. Intuitively this would result in different domains separated by domain walls carrying energy, as also happens in the Ising model described above.

Let us first focus on the edge of our configuration and consider the kink solutions. Say we start from a state where the entire edge is in the ground state $|0\rangle_+$ and apply the open Wilson line operator

$$W_1(x_1, x_2) = \exp \left[\frac{i}{\sqrt{8}} \int_{x_1}^{x_2} \partial_x \phi(x) dx \right], \quad (5.28)$$

which creates a domain in the $|0\rangle_-$ phase in between the points x_1 and x_2 . At the edge we only have the global symmetry of shifting $\phi(x)$ by a constant. Clearly the Wilson line on the edge is invariant under this transformation and creating these different domains does not require the introduction of the V_1 sectors at the endpoints. The kinks located around x_1 and x_2 however have finite energy, so restricting our consideration to the edge theory, we may conclude that the kinks are massive solitons which are not confined as there is only vacuum in between them.

As remarked before we can extend the operators $W_q(\mathcal{C})$ and $V_n(z)$ to well-defined operators referring to closed loops \mathcal{C} and points (punctures) z in the bulk. In discussing the phase structure of the broken phase \mathcal{U} , it is important to make a clear distinction between whether we permit insertions in the bulk of the confined sector $V_1(z)$ or not. This distinction can be made because there are two scales in the problem: the gap or mass of the V_n excitations, and the presumably smaller energy scale associated with the condensate. It is most natural to start with a situation where we do not include them, but we may still consider the Wilson loop operators with arbitrary q and in particular also with $q = 1$. The interpretation of closed loops is similar to the boundary and the Wilson loop operator now creates a domain of $-$ vacuum in the bulk, and a domain wall along

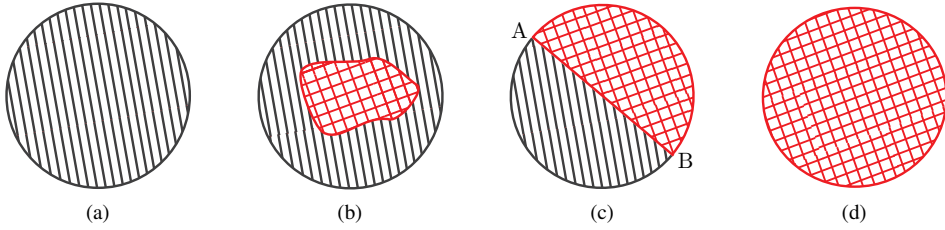


Figure 5.1: A disc in the broken phase \mathcal{U} with two possible vacua: the $+$ vacuum is indicated by grey stripes, and the $-$ vacuum by a red mesh. In fig. (a) we start with the disc entirely in the $+$ vacuum. In fig. (b) we have created a Wilson loop W_1 along a contour \mathcal{C} , which creates a $-$ vacuum inside it and a physical domain wall along the loop. It can be deformed to lie partially on the boundary as indicated in fig. (c). The boundary now has two different domains where the kinks located around point A and B carry energy and they are connected to the wall going across the disc through the bulk, which also carries energy. In fig. (d) the entire Wilson loop lies on the boundary and the entire disc is in the $-$ vacuum state.

the contour \mathcal{C} . It is interesting to deform this configuration as indicated in fig. 5.1. In fig. (a) and (b) we have sketched the situation we just discussed. However, the loop can be moved around at will, and in particular we may put it partially along the edge as in fig. (c). How do we interpret this physically? When looked at from the perspective of the boundary we see that at the points A and B where the closed loop leaves the boundary, the vacuum flips and therefore there should be a kink in the field on the boundary. The other part of the contour, going from B to A through the bulk, is a massive domain wall ending at the kink-antikink pair. The situation is comparable to the states created by $V_n(z)$ which represent massive localized anyons in the bulk and massless modes on the edge.

When there are different domains we have to probe the system locally to measure which domain we are in. We cannot simply use $V_4(z)$ as it is not gauge invariant. Instead we need to use the gauge invariant object in (5.16) with $n = 4$, which gives $+1$ if the end points are in the same vacuum and -1 if they are in different vacua, i.e. crossing the wall either an even or an odd number of times. The coloring of domains in fig. 5.1 is well defined at this stage, therefore in this restricted setting without V_1 quasiparticles the vacuum states can be unambiguously carried over to the bulk.

5.2.4 Confined particles

So far we have established a detailed, consistent picture of the physics of TSB except that we have to consider one more ingredient, and that is the role of the confined vertex operator $V_1(z)$ in the bulk of \mathcal{U} . We will see below that it plays a major role in the stability of domain walls.

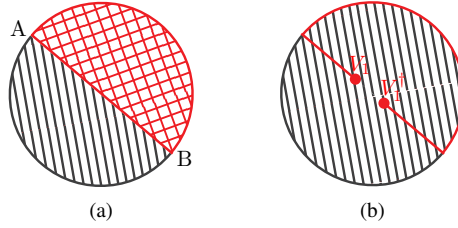


Figure 5.2: Fig. (a) shows a closed W_1 loop, which runs partially along the boundary and in fig. (b) the loop is broken through the creation of a $V_1-V_1^\dagger$ pair. Probing with a W_4 Wilson line to a point on the boundary is still consistently and unambiguously defined. It makes no difference whether this line crosses the wall or passes through the opening. In the one case the phase jump occurs because of the crossing, and in the other it comes from braiding with the V_1 vertex. However, it is also clear that the coloring of the domains in the bulk does not make any sense if we allow the V_1 anyons to be produced, but the coloring still makes sense if one restricts oneself only to the edge.

We can distinguish two types of instability. One is a *global* instability meaning that a closed loop in the bulk can shrink to zero. Since the domain wall has a fixed energy per unit length, shrinking lowers the total energy of the configuration and there is no topological obstruction to fully contract. More interesting is a *local* topological instability of the wall, where it can in principle break upon the creation of a $V_1-V_1^\dagger$ particle-hole pair attached to the new endpoints of the broken wall. This process is depicted in fig. 5.2. Whereas the V_1 quasiparticles were not confined on the boundary as we argued before, they are linearly confined in the bulk exactly because they have to be attached to a domain wall of finite energy. The walls are metastable because the creation of a massive pair requires an energy of at least twice the particle gap. Another important consequence of the metastability of the wall in the bulk, is that the domain structure of the vacuum is no longer protected.

A topological argument explaining this goes as follows [136]. In the unbroken phase V_1 is still present and we have a full $U(1)/\mathbb{Z}_8$ gauge group in the bulk with topological flux/particle sectors $\pi_1(U(1)/\mathbb{Z}_8) = \pi_0(\mathbb{Z}_8) = \mathbb{Z}_8$, corresponding to representations of the \mathbb{Z}_8 group generated by W_1 . After breaking, the gauge group is formally changed to $U(1)/\mathbb{Z}_4$ corresponding to the \mathbb{Z}_4 subgroup of \mathbb{Z}_8 consisting of the even elements, and $\pi_0(\mathbb{Z}_4)$ refers to the even sectors created by V_{2n} . The homotopy sequence of interest here is

$$\pi_0(\mathbb{Z}_4) \rightarrow \pi_0(\mathbb{Z}_8) \rightarrow \pi_0(\mathbb{Z}_8/\mathbb{Z}_4), \quad (5.29)$$

implying that the Image of the first mapping is the Kernel of the second. In physical

terms this means that the even sectors of $\pi_0(\mathbb{Z}_8)$ get mapped onto the trivial sector of $\pi_0(\mathbb{Z}_8/\mathbb{Z}_4) = \mathbb{Z}_2$, where the latter group labels per definition the new types of domain walls that arise in the broken phase. In other words, the odd charges of the $\pi_0(\mathbb{Z}_8)$ are mapped onto the nontrivial domain walls and are therefore confined, exactly as advertised.

The overall picture remains completely consistent if one takes into account that now there are two ways to go from a $+$ state created by $(V_n(x) + V_{n+4}(x))|0\rangle$ at a position x on the edge to the left of point A in fig. 5.2, to the corresponding $-$ state at a position on the right. The first option is to ‘cross’ the wall by transforming a vertex operator with W_1 using (5.19). The other is by moving the vertex operators involved through the bulk and around the endpoint at the opening in the wall, which in fact means acting with the monodromy operator. Let us demonstrate this explicitly by considering this question in the original unbroken \mathcal{A} theory, and see what can be carried over to the broken phase. Given that the monodromy, i.e. encircling an anyon V_n with V_m (in the original \mathcal{A} theory with $n, m = 0, \dots, 7$), yields a phase factor

$$\exp(2\pi i(h_{m+n} - h_n - h_m)) = e^{2\pi i nm/8}, \quad (5.30)$$

we can make some important observations. Since the \mathcal{A} sectors become combined (identified) as in (5.24) in the broken phase, encircling them around another \mathcal{T} sector gives different monodromy phases. For $n, m = 0, \dots, 3$ and $k, k' = 0, 1$, the different phases of the monodromy can be expressed as

$$\begin{aligned} & \frac{2\pi}{16} \left((n + m + 4k + 4k')^2 - (n + 4k)^2 - (m + 4k')^2 \right) = \\ & = \frac{2\pi}{8} (nm + 4nk' + 4mk) \pmod{2\pi}. \end{aligned} \quad (5.31)$$

Two \mathcal{T} sectors have consistent braiding if their monodromy is independent of k and k' , which leaves us with only the sectors $n = 0$ and $n = 2$ as expected. One also may verify that only these sectors are mutually local with respect to the new vacuum and therefore survive as unconfined particles. Note that from the monodromy phase we learn that if we have the fundamental quasiparticle corresponding to V_1 in the bulk and bring the new vacuum $V_0 \pm V_4$ around it, that would map the two vacua onto each other, i.e. $(V_0 \pm V_4) \rightarrow (V_0 \mp V_4)$. This means that the net effect of moving around the confined particle is the same as crossing the wall as we have described above, where the \pm state transforms under W_1 and gets mapped to the \mp state at the other side of the wall.

This shows once more that the wall is not locally stable, and it can break under the creation of a fundamental quasiparticle/hole pair, each of them remaining attached to the newly created end points. Alternatively one may consider starting from a disc entirely in

one of the vacua and creating the $V_1-V_1^\dagger$ pair somewhere in the bulk. When the particles are moved apart they stay connected by a wall which explicitly follows from (5.16). So their appearance will be exponentially suppressed not only because of their mass but also because of their interaction energy that rises linearly with distance, and they indeed are confined.

5.2.5 Unstable general Laughlin states

In this chapter we mainly focused on the specific Laughlin state at $\nu = 1/8$ in order to clearly present our results, but the construction is easily generalized to the other unstable Laughlin states that were presented in section 5.1. Even though the notation for fermionic and bosonic states is a bit different,

$$\text{Bosonic:} \quad M = 2l^2k \quad \mathcal{A} = U(1)_{l^2k} \quad l = 2, 3, \dots, \quad k = 1, 2, \dots \quad (5.32)$$

$$\text{Fermionic:} \quad M = l^2k \quad \mathcal{A} = U^+(1)_{2l^2k} \quad l = 3, 5, \dots, \quad k = 1, 3, \dots, \quad (5.33)$$

what they have in common is that V_{2lk} acquires a vacuum expectation value, resulting in l different vacua. There are $l - 1$ different Wilson loops as in (5.14), that create the different domains, and there are $l - 1$ distinct confined particles corresponding to V_n , with $n = 1, 2, \dots, l - 1$, that can be attached at the end of a Wilson line as in (5.28).

Let us end this chapter by summarizing our results. Even though there can be no backscattering in a chiral system, we have shown that certain chiral edges labeled by two integers l and k are not entirely protected because TSB may occur. When a condensate of bosonic particles forms, certain topological sectors can disappear in this condensate and others become confined. After breaking the topological symmetry we are left with a phase which is still chiral, but has less sectors in its spectrum.

Furthermore, we have extended our understanding of the original TSB picture proposed in 2002, by finding an explicit expression of an order parameter which obtains a finite expectation value in the broken phase. This leads to degenerate ground states and different domains separated by domain walls. Moreover this gives us a good understanding of the confined particles in the bulk, that turn out to be unconfined on the edge of the sample. We give simple criteria for the stability of the domain walls. This work also clearly shows the essential observable differences between an exact \mathcal{U} theory and the \mathcal{U} phase obtained after applying TSB to an \mathcal{A} theory.

Appendix

5.A CFT description of $U(1)$ chiral states

As explained in section 2.3 many FQH states have a CFT description. In the bulk, the wave functions can be expressed as CFT correlators and on the edge of a finite system the particle spectrum coincides with the CFT spectrum. In this chapter we focused on the Laughlin states, which describe Abelian FQH states at filling fraction $\nu = 1/M$, where M is a positive integer. These systems have a description in terms of simple chiral CFTs, namely the compactified boson. Therefore, we will use this section to present some results about this CFT. We will derive the spectrum and show for which particular compactification radii the CFT becomes rational, i.e. has a finite number of primary fields. For more information on CFTs in general, we refer the reader to [78].

The Lagrangian of the chiral compactified boson was given in (2.15). The boson field $\phi(x, t)$ is compactified on a circle of radius R , meaning that we identify $\phi \sim \phi + 2\pi R$. The modes of the conserved current form a Kac-Moody algebra and the spectrum of this system falls into irreps labeled by the lowest weight states $|n, m\rangle$ which have conformal weight

$$h_{n,m} = \frac{1}{2}(n/R + mR/2)^2. \quad (5.34)$$

There are an infinite number of primary fields in this theory, where n labels the charge and m the winding number of the field configuration corresponding to the boundary conditions $\phi(x + L, t) = \phi(x, t) + 2\pi mR$. Whenever R^2 is rational, i.e.

$$R = \sqrt{\frac{2p'}{p}}, \quad p, p' \text{ are coprime}, \quad (5.35)$$

the infinite number of lowest weight states can be rearranged into a finite number by adding a specific generator to the current algebra. The only available operators in the free boson theory are vertex operators $V_\alpha = e^{i\alpha\phi}$, and following ref. [78] the operator which is added to the chiral algebra is

$$i\partial\phi, \quad \Gamma^\pm = e^{\pm i\sqrt{2pp'}\phi}. \quad (5.36)$$

This operator Γ^+ has integer weight and is invariant under $\phi \rightarrow \phi + 2\pi R$. The primary fields of the extended theory must have local OPEs with the currents and are of the form

$$V_n = e^{in\phi/\sqrt{2pp'}} . \quad (5.37)$$

Their weights are

$$h_n = \frac{n^2}{4pp'} , \quad n = 0, \dots, 2pp' - 1 , \quad (5.38)$$

and the Hilbert space falls into irreps of the extended algebra which will be denoted by $U(1)_{pp'}$. Note that all of the above is invariant under the interchange $p \leftrightarrow p'$, which corresponds to the invariance under modular transformations.

5.B Laughlin states

How does $U(1)_{pp'}$ relate to the Laughlin states at $\nu = 1/M$? For the bosonic case it is quite straightforward, but for the fermionic states we need to be more careful as we will show below.

5.B.1 Bosonic Laughlin states

We first turn to the bosonic Laughlin states at filling fraction $\nu = 1/M$, with M even. The theory can be described by a compactified chiral boson at radius $R = \sqrt{M}$. Comparing to (5.35), we should choose $p' = M/2$ and $p = 1$, leading to an algebra $U(1)_{M/2}$. Note that this form can only apply to even M . The theory we start from has M sectors with conformal weights (spins)

$$h_n = \frac{n^2}{2M} , \quad n = 0, \dots, M - 1 . \quad (5.39)$$

The vertex operator that describes the physical boson of charge e is precisely the extended operator that gets added to the chiral algebra $V_e = e^{i\sqrt{M}\phi}$, with weight $h_e = M/2$, which is an integer for even M .

5.B.2 Fermionic Laughlin states

If we follow the same strategy for the fermionic Laughlin states we run into trouble. Take for instance the $\nu = 1/3$ Laughlin state. This corresponds to a compactified boson at $R = \sqrt{3}$. Following the definition in (5.35) we should choose $p' = 3$ and $p = 2$, which is a $U(1)_6$ algebra and has 12 sectors, with weights $h_n = n^2/24$. The charge e fermion corresponds to sector $f = 6$ and has spin $h_6 = 3/2$. From the physics of this particular

system we get an extra condition on the allowed vertex operators, since all quasiparticles need to be local with respect to the fermion. For instance, the monodromy with the fundamental quasiparticle is $\theta_{1,e} = 1/2$, from which it follows that they are nonlocal.

Moore and Read treated the fermionic case in [11]. They choose the electron operator $V_e = e^{i\sqrt{M}\phi}$ as extended generator even though it has half integer spin. As in appendix 5.A they choose the other operators such that they are mutually local with the electron operator. The weights of these other operators are $h_n = \frac{n^2}{2M}$, with $n = 0, \dots, M-1$ and they indeed carry the right quantum numbers associated with the quasiholes of the FQH state. The reason why we do not adopt their formulation is that they do not distinguish between the electron operator and the trivial operator, therefore we would never be able to distinguish between a fully gapped (edge) system and a $\nu = 1$ state.

Therefore we will follow a different strategy. For $\nu = 1/M$, with M odd we have a compactified boson at $R = \sqrt{M}$. Since M is odd we can choose $p' = M$ and $p = 2$ as coprime integers, resulting in a $U(1)_{2M}$ theory. The weights are

$$h_n = \frac{n^2}{8M}, \quad n = 0, \dots, 4M-1. \quad (5.40)$$

The sector with $f = 2M$ corresponds to the charge e fermion and it has spin $h_{2M} = M/2$. We want all the sectors to be local with respect to this operator, and the monodromy is given by

$$M_{n,f} = \frac{4Mn}{8M} = -\frac{n}{2}, \quad (5.41)$$

which means that only the even sectors are local and are good operators in this theory. Rewriting $2m = n$, we are left with $2M$ sectors, labeled by $m = 0, \dots, 2M-1$, with weights $h_m = \frac{m^2}{2M}$. Let us call this theory $U^+(1)_{2M}$, where the $+$ denotes the even sectors of $U(1)_{2M}$. The only difference with the literature is that we count up until twice the fermion.

CHAPTER 6

Boundaries between topological phases induced by a multilayer Bose condensate

This chapter is based on the following publication:

F.A. Bais, J.K. Slingerland, and S.M. Haaker, THEORY OF TOPOLOGICAL EDGES AND DOMAIN WALLS, *Phys. Rev. Lett.* **102**, 220403 (2009).

and the following unpublished work:

S.M. Haaker, F.A. Bais, and J.K. Slingerland, A QUANTUM GROUP APPROACH TO FRACTIONAL QUANTUM HALL HIERARCHIES, *working title*.

In this chapter¹ we study the boundaries between phases of different topological order. A clear understanding of such boundaries is very important but often lacking. In FQH systems, where experimental support for the existence of a variety of topological phases is strongest, observations are almost entirely restricted to edge transport, and proposed devices for probing the topological order rely on interference of tunneling currents between edges [13, 138, 139]. In such experiments the electron density is usually not constant throughout the sample and islands with different filling fractions form. In lattice models with several topological phases, one may induce phase boundaries by varying the local couplings. By applying TSB we will construct regions with different topological phases and study their boundaries. This technique was used in chapter 5 as well, where transitions between different Laughlin states were induced.

The transitions we discuss in the present chapter are between phases with different central charges, which alters the approach to some extent and involves the introduction of extra layers. This allows application in a greater variety of physical settings. In section 6.2 we work out two such examples, which involve Kitaev's spin model on the honeycomb lattice [77] and a domain wall between spin polarized and unpolarized non-Abelian FQH

¹Part of the results in this chapter appeared before in the master's thesis [137].

liquids [140]. In section 6.3 we discuss a transition between two Abelian FQH states belonging to the Haldane-Halperin (HH) hierarchy at $\nu = 1/3$ and $\nu = 2/5$, which we generalize to an arbitrary number of states in appendix 6.A. But let us first explain how to apply TSB to a system with an auxiliary layer.

6.1 Multilayer condensation

One way to match two different phases I and II at a domain wall is to treat them as independent systems without interaction and then bring the edges close together. The sectors that reside on the wall are then simply pairs of phase I and phase II sectors. However, this is not always the situation observed in experiments. For example, Camino et al. [141, 142] created a setup with a FQH state at filling fraction $\nu_I = 1/3$ surrounding a state at $\nu_{II} = 2/5$. They found that the boundary separating the two phases has excitations of charge $e/15$ which cannot be explained as a simple product of the $\nu_I = 1/3$ and $\nu_{II} = 2/5$ boundaries. In section 6.3 we will construct a similar situation and show how our approach agrees with the charge $e/15$ boundary excitation.

To describe these general interfaces, we start with two layers in phases I and III, which we allow to partially overlap as indicated in fig. 6.1. If we bring the layers close together a bosonic composite of excitations from the two layers could occur, and consequently, a condensate of such bosons may form. This condensation will lead to a different phase for the middle region, which we denote by phase II.

If we are given topological theories C_1 and C_3 describing phases I and III, the sectors of the layered system will initially be labeled by pairs $(a, b) \in C_1 \otimes C_3$. These sectors do not interact with each other, e.g.

$$(a_1, b_1) \times (a_2, b_2) = (a_1 \times a_2, b_1 \times b_2), \quad (6.1)$$

but combined their quantum dimensions multiply $d_{(a,b)} = d_a d_b$ and their spins will add $h_{(a,b)} = h_a + h_b$. This implies that even though the separate phases might not have a nontrivial bosonic particle, the combined phases could carry such a sector.

If we assume that a condensate of such bosonic quasiparticles forms this causes a change in the topological spectrum and fusion rules exactly along the same lines as was presented in section 2.2. Sectors of the $C_1 \otimes C_3$ theory branch into sectors of the intermediate phase \mathcal{T} according to branching rules of the form

$$(a, b) \rightarrow \sum_{c \in \mathcal{T}} N_{(a,b)}^c c. \quad (6.2)$$

While all \mathcal{T} sectors have good fusion rules, some do not inherit well-defined spin factors

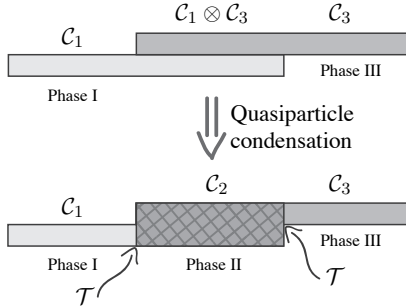


Figure 6.1: Side view of two overlapping layers supporting topological phases I and III. If we bring the layers close together a condensate may form in the overlap region leading to a phase II, which is no longer a direct product of phases I and III. The theory \mathcal{T} on the left boundary describes excitations that can be divided into bulk excitations of phase I and of phase II, and excitations that can only propagate along the boundary. On the right boundary a similar situation occurs for the same theory \mathcal{T} , now with I replaced by III.

from the uncondensed theory, because they have nontrivial braiding interaction with the condensed excitation and become confined. After all confined excitations are expelled from the bulk we are left with a C_2 theory, which describes the fusion and braiding of excitations in phase II.

We now make the crucial observation that, after condensation, excitations in all parts of the system can be labeled by sectors of the \mathcal{T} theory. More precisely, the bulk excitations of phase II correspond to unconfined \mathcal{T} sectors, while those of phases I and III are pairs (a, \mathbb{I}) and (\mathbb{I}, b) of $C_1 \otimes C_3$ labels, which correspond to \mathcal{T} sectors indicated by the branching rules in (6.2). Most importantly the excitations on the boundary between the phases are also \mathcal{T} sectors and we can investigate the kinematics of all processes that may occur when excitations are moved toward or through walls. For example, any C_1 particle that branches to an unconfined \mathcal{T} particle can pass through the boundary between phase I and II unnoticed and vice versa, while a C_1 particle that corresponds to a confined \mathcal{T} sector cannot enter the region in phase II. Reversely, \mathcal{T} particles that are confined in phase II but have lifts corresponding to a C_1 sector, can pass into the area in phase I after being driven out of phase II. Hence the excitations that must stay on the boundary are labeled by confined \mathcal{T} sectors which do not correspond to C_1 sectors.

For processes involving three or more excitations, we need to use the fusion rules of \mathcal{T} . Any process allowed by these rules could in principle occur. For example, a C_1 particle corresponding to a confined \mathcal{T} sector c could hit the phase boundary and split into a boundary excitation t and a bulk excitation u of phase II, provided that $c \in t \times u$ according to the fusion rules of \mathcal{T} . To actually perform the fusions involved, it will usually

| Ising | | | | \mathbb{Z}_2 toric code | | | | |
|-----------|---|------------|--------|---------------------------|---|-----|-----|------|
| $c = 1/2$ | 1 | σ | ψ | $c = 0$ | 1 | e | m | em |
| h | 0 | 1/16 | 1/2 | h | 0 | 0 | 0 | 1/2 |
| d | 1 | $\sqrt{2}$ | 1 | d | 1 | 1 | 1 | 1 |

Table 6.1: Quantum dimension and topological spin of the sectors of the Ising and toric code model.

be necessary to bring the quasiparticles from the bulk regions close to the boundary.

With this new approach where multiple layers are used, we can apply TSB to a wide variety of phases. In the next section we will study two different phase transitions between non-Abelian phases and investigate the excitations of the boundary between them.

6.2 Phase transition between non-Abelian states

After introducing the general idea of using auxiliary layers to create phase diagrams as depicted in fig. 6.1, we now move on to two explicit examples in the present section. Both of these involve topological phases that carry non-Abelian excitations. The first example covers Kitaev's honeycomb model and the second one treats two non-Abelian FQH states.

6.2.1 Kitaev's honeycomb and the toric code

Kitaev's honeycomb model [77] is a model of spins living on the sites of a honeycomb lattice and interacting through nearest neighbor Ising-like interactions. The model is exactly solvable and displays two types of phases.² There are three equivalent gapped Abelian topological phases with the same topological order as the \mathbb{Z}_2 toric code with central charge $c = 0$. And there is a gapless phase, which becomes gapped when a Zeeman term is added to the Hamiltonian and then displays non-Abelian topological order described by the Ising TQFT at $c = 1/2$.

The Abelian phase has four sectors with $\mathbb{Z}_2 \otimes \mathbb{Z}_2$ fusion rules and the Ising model has three sectors labeled by $\{1, \sigma, \psi\}$, where 1 denotes the vacuum. The Ising model was encountered before in section 2.1, but for clarity we mention the characteristics again. The nontrivial fusion rules are given by

$$\sigma \times \sigma = 1 + \psi, \quad \sigma \times \psi = \sigma, \quad \psi \times \psi = 1, \quad (6.3)$$

and the spins and quantum dimensions of the Ising model as well as the toric code are given in table 6.1.

²In extensions of the model, a third type of gapped phase has been found in [143].

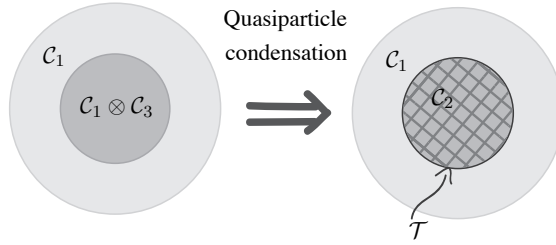


Figure 6.2: Starting from a disc in phase I which carries \mathcal{C}_1 excitations, we place a smaller disc \mathcal{C}_3 on top of it. We call this overlapping part region II and it contains sectors from $\mathcal{C}_1 \otimes \mathcal{C}_3$. After the formation of a quasiparticle condensate, region II contains the unconfined sectors given by \mathcal{C}_2 . The sectors at the boundary between the two phases are labeled by the intermediate phase \mathcal{T} .

We wish to consider a situation with an island in the Abelian phase surrounded by a medium in the Ising phase. As the two phases have different central charge we must use an auxiliary layer as discussed before. We take a large disc in the $\mathcal{C}_1 = \text{Ising}$ phase and place a smaller disc on top of it as depicted in fig. 6.2. \mathcal{C}_3 should be chosen in such a way that a Bose condensate can form, leaving the bulk of the small disc in the $\mathbb{Z}_2 \times \mathbb{Z}_2$ phase. The addition of the auxiliary layer should lower the central charge by $1/2$ and so we use an opposite chirality Ising model for it, which has the same fusion rules as the $c = 1/2$ Ising model and therefore the same quantum dimensions, but opposite topological spins.

We start from $\text{Ising} \otimes \overline{\text{Ising}}$ in region II and take a condensate in the bosonic (ψ, ψ) sector. This example has been worked out in detail in section X of ref. [81]. Condensation leads to the identifications

$$(1, 1) \sim (\psi, \psi) \quad (6.4)$$

$$(\psi, 1) \sim (1, \psi) \quad (6.5)$$

$$(\sigma, 1) \sim (\sigma, \psi) \quad (6.6)$$

$$(1, \sigma) \sim (\psi, \sigma), \quad (6.7)$$

while the remaining sector is fixed under fusion with the condensate and has to split

$$(\sigma, \sigma) \rightarrow (\sigma, \sigma)_1 + (\sigma, \sigma)_2. \quad (6.8)$$

Hence, the intermediate \mathcal{T} theory has six sectors and one finds that it has $\text{Ising} \otimes \mathbb{Z}_2$ fusion rules.

Next we analyze the braiding interactions with the condensate to find which of these

$$\mathcal{M}(4, 5)$$

| | | | | | | |
|------------|-------------------|------------------------------------|------------------------------------|-------------------|---|-------------------|
| $c = 7/10$ | 1 | ϵ | ϵ' | ϵ'' | $\tilde{\sigma}$ | $\tilde{\sigma}'$ |
| h | 0 | $\frac{1}{10}$ | $\frac{3}{5}$ | $\frac{3}{2}$ | $\frac{3}{80}$ | $\frac{7}{16}$ |
| d | 1 | $\frac{1+\sqrt{5}}{2}$ | $\frac{1+\sqrt{5}}{2}$ | 1 | $\frac{1+\sqrt{5}}{\sqrt{2}}$ | $\sqrt{2}$ |
| | ϵ | $1 + \epsilon'$ | | | | |
| | ϵ' | $\epsilon + \epsilon''$ | $1 + \epsilon'$ | | | |
| | ϵ'' | ϵ' | ϵ | 1 | | |
| | $\tilde{\sigma}$ | $\tilde{\sigma} + \tilde{\sigma}'$ | $\tilde{\sigma} + \tilde{\sigma}'$ | $\tilde{\sigma}$ | $1 + \epsilon + \epsilon' + \epsilon''$ | |
| | $\tilde{\sigma}'$ | $\tilde{\sigma}$ | $\tilde{\sigma}$ | $\tilde{\sigma}'$ | $\epsilon + \epsilon'$ | $1 + \epsilon''$ |

 Table 6.2: Spins, quantum dimensions and fusion rules of the tri-critical Ising model $\mathcal{M}(4, 5)$.

\mathcal{T} sectors become confined. It turns out that the sectors $(\sigma, 1)$ and $(1, \sigma)$ have nontrivial monodromy with (ψ, ψ) and hence become confined. When we check the spins and fusion rules of the remaining unconfined sectors $\{(1, 1), (\sigma, \sigma)_1, (\sigma, \sigma)_2, (\psi, 1)\}$, they correspond precisely to the toric code whose sectors $1, e, m$ and em are given in table 6.1.

Let us now look at the wall in between the phases. Of the nontrivial excitations in the interior bulk, the fermionic $(\psi, 1)$ excitation can freely move through the wall into the exterior region while the other two bulk excitations cannot. This corresponds well to the results of ref. [144] where it was shown that free fermionic excitations occur throughout the phase diagram. The confined excitations are expelled from the interior, but the $(\sigma, 1)$ excitation can move into the exterior region, while the other $(1, \sigma)$ excitation is strictly confined to the wall.

Now consider the following process, where a $(\sigma, 1)$ excitation from the exterior region hits the boundary. From the fusion rules of the \mathcal{T} theory we see that

$$(\sigma, 1) = (1, \sigma) \times (\sigma, \sigma)_1 = (1, \sigma) \times (\sigma, \sigma)_2. \quad (6.9)$$

Hence, the $(\sigma, 1)$ particle can split into a boundary excitation and either an e or an m type toric code sector. This corresponds well with the results of ref. [145], where σ -like excitations were exhibited in the toric code using superpositions of e and m type excitations. Pushing another $(\sigma, 1)$ particle through the phase boundary will allow the confined $(1, \sigma)$ excitations to annihilate, yielding either $(1, 1)$ or $(\psi, 1)$. This depends on the fusion channel the initial two $(\sigma, 1)$ particles were in, thus conserving \mathcal{T} charge.

6.2.2 The Pfaffian/NASS interface

Now we turn to the interface between the MR Pfaffian FQH state [11] and the non-Abelian spin-singlet (NASS) state proposed by Ardonne and Schoutens [146, 147], which are candidate states for QH liquids at filling fraction $\nu = 5/2$ and $\nu = 18/7$, respectively. Such an interface was also considered in ref. [140].

The NASS state was originally proposed as a candidate state for the plateau at $\nu = 18/7$, but numerical calculations show that with Coulomb interactions it is a better candidate for the LLL at $\nu = 4/7$. This would suggest that the study of an interface between MR and NASS is solely a theoretical exercise, but preliminary studies [148] indicate that there exists well-chosen modifications of the Coulomb interaction that could stabilize both the MR and NASS phases in the second LL. Moreover, we remark that FQH states can in principle be produced in cold atoms with artificial gauge fields, thus in practice an interface between a bosonic MR state at $\nu = 1$ and a bosonic NASS state at $\nu = 4/3$ seems to be promising [149].

In this section we leave out the $U(1)$ charge factors and focus on the non-Abelian parts of the MR and NASS theories which are the same regardless of the LL they are in. The condensation process that drives the phase transition only takes place in the neutral part for these particular models and the $U(1)$ charges can be put back in at any point.

Let us return to fig. 6.2 and consider a disc with a $C_1 = \text{Ising}$ CFT, corresponding to the non-Abelian part of the MR state, with a smaller disc with $C_3 = \mathcal{M}(4, 5)$ on top of that. The latter CFT is a minimal model with $c = 7/10$ corresponding to a tri-critical Ising model [78]. The field content of the Ising and $\mathcal{M}(4, 5)$ theories are given in tables 6.1 and 6.2, respectively.

In the overlapping region we start from a theory $\text{Ising} \otimes \mathcal{M}(4, 5)$. The (ψ, ϵ'') sector is the only bosonic channel and as this is a simple current it is straightforward to determine the fate of the various fields in the model. Of the initial 18 sectors, 16 become pairwise identified, because they are equivalent modulo fusion with (ψ, ϵ'') . The remaining two sectors $(\sigma, \tilde{\sigma})$ and $(\sigma, \tilde{\sigma}')$, are invariant under fusion with the condensate and therefore split, resulting in a total of 12 \mathcal{T} sectors, which are listed at the top of table 6.4. An analysis along the lines of ref. [81] shows that the fusion rules of the intermediate phase are given by $\mathcal{T} = \mathcal{M}(4, 5) \otimes \mathbb{Z}_2$. Again, not all of the \mathcal{T} fields can live in the bulk of region II and after explicitly calculating the monodromies with the condensate, we find that the \mathcal{T} sectors that are not confined correspond to the sectors of the NASS state, and form the residual bulk theory in region II. The quantum numbers and fusion rules of the NASS sectors are given in table 6.3.

In table 6.4 we have explicitly indicated which \mathcal{T} sectors correspond to excitations in the various regions, and which are strictly confined to particular walls. Note that in this table the configuration depicted in fig. 6.1 is considered, meaning that there are three different phases.

| \mathcal{U} | $(1, 1)$ | $(\sigma, \bar{\sigma})_1$ | $(\sigma, \bar{\sigma})_2$ | $(1, \epsilon)$ | $(1, \epsilon')$ | $(\sigma, \bar{\sigma}')_1$ | $(\sigma, \bar{\sigma}')_2$ | $(1, \epsilon'')$ |
|---------------|---------------------|------------------------------|------------------------------|------------------------|------------------------|-----------------------------|-----------------------------|-------------------|
| NASS | 1 | σ_\uparrow | σ_\downarrow | σ_3 | ρ | ψ_1 | ψ_2 | ψ_{12} |
| h | 0 | $\frac{1}{10}$ | $\frac{1}{10}$ | $\frac{1}{10}$ | $\frac{3}{5}$ | $\frac{1}{2}$ | $\frac{1}{2}$ | $\frac{1}{2}$ |
| d | 1 | $\frac{1+\sqrt{5}}{2}$ | $\frac{1+\sqrt{5}}{2}$ | $\frac{1+\sqrt{5}}{2}$ | $\frac{1+\sqrt{5}}{2}$ | 1 | 1 | 1 |
| | σ_\uparrow | $1 + \rho$ | | | | | | |
| | σ_\downarrow | $\psi_{12} + \sigma_3$ | $1 + \rho$ | | | | | |
| | σ_3 | $\psi_1 + \sigma_\downarrow$ | $\psi_2 + \sigma_\uparrow$ | $1 + \rho$ | | | | |
| | ρ | $\psi_2 + \sigma_\uparrow$ | $\psi_1 + \sigma_\downarrow$ | $\psi_{12} + \sigma_3$ | $1 + \rho$ | | | |
| | ψ_1 | σ_3 | ρ | σ_\uparrow | σ_\downarrow | 1 | | |
| | ψ_2 | ρ | σ_3 | σ_\downarrow | σ_\uparrow | ψ_{12} | 1 | |
| | ψ_{12} | σ_\downarrow | σ_\uparrow | ρ | σ_3 | ψ_2 | ψ_1 | 1 |

Table 6.3: The sectors of the broken unconfined phase \mathcal{U} in region II are given in the first row. They turn out to be the same as the non-Abelian part of the NASS state. The sectors and their quantum numbers and fusion rules are given.

Let us highlight a few processes which could occur in such a phase diagram. The ψ_{12} sector of the NASS phase is identified with the MR sector ψ , which means that the ψ or ψ_{12} excitations can propagate right through the wall separating the two phases. Again, the fusion rules of the \mathcal{T} theory fix the kinematically allowed channels by which particles hitting the wall can split. For instance, from the \mathcal{T} fusion rule $\sigma \times \bar{\sigma} = \sigma_\uparrow + \sigma_\downarrow$, we find that a σ_\uparrow coming from region II can split into a σ going into the MR region and a $\bar{\sigma}$ staying on the wall. However, since $\bar{\sigma} \times \sigma^* = \sigma_\uparrow + \sigma_\downarrow + \psi_1 + \psi_2$ is also a correct fusion rule, the σ_\uparrow excitation may instead split into two wall-excitations $\bar{\sigma}$ and σ^* . Likewise, this scenario may be turned around by noticing that two strict boundary excitations may fuse into a state that is not confined to the wall. Obviously there are many more possible processes, but we refrain from listing them all here.

A final comment concerns the relaxation of qubits near a wall [150]. If we encode a topological qubit in the NASS phase, for example in the fusion channel of a pair of excitations, the qubit may relax to the lowest energy state by transferring a neutral excitation to the boundary. For example, pairs of σ type excitations have fusion rules $\sigma_3 \times \sigma_3 = 1 + \rho$ and $\sigma_\downarrow \times \sigma_\uparrow = \psi_{12} + \sigma_3$, so these pairs can relax under emission of a ρ excitation. This excitation may convert into one of the pairs $\sigma^* \times \sigma^*$, $\bar{\sigma} \times \bar{\sigma}$, or $\bar{\sigma} \times \bar{\sigma}'$, which are all strictly confined to the interface. Alternatively we may have $\rho \rightarrow \sigma^* \times \sigma$ where σ^* is confined to the wall but σ can enter the MR region.

Having examined two specific examples of a phase transition between non-Abelian topo-

| | | | | | | | | | | | | |
|---|----------------------------------|--------------------------|------------------------|---|---|---------------------------|----------|-------------------------------------|---|--|--|---|
| \mathcal{T} theory | 1 | σ_\uparrow | σ_\downarrow | σ_3 | ρ | ψ_1 | ψ_2 | ψ_{12} | σ | $\bar{\sigma}$ | $\bar{\sigma}'$ | σ^* |
| Corresponding sectors in Ising $\otimes \mathcal{M}(4,5)$ | (1, 1) (ψ, ϵ'') | $(\sigma, \bar{\sigma})$ | | (1, ϵ) (ψ, ϵ') | (1, ϵ') (ψ, ϵ) | $(\sigma, \bar{\sigma}')$ | | (1, ϵ'') ($\psi, 1$) | ($\sigma, 1$) (σ, ϵ'') | (1, $\bar{\sigma}$) ($\psi, \bar{\sigma}$) | (1, $\bar{\sigma}'$) ($\psi, \bar{\sigma}'$) | (σ, ϵ) (σ, ϵ') |
| d | 1 | $\frac{1+\sqrt{5}}{2}$ | $\frac{1+\sqrt{5}}{2}$ | $\frac{1+\sqrt{5}}{2}$ | $\frac{1+\sqrt{5}}{2}$ | 1 | 1 | 1 | $\sqrt{2}$ | $\frac{1+\sqrt{5}}{\sqrt{2}}$ | $\sqrt{2}$ | $\frac{1+\sqrt{5}}{\sqrt{2}}$ |
| Phase I : MR | 1 | | | | | | | ψ | σ | | | |
| Phase II : NASS | 1 | σ_\uparrow | σ_\downarrow | σ_3 | ρ | ψ_1 | ψ_2 | ψ_{12} | | | | |
| Confined on I/II wall | | | | | | | | | | $\bar{\sigma}$ | $\bar{\sigma}'$ | σ^* |
| Phase III : $\mathcal{M}(4,5)$ | 1 | | | ϵ | ϵ' | | | ϵ'' | | $\bar{\sigma}$ | $\bar{\sigma}'$ | σ^* |
| Confined on II/III wall | | | | | | | | | σ | | | σ^* |

Table 6.4: The field content of the \mathcal{T} theory resulting from a (ψ, ϵ'') condensate in the Ising $\otimes \mathcal{M}(4,5)$ model is listed in the top row. The following rows give the correspondence between these \mathcal{T} sectors and the excitations of the different phases and walls. The sectors $\bar{\sigma}, \bar{\sigma}'$ and σ^* are strictly confined to the I/II boundary. The same \mathcal{T} theory describes a domain wall between NASS and $\mathcal{M}(4,5)$ phases, where σ and σ^* would be strictly confined to the II/III boundary.

logical phases at different central charges, we return to Abelian phase transitions in the next section.

6.3 Phase transitions between different levels of the HH hierarchy

In the previous section we discussed phase transitions between non-Abelian phases due to Bose condensation of a topological sector. We showed how we can circumvent the problem of having phases at different central charges by adding an auxiliary layer to the system, and how this gives a good description of the boundary between the two phases. In the present section we will discuss a transition between two FQH states belonging to the same hierarchy, but which have different filling fractions. In chapter 5 we treated very specific examples of Laughlin states that contain a bosonic sector in their particle spectrum, but in this section we want to describe a transition from a phase that does not contain such a bosonic candidate. Once more we have to use an auxiliary layer to induce the transition and be able to investigate the boundary between these phases.

We will discuss a transition from a Laughlin state \mathcal{A}_0 at $\nu = 1/3$ to a state \mathcal{U}_1 at the 1st level of the HH hierarchy at filling fraction $\nu = 2/5$. More details on the HH hierarchy were presented in section 2.3. We choose this specific example to motivate our formalism and give a general treatment of the entire HH hierarchy in appendix 6.A.

As explained in appendix 5.B, excitations of the initial phase are labeled by irreps of the quantum group $\mathcal{A}_0 = U^+(1)_6$, which has a total of six sectors corresponding to the CFT vertex operators

$$V_n(z) = e^{in\phi(z)/\sqrt{3}}, \quad n = 0, \dots, 5. \quad (6.10)$$

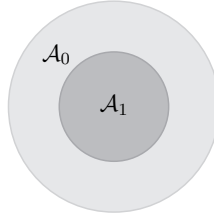


Figure 6.3: Phase diagram of the initial situation before the formation of a condensate. Since $\mathcal{A}_0 \subset \mathcal{A}_1$ the boundary between the two regions has sectors labeled by \mathcal{A}_1 .

The electron operator is given by $V_3 = e^{i\sqrt{3}\phi}$, and $V_6 = e^{2i\sqrt{3}\phi}$ is added to the current algebra resulting in this finite number of sectors. In terms of the K matrix (see section 2.3), this phase is characterized by $K_{\mathcal{A}_0} = 3$ and has charge vector $t_{\mathcal{A}_0} = 1$. At this point there is no big advantage to using the K matrix approach over the explicit CFT operators, as both give all the relevant quantum numbers. But when we treat a general level of the hierarchy in appendix 6.A we will encounter more complicated structures, which makes the K matrix formalism the preferable one, and therefore we adopt it right away.

The electric charges (in units $e = 1$), monodromy and topological spins of the different sectors are

$$Q_n = t_{\mathcal{A}_0} \cdot K_{\mathcal{A}_0}^{-1} \cdot n = \frac{n}{3} \quad (6.11)$$

$$M_{n,m} = n \cdot K_{\mathcal{A}_0}^{-1} \cdot m = \frac{nm}{3} \quad (6.12)$$

$$h_n = \frac{1}{2} M_{n,n} = \frac{n^2}{6}, \quad (6.13)$$

which confirms the fermionic nature and charge of the electron $n = 3$. Moreover, note that all sectors are local with respect to the electron operator. Since we will be dealing with Abelian theories throughout the rest of this chapter, we will not be mentioning the quantum dimension of the sectors explicitly as they are all equal to unity. We can easily see that none of these excitations are a candidate to form the condensate, as \mathcal{A}_0 does not contain any bosonic sectors.

\mathcal{A}_1 phase

We add a conveniently chosen auxiliary layer to \mathcal{A}_0 , which we choose to be a fermionic Laughlin state of the same chirality at filling fraction $\nu = 1/15$. It is described by a $U(1)_{30}^+$ theory. As we wish to investigate a boundary between a $\nu_0 = 1/3$ state and

$\nu_1 = 2/5$, we add a smaller auxiliary layer to \mathcal{A}_0 , thus creating a system as depicted in fig. 6.3 in which region I consists of a phase with $\mathcal{A}_0 = U^+(1)_6$ and region II with $\mathcal{A}_1 = U^+(1)_6 \otimes U^+(1)_{30}$. The phase in region II is now described by

$$K_{\mathcal{A}_1} = \begin{pmatrix} 3 & 0 \\ 0 & 15 \end{pmatrix}, \quad \mathfrak{t}_{\mathcal{A}_1} = \begin{pmatrix} 1 \\ 1 \end{pmatrix}. \quad (6.14)$$

This is a double layered phase where both layers carry electric charge. The filling fraction, charge, and monodromy are given by (see eqs. (2.11–2.13))

$$\nu_{\mathcal{A}_1} = \frac{2}{5} \quad (6.15)$$

$$Q_1 = \frac{l_1}{3} + \frac{l_2}{15} \quad (6.16)$$

$$M_{1,\mathbf{m}} = \frac{l_1 m_1}{3} + \frac{l_2 m_2}{15}. \quad (6.17)$$

\mathcal{T}_1 phase

\mathcal{A}_1 has more than one nontrivial boson, but we choose to let the charge neutral (modulo $2e$) boson $\mathbf{B}_1 = (1, -5) \sim (1, 25)$ condense. That this is indeed a bosonic sector follows from

$$h_{(1,-5)} = \frac{1}{6} + \frac{(-5)^2}{30} \in \mathbb{Z}. \quad (6.18)$$

When these sectors form a condensate a transition to a new phase \mathcal{U}_1 is driven. In light of the results of chapter 5, this means that the operator creating such a bosonic particle gets a finite expectation value. Since $(1, -5)$ is a simple current of order six, there are six different possible vacua. In the present chapter we will just consider one of these vacua, say

$$|v\rangle = \sum_{v'=0}^5 (v', -5v'), \quad (6.19)$$

but keep in mind that the formation of different domains within the final \mathcal{U}_1 phase due to spontaneous symmetry breaking also holds in this context. The other states rearrange as

follows

$$|a\rangle = \sum_{a'=0}^5 (a', a - 5a'), \quad a = 1, \dots, 29, \quad (6.20)$$

and together they have fusion rules \mathbb{Z}_{30} forming the intermediate phase \mathcal{T}_1 .

\mathcal{U}_1 phase

Next, we will check for consistent braiding, i.e. the sectors that survive should have trivial monodromy with the condensate. Since a \mathcal{T}_1 sector consists of several \mathcal{A}_1 sectors, all of these should have trivial monodromy with all the lifts of the \mathcal{T}_1 vacuum $|v\rangle$. Let us first write an expression for the monodromy of two \mathcal{T}_1 sectors $|a\rangle$ and $|b\rangle$

$$\begin{aligned} M_{a,b} &= (a', a - 5a') \cdot K_{\mathcal{A}_1}^{-1} \cdot (b', b - 5b')^T \\ &= 2a'b' + \frac{1}{15}ab - \frac{1}{3}(ab' + a'b). \end{aligned} \quad (6.21)$$

This should be independent of a' and b' modulo integers. Therefore it follows that $a, b \in 3\mathbb{Z}$. The monodromy of $|a\rangle$ with the condensate is given by

$$M_{a,v} = 2a'v' - \frac{av'}{3}, \quad (6.22)$$

resulting in the same condition, namely $a \in 3\mathbb{Z}$ for the unconfined sectors. After all confined excitations are expelled from the bulk of region II, for the same reasons as explained in chapter 5, we are left with a broken unconfined phase

$$\mathcal{U}_1 = \{|3u\rangle | u = 0, 1, \dots, 9\}. \quad (6.23)$$

These sectors form a closed set under fusion and have well-defined braiding statistics. The monodromy of the unconfined sectors in region II is

$$\begin{aligned} M_{u_1, u_2} &= (u'_1, 3u_1 - 5u'_1) \cdot K_{\mathcal{A}_1}^{-1} \cdot (u'_2, 3u_2 - 5u'_2)^T \\ &= \frac{3}{5}u_1u_2 \pmod{1}, \end{aligned} \quad (6.24)$$

which corresponds to a topological spin of $h_u = 3u^2/10$.

Comparing to HH hierarchy state

The easiest way to recognize which state we have obtained, is by returning to the original \mathcal{A}_1 sectors. The monodromy of a state $\mathbf{l} = (l_1, l_2)$ with the condensate is

$$M_{\mathbf{l}, \mathbf{B}_1} = \frac{l_1 - l_2}{3}, \quad (6.25)$$

so an unconfined sector has lifts with $l_1 - l_2 \in 3\mathbb{Z}$. An arbitrary integer vector \mathbf{l} can be mapped to an unconfined \mathcal{U}_1 sector by the transformation

$$W = \begin{pmatrix} 1 & 0 \\ 1 & 3 \end{pmatrix} : \quad \mathbf{l} \mapsto W\mathbf{l} = \begin{pmatrix} l_1 \\ l_1 + 3l_2 \end{pmatrix}. \quad (6.26)$$

Let us check what this means for the monodromy in the initial \mathcal{A}_1 phase of two states $W\mathbf{l}$ and $W\mathbf{m}$ mapped in such a way

$$\begin{aligned} M_{W\mathbf{l}, W\mathbf{m}} &= (W\mathbf{l})^T \cdot K_{\mathcal{A}_1}^{-1} \cdot (W\mathbf{m}) \\ &= \mathbf{l}^T \cdot (W^T \cdot K_{\mathcal{A}_1}^{-1} \cdot W) \cdot \mathbf{m}. \end{aligned} \quad (6.27)$$

We recognize this as the monodromy of two sectors \mathbf{l} and \mathbf{m} in a different theory with K matrix

$$K_{\mathcal{U}_1}^{-1} = W^T \cdot K_{\mathcal{A}_1}^{-1} \cdot W = \frac{1}{5} \begin{pmatrix} 2 & 1 \\ 1 & 3 \end{pmatrix}. \quad (6.28)$$

Calculating the charge of a $W\mathbf{l}$ sector we find

$$\begin{aligned} Q_{W\mathbf{l}} &= \mathbf{t}^T \cdot K_{\mathcal{A}_1}^{-1} \cdot (W\mathbf{l}) \\ &= (W^{-1}\mathbf{t})^T \cdot (W^T \cdot K_{\mathcal{A}_1}^{-1} \cdot W) \cdot \mathbf{l} \end{aligned} \quad (6.29)$$

where we define a new charge vector $\mathbf{t}_{\mathcal{U}_1} = W^{-1}\mathbf{t}_{\mathcal{A}_1}$. All of this leads to a new phase characterized by

$$K_{\mathcal{U}_1} = \begin{pmatrix} 3 & -1 \\ -1 & 2 \end{pmatrix}, \quad \mathbf{t}_{\mathcal{U}_1} = \begin{pmatrix} 1 \\ 0 \end{pmatrix}, \quad (6.30)$$

which is precisely the $\nu = 2/5$ FQH state at the 1st level of the HH hierarchy as in (2.14). To summarize, the connection between the two phases is

$$\mathbf{t}_{\mathcal{A}_1} = W \mathbf{t}_{\mathcal{U}_1} \quad (6.31)$$

$$K_{\mathcal{A}_1} = W K_{\mathcal{U}_1} W^T . \quad (6.32)$$

Boundary excitations

As was discussed in section 6.2, the particles in both region I and II as well as on the boundary separating them, can be expressed in terms of \mathcal{T}_1 sectors. In region I described by \mathcal{A}_0 , the sectors are labeled $\mathbf{l}_{\mathcal{A}_0} = (l_1, 0)_{\mathcal{A}_1}$, which is a lift of the \mathcal{T}_1 sector

$$|a = 5l_1\rangle = \sum_{l'=0}^5 (l', 5l_1 - 5l')_{\mathcal{A}_1}, \quad l_1 = 0, \dots, 5 . \quad (6.33)$$

To express the particles of \mathcal{U}_1 in terms of the \mathcal{T}_1 sectors, let us first establish a connection between the \mathcal{A}_1 sectors and those of \mathcal{U}_1 in terms of the W matrix. We can go back and forth between them as follows

$$\mathbf{l} \in \mathcal{A}_1 \Rightarrow W^{-1} \mathbf{l} \in \mathcal{U}_1, \quad \text{provided } l_1 - l_2 \in 3\mathbb{Z} \quad (6.34)$$

$$\mathbf{l} \in \mathcal{U}_1 \Rightarrow W \mathbf{l} \in \mathcal{A}_1 . \quad (6.35)$$

We know from (6.23) that an unconfined particle has $|a = 3u\rangle$, which can be expressed in \mathcal{U}_1 sectors as

$$|3u\rangle = \sum_{u'=0}^5 (u', 3u - 5u')_{\mathcal{A}_1} \quad (6.36)$$

$$= \sum_{u'=0}^5 (u', u - 2u')_{\mathcal{U}_1}, \quad u = 0, \dots, 9 . \quad (6.37)$$

We can now draw the following conclusions. First of all, the \mathcal{T}_1 sectors which are of the form in (6.33) and (6.37) can move into the bulk of region I and region II, respectively. There is one excitation that can move into both regions and it is given by $|a = 15\rangle$. In region I it carries a label $\mathbf{l} = (3, 0)_{\mathcal{A}_1}$ and in region II $\mathbf{l}_{\mathcal{U}_1} = W^{-1} \mathbf{l}_{\mathcal{A}_1} = (3, -1)$. We immediately see that this is the electron operator in both regions. Lastly we may

conclude that the fundamental quasiparticle that lives on the boundary between phase I and II is given by $|a = 1\rangle$, it has charge $Q = e/15$ and this excitation is strictly confined to the wall. These results agree perfectly with those of Camino et al. mentioned in the introduction of this chapter [141, 142].

In this chapter we have investigated phase transitions between FQH states at different filling fraction. We used the formalism of TSB, where we had to add an auxiliary layer to an initial phase in order to obtain a bosonic quasiparticle that could condense and drive the phase transition. Adding a smaller layer on top of the original phase \mathcal{A}_0 enabled us to study a boundary between \mathcal{A}_0 and the broken unconfined phase \mathcal{U}_1 , as was explained in the first section.

The second section of this chapter was concerned with a transition between non-Abelian states. We started with a transition between an Ising CFT and the gapped \mathbb{Z}_2 toric code, by using an auxiliary layer which was also an Ising CFT but of opposite chirality. After a careful treatment of the boundary between the two phases, we could deduce that its gapless modes were again described by an Ising CFT. The second type of transition we studied was between two non-Abelian FQH states, namely the MR and the NASS state. As auxiliary layer we used a minimal model $\mathcal{M}(4, 5)$ with central charge $c = 7/10$. After the transition we ended up with a MR and a NASS phase separated by a boundary, whose gapless excitations corresponded precisely to the $\mathcal{M}(4, 5)$ CFT. This gave us a detailed dictionary of which particles may move into the bulk of either phase I or phase II and which are strictly confined to the boundary.

In the last part of this chapter we used TSB to describe phase transitions between different levels of the FQH hierarchy picture. Explicitly, we considered the HH hierarchy, which is a hierarchy of Abelian states in the lowest Landau level, building on the Laughlin state. We presented an explicit example of a phase transition between a $\nu = 1/3$ Laughlin state and a $\nu = 2/5$ state at the first level of the hierarchy. A detailed account was given regarding which auxiliary layer should be used and what the connection is between the two phases in terms of a W matrix. We gave expressions of the spectrum on the boundary between the two adjacent phases. The spins and electric charges are in agreement with what is found in the literature. In the appendix we generalize our derivation to a transition between two arbitrary levels of the HH hierarchy.

Appendix

6.A General HH hierarchy

In section 6.3 we focused on one specific example of a phase transition between states belonging to the same FQH hierarchy, and in this appendix these ideas are extended to transitions at a general level of the hierarchy. First we consider a transition between an arbitrary 0th and 1st level of the HH hierarchy, and in the second part we move on to transitions between an arbitrary number of levels of the HH hierarchy.

6.A.1 From the 0th to the 1st level

The K matrix that describes a state at the k th level of the HH hierarchy was given in (2.14). It shows that the 0th level of this hierarchy corresponds to

$$K = m_0, \quad t = 1, \quad (6.38)$$

for m_0 a positive odd integer. It describes a FQH state at filling fraction $\nu = 1/m_0$ and is recognized as a Laughlin state, which we encountered in chapter 5. The vertex operators corresponding to the insertion of an electron and fundamental quasiparticle are

$$V_e = e^{i\sqrt{m_0}\phi_0} \quad (6.39)$$

$$V_{qp} = e^{i\frac{1}{\sqrt{m_0}}\phi_0}, \quad (6.40)$$

and the entire topological spectrum of phase I can be labeled by irreps of the quantum group

$$\mathcal{A}_0 = U^+(1)_{2m_0}. \quad (6.41)$$

The particles have \mathbb{Z}_{2m_0} fusion rules and a sector corresponding to an insertion of $V_n = e^{in\phi_0/\sqrt{m_0}}$ has charge and monodromy

$$Q_n = \frac{n}{m_0} \quad (6.42)$$

$$M_{n,n'} = \frac{nn'}{m_0}. \quad (6.43)$$

Note that the electron operator $n = m_0$ has unit charge and is local with respect to all other sectors in the theory.

To get to the 1st level of the hierarchy we add a smaller auxiliary layer to this Laughlin state. We know that the state at the next level has K matrix

$$K = \begin{pmatrix} K_{00} & K_{01} \\ K_{10} & K_{11} \end{pmatrix}, \quad (6.44)$$

and we use this knowledge to choose an auxiliary layer in region II such that

$$\mathcal{A}_1 = U^+(1)_{2m_0} \otimes U^+(1)_{2m_1 m_0^2}, \quad (6.45)$$

where $m_{i>0} = K_{ii} - \frac{1}{m_{i-1}}$. This phase can be described by K matrix and charge vector

$$K_{\mathcal{A}_1} = \begin{pmatrix} m_0 & 0 \\ 0 & m_1 m_0^2 \end{pmatrix}, \quad \mathbf{t}_{\mathcal{A}_1} = \begin{pmatrix} 1 \\ 1 \end{pmatrix}. \quad (6.46)$$

We can check explicitly that a charge neutral sector \mathbf{B}_1 , i.e. for which

$$Q_{\mathbf{B}_1} = 0, \quad (6.47)$$

is of the form $\mathbf{B}_1 = (1, -m_0 m_1)$ and that it has topological spin

$$h_{\mathbf{B}_1} = \frac{1}{2m_0} + \frac{m_1}{2} = \frac{K_{11}}{2}, \quad (6.48)$$

which is an integer because $K_{11} \in 2\mathbb{Z}$ by definition. It is therefore a suitable candidate to form a quasiparticle condensate. When it condenses, the sectors of \mathcal{A}_1 form orbits of length $2m_0$ under fusion with the condensate \mathbf{B}_1 , resulting in an intermediate phase \mathcal{T}_1 with sectors

$$|a\rangle = \sum_{a'=0}^{2m_0-1} (a', a - m_0 m_1 a'), \quad a \in \mathbb{Z}_{2|m_1 m_0^2|}. \quad (6.49)$$

We can check for confinement by considering the monodromy of the different lifts of

these sectors

$$M_{a,b} = \frac{ab}{m_1 m_0^2} - \frac{1}{m_0} (ab' + a'b) \pmod{1}. \quad (6.50)$$

As this should be independent of a' and b' , the unconfined sectors are those for which $a, b \in m_0 \mathbb{Z}$. The particle spectrum of the unconfined broken phase \mathcal{U}_1 is therefore given by

$$\mathcal{U}_1 = \{|m_0 u\rangle | u \in \mathbb{Z}_{2|m_0 m_1|}\}, \quad u \in \mathbb{Z}_{2|m_1 m_0|}. \quad (6.51)$$

In order to find the HH hierarchy state that corresponds to this particle spectrum we use the transformation

$$W = \begin{pmatrix} 1 & 0 \\ 1 & -K_{01} m_0 \end{pmatrix}, \quad (6.52)$$

which results in a K matrix and charge vector for the phase described by \mathcal{U}_1

$$\mathbf{t}_{\mathcal{U}_1} = W^{-1} \mathbf{t}_{\mathcal{A}_1} = \begin{pmatrix} 1 \\ 0 \end{pmatrix} \quad (6.53)$$

$$K_{\mathcal{U}_1} = W^{-1} K_{\mathcal{A}_1} (W^T)^{-1} = \begin{pmatrix} K_{00} & K_{01} \\ K_{10} & K_{11} \end{pmatrix}. \quad (6.54)$$

From this we deduce that the broken unconfined phase in region II indeed corresponds to the 1st level of the HH hierarchy.

Boundary excitations

Let us investigate which particles are allowed in region I and/or II. Region I is described by (6.38), region II by (6.54) and the boundary between the two has excitations given in (6.49). How do we go back and forth between these different types of labeling? The easiest thing to do is to express all sectors in terms of \mathcal{T}_1 labels.

The particles in region I can be written as $\mathbf{l}_{\mathcal{A}_0} = (l, 0)_{\mathcal{A}_1}$ and these correspond to boundary excitations $|m_0 m_1 l\rangle$, with $l \in \mathbb{Z}_{2m_0}$. In order to translate the sectors in region II to \mathcal{A}_1 particles we will use the W matrix

$$\mathbf{l} \in \mathcal{A}_1 \Rightarrow W^{-1} \mathbf{l} \in \mathcal{U}_1, \quad \text{provided } l_1 - l_2 \in m_0 \mathbb{Z} \quad (6.55)$$

$$\mathbf{l} \in \mathcal{U}_1 \Rightarrow W \mathbf{l} \in \mathcal{A}_1. \quad (6.56)$$

We use the first line to express the boundary excitations into \mathcal{U}_1 particles

$$|m_0 u\rangle = \sum_{u'=0}^{2m_0-1} (u', -K_{01}u + K_{01}K_{11}u')_{\mathcal{U}_1}, \quad u \in \mathbb{Z}_{2|m_1 m_0|}. \quad (6.57)$$

All the boundary excitations that are not of the form $|m_0 m_1 l\rangle$ with $l \in \mathbb{Z}_{2m_0}$, or $|m_0 u\rangle$ with $u \in \mathbb{Z}_{2|m_1 m_0|}$, are strictly confined to the boundary and cannot move into region I nor II. The fundamental particle at the boundary $|a = 1\rangle$ is one of these strictly confined sectors and it has charge $Q = \frac{1}{m_1 m_0^2}$. On the other hand, there is one nontrivial particle that can travel undisturbed from region I to region II and it is the electron $\mathbf{l}_e = (m_0, 0)_{\mathcal{A}_1}$. At the boundary it belongs to the orbit $|m_1 m_0^2\rangle$ and in region II it is given by $\mathbf{l}_{\mathcal{U}_1} = W^{-1} \mathbf{l}_{\mathcal{A}_1} = (m_0, K_{01})$.

6.A.2 Transitions to k th level of the HH hierarchy

The above strategy can be repeated k times which will lead to the k th level of the HH hierarchy, with $k + 1$ different regions. All the information we need is contained in the K matrix. In the following we will sketch how this works and give general formulas for this breaking process.

The 0th level is again described by $\mathcal{A}_0 = U^+(1)_{2m_0}$ and to obtain k levels on top of \mathcal{A}_0 we should start with k auxiliary layers, resulting in an initial phase structure

$$\mathcal{A}_k = U^+(1)_{2m_0} \otimes U^+(1)_{2m_1 m_0^2} \otimes \cdots \otimes U^+(1)_{2m_k m_{k-1}^2 \dots m_0^2}. \quad (6.58)$$

This initial phase is described by the following K matrix and charge vector

$$K_{\mathcal{A}_k} = \text{Diag}(m_0, m_1 m_0^2, \dots, m_k m_{k-1}^2 \dots m_0^2) \quad (6.59)$$

$$\mathbf{t}_{\mathcal{A}_k} = (1, 1, \dots, 1)^T. \quad (6.60)$$

Note that \mathcal{A}_k is the full theory for the innermost region, but it can be used to describe all of them, for instance in the outermost region we would have $\mathcal{A}_0 = U^+(1)_{2m_0} \otimes \{0\} \otimes \cdots \otimes \{0\} \subset \mathcal{A}_k$.

To induce phase transitions between the $k + 1$ regions we start by condensing the first boson $\mathbf{B}_1 = (1, -m_1 m_0, 0, \dots, 0)$ and repeat the exercise of the previous subsection. Ultimately we end up with unconfined sectors $\mathbf{l} = (0, m_0 u, l_3, l_4, \dots, l_{k+1})_{\mathcal{A}_k}$. We repeat

this process, and the bosons that drive the k different phase transitions are

$$\mathbf{B}_{j>1} = \underbrace{(0, 0, \dots, 0, m_{j-2} \dots m_0, -m_j \dots m_0)}_{j-1 \text{ times}}, \underbrace{(0, \dots, 0)}_{k-j \text{ times}}. \quad (6.61)$$

It can be easily checked that these are indeed charge neutral bosons whenever the K matrices have $K_{ii} \in 2\mathbb{Z}, i > 0$ as is the case for the HH hierarchy. When \mathbf{B}_j condenses the sectors rearrange in orbits of length $2|m_{j-1} \dots m_0|$ and the \mathcal{T}_j sectors can be written as

$$|a\rangle = \sum_{a'=0}^{2|m_{j-1} \dots m_0|-1} (0, \dots, 0, m_{j-2} \dots m_0 a', a - m_j \dots m_0 a', l_{j+2}, \dots, l_{k+1}), \quad (6.62)$$

with $a \in \mathbb{Z}_{2|m_j m_{j-1}^2 \dots m_0^2|}$. From the monodromy of two such sectors we learn that the unconfined particles have $a \in m_{j-1} \dots m_0 \mathbb{Z}$, resulting in a number of $2|m_j \dots m_0|$ unconfined sectors.

When all k bosons have condensed we obtain the phase diagram with $k+1$ different phases \mathcal{U}_j , for $j = 0, \dots, k$ and $\mathcal{U}_0 = \mathcal{A}_0$. Every two adjacent phases \mathcal{U}_{j-1} and \mathcal{U}_j are separated by a wall \mathcal{T}_j which has sectors

$$|a\rangle_{\mathcal{T}_j} = \sum_{a'=0}^{2|m_{j-1} \dots m_0|-1} (0, \dots, 0, m_{j-2} \dots m_0 a', a - m_j \dots m_0 a', 0, \dots, 0). \quad (6.63)$$

They have $\mathbb{Z}_{2|m_j m_{j-1}^2 \dots m_0^2|}$ fusion rules and the fundamental excitation with $a = 1$ has charge $Q_1 = \frac{1}{m_j m_{j-1}^2 \dots m_0^2}$ and is strictly confined to the boundary. The sectors that can move into the phase \mathcal{U}_{j-1} and \mathcal{U}_j are, respectively,

$$|a = m_j \dots m_0 u\rangle \quad u \in \mathbb{Z}_{2|m_{j-1} \dots m_0|} \quad (6.64)$$

$$|a = m_{j-1} \dots m_0 u'\rangle \quad u' \in \mathbb{Z}_{2|m_j \dots m_0|}. \quad (6.65)$$

There is one \mathcal{T}_j sector that can move into both phases. It has charge $Q = e$, half-integer spin, and it is given by $|a = m_j m_{j-1}^2 \dots m_0^2\rangle$.

The W matrix that transforms the $K_{\mathcal{A}_k}$ matrix into the $K_{\mathcal{U}_k}$ matrix corresponding to

the k th level of the HH hierarchy is

$$W = \begin{pmatrix} 1 & 0 & 0 & 0 & \dots & 0 \\ 1 & -K_{01}m_0 & 0 & 0 & \dots & 0 \\ 1 & -K_{01}m_0 & (-K_{01}m_0)(-K_{12}m_1) & 0 & \dots & 0 \\ \vdots & \vdots & \vdots & \ddots & & \vdots \\ \vdots & \vdots & \vdots & \ddots & & 0 \\ 1 & -K_{01}m_0 & (-K_{01}m_0)(-K_{12}m_1) & \dots & \dots & (-K_{k-1,k}m_{k-1}) \dots (-K_{01}m_0) \end{pmatrix} \quad (6.66)$$

CHAPTER 7

Outlook

Part of doing research is that the job is never completely done: answers usually raise new questions. Therefore, in this last chapter we will present some of the questions that naturally follow from the results presented in this thesis, and we will indicate possible paths for future research.

Topological invariant The Hamiltonian in (3.1) was proposed as a continuum model for a three-dimensional topological insulator, but so far no explicit topological invariant has been written down to unambiguously confirm this. The classification of topological insulators [17–19] suggests that in three dimensions for a system with TRS, the invariant should take values in \mathbb{Z}_2 , but these results are obtained from lattice models. The problem with the model we investigate is that the number of available states grows with distance, so it is not possible to define a (magnetic) Brillouin zone.

A route that could be pursued is to investigate edge states. When the edge does not break the TRS and our system is indeed a topological insulator, then the edge to a trivial phase necessarily has to carry protected gapless edge modes. It might be easier to choose a different gauge in the formulation of (3.2) and consider a half infinite system with a boundary along the \hat{z} -axis. The system could be probed by, for instance, the insertion of some (possibly non-Abelian) flux along the lines of the Laughlin argument.

Fractional topological insulators Still focusing on the model of (3.1) we would like to remark that flat energy bands are very interesting if one wants to study interactions. Analogous to the FQHE, we could partially fill the LLL and try to find an interaction term that makes the partially filled system an exact ground state. This would be an interesting candidate for a fractional topological insulator, which would then exhibit fractionally charged particles. Studying interactions is most easily done on a compact manifold like the three-sphere, because such a system would only have a finite number of states making it feasible to do numerics. This construction would give a continuum version of the fractional Chern insulators.

Geometric picture Our results in chapter 3 suggest a geometrical picture for three-dimensional Landau levels based on four-dimensional Anti de Sitter space (AdS4), whose isometries are precisely $SO(3, 2)$. We have established that, as far as their quantum orbitals are concerned, particles in the three-dimensional Landau levels experience a geometry that is a radial deformation of AdS4 rather than flat space. We expect that this qualitative observation can be made more precise, for example in the form of accurate statements about magnetic translations.

Higher dimensions and spin representations Another observation about chapter 3 is that in three dimensions one may choose a different spin representation in the Hamiltonian, $H = H_0 - \alpha \mathbf{L} \cdot \mathbf{S}$, where α is a constant. For spin- s particles this gives us $2s + 1$ branches, of which one can always be made flat by adjusting the coefficient α . Presumably a higher spin representation will not change the fundamental structure, but will change the representation content to a corresponding higher spin representation of the group $SO(3, 2)$.

The system can also be analyzed in higher dimensions to determine whether a generic hierarchy of symmetries arises similar to what happens for the ordinary harmonic oscillator, which has a $SU(d)$ symmetry in d -dimensional space.

TSB with more domains In chapter 5 we extended our understanding of TSB by recognizing a ground state degeneracy after the formation of a condensate. This degeneracy could result in the formation of different domains in the bulk and on the boundary of a system in the broken unconfined \mathcal{U} phase. We discussed the specific example of a chiral compactified boson CFT and mainly focused on a system with a two-dimensional ground state manifold.

It would be intriguing to extend these derivations to systems with more structure. For instance, the FQH state at $\nu = 1/9$ allows a similar discussion as was already presented in section 5.1. Now we obtain three degenerate ground states and we can imagine that three different domains may touch at a point somewhere in the bulk of the system. It would be interesting to investigate what could happen at such a point.

Also we can imagine starting from a bulk in one of the ground states and then creating two different domains somewhere in the bulk by acting with the Wilson loop operators W_1 and W_2 . Now if we break both loops into Wilson lines by attaching $V_1-V_1^\dagger$ and $V_2-V_2^\dagger$ pairs at the endpoints we still have two gauge invariant operators. But what would happen if we fuse an endpoint of the first line with an endpoint of the other Wilson line? This would again create a loop but now with point excitations attached to the loop.

Domains in non-Abelian system In chapter 5 we have only focused on the $U(1)$ CFTs, but another interesting generalization are systems which are described by a WZW theory. Also, the NASS state discussed in section 6.2, would be a nice starting point. One could investigate how the non-Abelian nature of the quasiparticles affects the formation and stability of domain walls in the NASS state when it is obtained from breaking Ising $\otimes \mathcal{M}(4, 5)$.

Effective theory TSB We would like to show explicitly how TSB occurs from the effective Lagrangian of the topological phase. This could give much insight into the precise energy scales of the problem, and could ultimately help in designing experiments where these phase transitions could be explicitly realized.

TSB and other hierarchies The HH hierarchy that was constructed in chapter 6 by applying TSB to multilayered systems, could be generalized to other hierarchies and possibly be used to create entirely new ones. One particular hierarchy that we want to study in future work is the Bonderson-Slingerland (BS) hierarchy, which describes FQH states in the second Landau level. It contains non-Abelian states as opposed to the HH hierarchy. One of the states of this hierarchy is a candidate for the plateau observed at $\nu = 12/5$ and its neutral sectors are labeled by the Ising model [151].

It would be especially interesting to investigate possible boundaries with other FQH states. One obvious route is to study a transition between this state and one that has the same neutral sectors as the NASS state. This is because the parent state of the $\nu = 12/5$ phase of the BS hierarchy is precisely the MR state. Presumably, adding a layer of $\mathcal{M}(4, 5)$ to this BS state would drive a transition to some ‘daughter’ state of the NASS phase.

TSB and orbifolds We would like to conclude the outlook by pointing out a possible connection between TSB and orbifolds. Breaking an initial phase with Ising \otimes Ising sectors by condensing (ψ, ψ) , results in a compactified boson theory at radius $R = 2$, which was described in appendix 5.A and corresponds to $U(1)_2$. Conversely, the \mathbb{Z}_2 orbifold of a $U(1)_2$ theory is equivalent to Ising \otimes Ising.

According to ref. [78], in general the partition function of a \mathbb{Z}_2 orbifolded theory at radius R obeys

$$Z_{\text{orb}}(R) = \frac{1}{2} (Z(R) + 2Z(2\sqrt{2}) - Z(\sqrt{2})) . \quad (7.1)$$

For radii of the form $R = \sqrt{2p}$ with p a positive integer, it can be shown that the orbifold of $U(1)_p$ is some generalized Ising \otimes Ising model. This model has $p + 7$ operators and one of these has conformal weight 1. We can break this generalized model, which we will denote by Ising^(p), by condensing this boson to obtain $U(1)_p$ as broken unconfined phase. For $p = 4$, we get

$$(\text{Ising})^4 \xrightarrow{\text{TSB}} U(1)_4 \xrightarrow{\text{TSB}} U(1)_1 , \quad (7.2)$$

and conversely by \mathbb{Z}_2 orbifolding (see (7.1))

$$(\text{Ising})^4 \xleftarrow{\mathbb{Z}_2} U(1)_4 \xleftarrow{\mathbb{Z}_2} U(1)_1 . \quad (7.3)$$

Whenever $p = k^2$ applying TSB gives

$$(\text{Ising})^{k^2} \xrightarrow{\text{TSB}} U(1)_{k^2} \xrightarrow{\text{TSB}} U(1)_1 . \quad (7.4)$$

Orbifolding takes us in the other direction

$$(\text{Ising})^{k^2} \xleftarrow{\mathbb{Z}_2} U(1)_{k^2} \xleftarrow{?} U(1)_1 . \quad (7.5)$$

It seems tempting to conjecture that the missing link, $U(1)_{k^2} \leftarrow U(1)_1$, could be accomplished by a \mathbb{Z}_k orbifold, which corresponds to the fusion rules of the different vacua of $U(1)_{k^2}$ when breaking to $U(1)_1$.

Bibliography

- [1] K. VON KLITZING, G. DORDA, AND M. PEPPER. New method for high-accuracy determination of the fine-structure constant based on quantized Hall resistance. *Phys. Rev. Lett.*, **45**, 494, 1980.
- [2] R.B. LAUGHLIN. Quantized Hall conductivity in two dimensions. *Phys. Rev. B*, **23**, 5632, 1981.
- [3] D.J. THOULESS, M. KOHMOTO, M.P. NIGHTINGALE, AND M. DEN NIJS. Quantized Hall conductance in a two-dimensional periodic potential. *Phys. Rev. Lett.*, **49**, 405, 1982.
- [4] J.E. AVRON, R. SEILER, AND B. SIMON. Homotopy and quantization in condensed matter physics. *Phys. Rev. Lett.*, **51**, 51, 1983.
- [5] B. SIMON. Holonomy, the quantum adiabatic theorem, and Berry's phase. *Phys. Rev. Lett.*, **51**, 2167, 1983.
- [6] M. KOHMOTO. Topological invariant and the quantization of the Hall conductance. *Ann. Phys.*, **160**, 343, 1985.
- [7] D.C. TSUI, H.L. STÖRMER, AND A.C. GOSSARD. Two-dimensional magneto-transport in the extreme quantum limit. *Phys. Rev. Lett.*, **48**, 1559, 1982.
- [8] R.B. LAUGHLIN. Anomalous quantum Hall effect: an incompressible quantum fluid with fractionally charged excitations. *Phys. Rev. Lett.*, **50**, 1395, 1983.
- [9] R. DE PICCIOTTO, M. REZNIKOV, M. HEIBLUM, V. UMANSKY, G. BUNIN, AND D. MAHALU. Direct observation of a fractional charge. *Nature*, **389**, 162, 1997.
- [10] L. SAMINADAYAR, D.C. GLATTLI, Y. JIN, AND B. ETIENNE. Observation of the $e/3$ fractionally charged Laughlin quasiparticle. *Phys. Rev. Lett.*, **79**, 2526, 1997.
- [11] G. MOORE AND N. READ. Nonabelions in the fractional quantum Hall effect. *Nuclear Physics B*, **360**, 362, 1991.
- [12] M. GREITER, X.G. WEN, AND F. WILCZEK. Paired Hall states. *Nucl. Phys. B*, **374**, 567, 1992.
- [13] C. NAYAK, S.H. SIMON, A. STERN, M. FREEDMAN, AND S. DAS SARMA. Non-Abelian anyons and topological quantum computation. *Rev. Mod. Phys.*, **80**, 1083, 2008.

- [14] C.L. KANE AND E.J. MELE. Quantum spin Hall effect in graphene. *Phys. Rev. Lett.*, **95**, 226801, 2005.
- [15] B.A. BERNEVIG AND S.-C. ZHANG. Quantum spin Hall effect. *Phys. Rev. Lett.*, **96**, 106802, 2006.
- [16] M. KÖNIG, S. WIEDMANN, C. BRÜNE, A. ROTH, H. BUHMANN, L.W. MOLENKAMP, X.-L. QI, AND S.-C. ZHANG. Quantum spin Hall insulator state in HgTe quantum wells. *Science*, **318**, 766, 2007.
- [17] A.P. SCHNYDER, S. RYU, A. FURUSAKI, AND A.W.W. LUDWIG. Classification of topological insulators and superconductors in three spatial dimensions. *Phys. Rev. B*, **78**, 195125, 2008.
- [18] A. KITAEV. Periodic table for topological insulators and superconductors. *AIP Conf. Proc.*, **1134**, 22, 2009.
- [19] S. RYU, A.P. SCHNYDER, A. FURUSAKI, AND A.W.W. LUDWIG. Topological insulators and superconductors: Tenfold way and dimensional hierarchy. *New J. Phys.*, **12**, 065010, 2010.
- [20] A.Y. KITAEV. Unpaired Majorana fermions in quantum wires. *Phys.-Usp.*, **44**, 131, 2001.
- [21] G.E. VOLOVIK. Fermion zero modes on vortices in chiral superconductors. *JETP Lett.*, **70**, 609, 1999.
- [22] N. READ AND D. GREEN. Paired states of fermions in two dimensions with breaking of parity and time-reversal symmetries and the fractional quantum Hall effect. *Phys. Rev. B*, **61**, 10267, 2000.
- [23] E. MAJORANA. Teoria simmetrica dell'elettrone e del positrone. *Nuovo Cimento*, **14**, 171, 1937.
- [24] V. MOURIK, K. ZUO, S.M. FROLOV, S.R. PLISSARD, E.P.A.M. BAKKERS, AND L.P. KOUWENHOVEN. Signatures of Majorana fermions in hybrid superconductor-semiconductor nanowire devices. *Science*, **336**, 1003, 2012.
- [25] A. DAS, Y. RONEN, Y. MOST, Y. OREG, M. HEIBLUM, AND H. SHTRIKMAN. Zero-bias peaks and splitting in an Al-InAs nanowire topological superconductor as a signature of Majorana fermions. *Nature*, **8**, 887, 2012.
- [26] L.P. ROKHINSON, X. LIU, AND J.K. FURDYNA. The fractional a.c. Josephson effect in a semiconductor-superconductor nanowire as a signature of Majorana particles. *Nat. Phys.*, **8**, 795, 2012.

-
- [27] M.T. DENG, C.L. YU, G.Y. HUANG, M. LARSSON, P. CAROFF, AND H.Q. XU. Anomalous zero-bias conductance peak in a Nb-InSb nanowire-Nb hybrid device. *Nano Lett.*, **12**, 6414, 2012.
- [28] A.D.K. FINCK, D.J. VAN HARLINGEN, P.K. MOHSENI, K. JUNG, AND X. LI. Anomalous modulation of a zero-bias peak in a hybrid nanowire-superconductor device. *Phys. Rev. Lett.*, **110**, 126406, 2013.
- [29] H.O.H. CHURCHILL, V. FATEMI, K. GROVE-RASMUSSEN, M.T. DENG, P. CAROFF, H.Q. XU, AND C.M. MARCUS. Superconductor-nanowire devices from tunneling to the multichannel regime: zero-bias oscillations and magnetoconductance crossover. *Phys. Rev. B*, **87**, 241401, 2013.
- [30] I. M. JAMES, EDITOR. *History of Topology*. Elsevier, 1999. Chapter 12.
- [31] P.A.M. DIRAC. Quantised singularities in the electromagnetic field. *Proc. R. Soc. Lond. A*, **133**, 60, 1931.
- [32] X.G. WEN. Topological orders and edge excitations in fqh states. *Adv. Phys.*, **44**, 405, 1995.
- [33] C.L. KANE AND E.J. MELE. \mathbb{Z}_2 topological order and the quantum spin Hall effects. *Phys. Rev. Lett.*, **95**, 146802, 2005.
- [34] B.A. BERNEVIG. *Topological insulators and topological superconductors*. Princeton University Press, 2013.
- [35] R.E. PRANGE AND S.M. GIRVIN, EDITORS. *The quantum Hall effect*. Springer-Verlag, New York, 1987.
- [36] S.M. GIRVIN. The quantum Hall effect: Novel excitations and broken symmetries. arXiv:9907002, 1998.
- [37] J.E. AVRON, D. OSADCHY, AND R. SEILER. A topological look at the quantum Hall effect. *Physics Today*, **56**, 38, 2003.
- [38] B. DOUÇOT. Introduction to the theory of the integer quantum Hall effect. *C. R. Physique*, **12**, 323, 2011.
- [39] L.D. LANDAU. Diagnetismus der Metalle. *Z. Phys.*, **64**, 629, 1930.
- [40] D. XIAO, M.-C. CHANG, AND Q. NIU. Berry phase effects on electronic properties. *Rev. Mod. Phys.*, **82**, 1959, 2010.

- [41] M.V. BERRY. Quantal phase factors accompanying adiabatic changes. *Proc. R. Soc. Lond. A*, **392**, 45, 1984.
- [42] J.E. AVRON AND R. SEILER. Quantization of the Hall conductance for general multiparticle Schrödinger Hamiltonians. *Phys. Rev. Lett.*, **54**, 259, 1985.
- [43] Q. NIU, D.J. THOULESS, AND Y.-S. WU. Quantized Hall conductance as a topological invariant. *Phys. Rev. B*, **31**, 3372, 1985.
- [44] I. BLOCH, J. DALIBARD, AND W. ZWERGER. Many-body physics with ultracold gases. *Rev. Mod. Phys.*, **80**, 885, 2008.
- [45] K.W. MADISON, F. CHEVY, W. WOHLLEBEN, AND J. DALIBARD. Vortex formation in a stirred Bose-Einstein condensate. *Phys. Rev. Lett.*, **84**, 806, 2000.
- [46] N.R. COOPER. Rapidly rotating atomic gases. *Adv. Phys.*, **57**, 539, 2008.
- [47] A.A. ABRIKOSOV. Nobel Lecture: Type-II superconductors and the vortex lattices. *Rev. Mod. Phys.*, **76**, 975, 2004.
- [48] Y.-J. LIN, R.L. COMPTON, K. JIMÉNEZ-GARCÍA, J.V. PORTO, AND I.B. SPIELMAN. Synthetic magnetic fields for ultracold neutral atoms. *Nature*, **462**, 628, 2009.
- [49] V. SCHWEIKHARD, I. CODDINGTON, P. ENGELS, V.P. MOGENDORFF, AND E.A. CORNELL. Rapidly rotating Bose-Einstein condens in and near the lowest Landau level. *Phys. Rev. Lett.*, **92**, 040404, 2004.
- [50] G. JUZELIŪNAS AND P. ÖHBERG. Slow light in degenerate Fermi gases. *Phys. Rev. Lett.*, **93**, 033602, 2004.
- [51] J. DALIBARD, F. GERBIER, G. JUZELIŪNAS, AND P. ÖHBERG. Artificial gauge potentials for neutral atoms. *Rev. Mod. Phys.*, **83**, 1523, 2011.
- [52] D. JAKSCH AND P. ZOLLER. Creation of effective magnetic fields in optical lattices: the Hofstadter butterfly for cold neutral atoms. *New J. Phys.*, **5**, 56, 2003.
- [53] D.R. HOFSTADTER. Energy levels and wave functions of Bloch electrons in rational and irrational magnetic fields. *Phys. Rev. B*, **14**, 2239, 1976.
- [54] F. WILCZEK AND A. ZEE. Appearance of gauge structure in simple dynamical systems. *Phys. Rev. Lett.*, **52**, 2111, 1984.
- [55] L.S. BROWN AND W.I. WEISBERGER. Vacuum polarization in uniform non-Abelian gauge fields. *Nucl. Phys. B*, **157**, 285, 1979.

-
- [56] F.A. BAIS. Flux metamorphosis. *Nucl. Phys. B*, **170**, 32, 1980.
- [57] J. RUSECKAS, G. JUZELIŪNAS, P. ÖHBERG, AND M. FLEISCHHAUER. Non-Abelian gauge potentials for ultracold atoms with degenerate dark states. *Phys. Rev. Lett.*, **95**, 010404, 2005.
- [58] K. OSTERLOH, M. BAIG, L. SANTOS, P. ZOLLER, AND M. LEWENSTEIN. Cold atoms in non-Abelian gauge potentials: from the Hofstadter “moth” to lattice gauge theory. *Phys. Rev. Lett.*, **95**, 010403, 2005.
- [59] M.Z. HASAN AND C.L. KANE. Topological insulators. *Rev. Mod. Phys.*, **82**, 3045, 2010.
- [60] X.-L. QI AND S.-C. ZHANG. Topological insulators and superconductors. *Rev. Mod. Phys.*, **83**, 1057, 2011.
- [61] B.A. BERNEVIG, T.L. HUGHES, AND S.-C. ZHANG. Quantum spin Hall effect and topological phase transitions in HgTe quantum wells. *Science*, **314**, 1757, 2006.
- [62] N. GOLDMAN, I. SATIJA, P. NIKOLIC, A. BERMUDEZ, M.A. MARTIN-DELGADO, M. LEWENSTEIN, AND I.B. SPIELMAN. Realistic time-reversal invariant topological insulators with neutral atoms. *Phys. Rev. Lett.*, **105**, 255302, 2010.
- [63] G. LIU, S.-L. ZHU, S. JIANG, F. SUN, AND W.M. LIU. Simulating and detecting the quantum spin Hall effect in the kagome optical lattice. *Phys. Rev. A*, **82**, 053605, 2010.
- [64] F. WILCZEK. Majorana returns. *Nat. Phys.*, **5**, 614, 2009.
- [65] J. ALICEA. New directions in the pursuit of Majorana fermions in solid state systems. *Rep. Prog. Phys.*, **75**, 076501, 2012.
- [66] L. FU AND C.L. KANE. Superconducting proximity effect and Majorana fermions at the surface of a topological insulator. *Phys. Rev. Lett.*, **100**, 096407, 2008.
- [67] R.M. LUTCHYN, J.D. SAU, AND S. DAS SARMA. Majorana fermions and a topological phase transition in semiconductor-superconductor heterostructures. *Phys. Rev. Lett.*, **105**, 077001, 2010.
- [68] Y. OREG, G. REFAEL, AND F. VON OPPEN. Helical liquids and Majorana bound states in quantum wires. *Phys. Rev. Lett.*, **105**, 177002, 2010.

- [69] X.-G. WEN. *Quantum field theory of many-body systems*. Oxford University Press, 2004.
- [70] F.D.M. HALDANE. Many-particle translational symmetries of two-dimensional electrons at rational Landau-level filling. *Phys. Rev. Lett.*, **55**, 2095, 1985.
- [71] B.I. HALPERIN. Statistics of quasiparticles and the hierarchy of fractional quantized Hall states. *Phys. Rev. Lett.*, **52**, 1583, 1984.
- [72] D. AROVAS, J.R. SCHRIEFFER, AND F. WILCZEK. Fractional statistics and the quantum Hall effect. *Phys. Rev. Lett.*, **53**, 722, 1984.
- [73] B.I. HALPERIN. Quantized Hall conductance, current-carrying edge states, and the existence of extended states in a two-dimensional disordered potential. *Phys. Rev. B*, **25**, 2185, 1982.
- [74] X.G. WEN. Theory of the edge states in fractional quantum Hall effects. *Int. J. Mod. Phys. B*, **6**, 1711, 1992.
- [75] J.K. SLINGERLAND. *Hopf symmetry and its breaking*. PhD thesis, University of Amsterdam, 2002.
- [76] J. PRESKILL. Lecture notes for physics 219: Quantum computation. Chapter 9: Topological quantum computation, 2004.
- [77] A. KITAEV. Anyons in an exactly solved model and beyond. *Annals of Physics*, **321**, 2, 2006.
- [78] P. DI FRANCESCO, P. MATHIEU, AND D. SÉNÉCHAL. *Conformal Field Theory*. Springer, 1997.
- [79] F.A. BAIS, B.J. SCHROERS, AND J.K. SLINGERLAND. Broken quantum symmetry and confinement phases in planar physics. *Phys. Rev. Lett.*, **89**, 181601, 2002.
- [80] F.A. BAIS, B.J. SCHROERS, AND J.K. SLINGERLAND. Hopf symmetry breaking and confinement in $(2 + 1)$ -dimensional gauge theory. *JHEP*, **0305**(068), 2003.
- [81] F.A. BAIS AND J.K. SLINGERLAND. Condensate-induced transitions between topologically ordered phases. *Phys. Rev. B*, **79**, 045316, 2009.
- [82] F.A. BAIS, J.K. SLINGERLAND, AND S.M. HAAKER. Theory of topological edges and domain walls. *Phys. Rev. Lett.*, **102**, 220403, 2009.

-
- [83] F.A. BAIS AND J.C. ROMERS. Anyonic order parameters for discrete gauge theories on the lattice. *Ann. Phys.*, **324**, 1168, 2009.
- [84] M. BARKESHLI AND X.-G. WEN. Anyon condensation and continuous topological phase transitions in non-Abelian fractional quantum Hall states. *Phys. Rev. Lett.*, **105**, 216804, 2010.
- [85] M. BARKESHLI AND X.-G. WEN. Bilayer quantum Hall phase transitions and the orbifold non-Abelian fractional quantum Hall states. *Phys. Rev. B*, **84**, 115121, 2011.
- [86] F.A. BAIS AND J.C. ROMERS. The modular S-matrix as order parameter for topological phase transitions. *New J. Phys.*, **14**, 035024, 2012.
- [87] S.M. HAAKER, F.A. BAIS, AND J.K. SLINGERLAND. A quantum group approach to fractional quantum Hall hierarchies. *In preparation*.
- [88] L. KONG. A mathematical theory of anyon condensation. arXiv: 1307.8244v3, 2013.
- [89] A. KITAEV AND L. KONG. Models for gapped boundaries and domain walls. *Commun. Math. Phys.*, **313**, 351, 2012.
- [90] S.M. GIRVIN AND A.H. MACDONALD. Off-diagonal long-range order, oblique confinement, and the fractional quantum Hall effect. *Phys. Rev. Lett.*, **58**, 1252, 1987.
- [91] S.-C. ZHANG, T.H. HANSSON, AND S. KIVELSON. Effective-field-theory model for the fractional quantum Hall effect. *Phys. Rev. Lett.*, **62**, 82, 1989.
- [92] X.G. WEN AND Q. NIU. Ground-state degeneracy of the fractional quantum Hall states in the presence of a random potential and on high-genus Riemann surfaces. *Phys. Rev. B*, **41**, 9377, 1990.
- [93] F.D.M. HALDANE. Fractional quantization of the Hall effect: a hierarchy of incompressible quantum fluid states. *Phys. Rev. Lett.*, **51**, 605, 1983.
- [94] E. WITTEN. Quantum field theory and the Jones polynomial. *Commun. Math. Phys.*, **121**, 351, 1989.
- [95] R. WILLET, J.P. EISENSTEIN, H.L. STÖRMER, D.C. TSUI, A.C. GOSSARD, AND J.H. ENGLISH. Observation of an even-denominator quantum number in the fractional quantum Hall effect. *Phys. Rev. Lett.*, **59**, 1776, 1987.

- [96] W. PAN, J.-S. XIA, V. SHVARTS, D.E. ADAMS, H.L. STÖRMER, D.C. TSUI L.N. PFEIFFER, K.W. BALDWIN, AND K.W. WEST. Exact quantization of the even-denominator fractional quantum Hall states at $\nu = 5/2$ Landau level filling factor. *Phys. Rev. Lett.*, **83**, 3530, 1999.
- [97] E. ARDONNE. *A conformal field theory description of fractional quantum Hall states*. PhD thesis, University of Amsterdam, 2002.
- [98] B. BLOK AND X.G. WEN. Many-body systems with non-abelian statistics. *Nucl. Phys. B*, **374**, 615, 1992.
- [99] V. GURARIE AND C. NAYAK. A plasma analogy and Berry matrices for non-abelian quantum Hall states. *Nucl. Phys. B*, **506**, 685, 1997.
- [100] P. BONDERSON, V. GURARIE, AND C. NAYAK. Plasma analogy and non-Abelian statistics for Ising-type quantum Hall states. *Phys. Rev. B*, **83**, 075303, 2011.
- [101] X.G. WEN. Chiral Luttinger liquid and the edge excitations in the fractional quantum Hall states. *Phys. Rev. B*, **41**, 12838, 1990.
- [102] X.G. WEN. Gapless boundary excitations in the quantum Hall states and in the chiral spin states. *Phys. Rev. B*, **43**, 11025, 1991.
- [103] D.J. GROSS, J.A. HARVEY, E. MARTINEC, AND R. ROHM. Heterotic string theory (I). The free heterotic string. *Nucl. Phys. B*, **256**, 253, 1985.
- [104] R. FLOREANINI AND R. JACKIW. Self-dual fields as charge-density solitons. *Phys. Rev. Lett.*, **59**, 1873, 1987.
- [105] Y. LI AND C. WU. High-dimensional topological insulators with quaternionic analytic Landau levels. *Phys. Rev. Lett.*, **110**, 216802, 2013.
- [106] H. UI AND G. TAKEDA. Does accidental degeneracy imply a symmetry group? *Prog. Theor. Phys.*, **72**, 266, 1984.
- [107] A. CAPPELLI, C.A. TRUGENBERGER, AND G.R. ZEMBA. Infinite symmetry in the quantum Hall effect. *Nucl. Phys. B*, **396**, 465, 1993.
- [108] M. FLOHR AND R. VARNHAGEN. Infinite symmetry in the fractional quantum Hall effect. *J. Phys. A: Math. Gen.*, **27**, 3999, 1994.
- [109] J.B. EHRMAN. On the unitary irreducible representations of the universal covering group of the $3 + 2$ deSitter groups. *Proc. Cambridge Philos. Soc.*, **53**, 290, 1956.

-
- [110] P.A.M. DIRAC. A remarkable representation of the $3+2$ de Sitter group. *J. Math. Phys.*, **4**, 901, 1963.
- [111] N.T. EVANS. Discrete series for the universal covering group of the $3+2$ de Sitter groups. *J. Math. Phys.*, **8**, 170, 1967.
- [112] HARISH-CHANDRA. Infinite irreducible representations of the Lorentz group. *Proc. R. Soc. London Ser. A*, **189**, 372, 1947.
- [113] T. HOLSTEIN AND H. PRIMAKOFF. Field dependence of the intrinsic domain magnetization of a ferromagnet. *Phys. Rev.*, **58**, 1098, 1940.
- [114] V. BARGMANN. Irreducible unitary representations of the Lorentz groups. *Ann. Math.*, **48**, 568, 1947.
- [115] B.G. WYBOURNE. *Classical groups for physicists*. John Wiley & Sons, 1974.
- [116] B. BAGCHI. *Supersymmetry in quantum and classical mechanics*. Chapman & Hall/CRC, 2001.
- [117] N. MUKUNDA. Unitary representations of the group $O(2, 1)$ in an $O(1, 1)$ basis. *J. Math. Phys.*, **8**, 2210, 1967.
- [118] J.G. KURIYAN, N. MUKUNDA, AND E.C.G SUDARSHAN. Master analytic representation: reduction of $O(2, 1)$ in an $O(1, 1)$ basis. *J. Math. Phys.*, **9**, 2100, 1968.
- [119] G. 'T HOOFT. Magnetic monopoles in unified gauge theories. *Nucl. Phys. B*, **79**, 276, 1974.
- [120] A.M. POLYAKOV. Particle spectrum in the quantum field theory. *JETP Lett.*, **20**, 194, 1974.
- [121] N. GOLDMAN, A. KUBASIAK, P. GASPARD, AND M. LEWENSTEIN. Ultracold atomic gases in non-Abelian gauge potentials: The case of constant Wilson loop. *Phys. Rev. A*, **79**, 023624, 2009.
- [122] N. GOLDMAN, A. KUBASIAK, A. BERMUDEZ, P. GASPARD, M. LEWENSTEIN, AND M.A. MARTIN-DELGADO. Non-Abelian optical lattices: Anomalous quantum Hall effect and Dirac fermions. *Phys. Rev. Lett.*, **103**, 035301, 2009.
- [123] M. BURRELLO AND A. TROMBETTONI. Non-Abelian anyons from degenerate Landau levels of ultracold atoms in artificial gauge potentials. *Phys. Rev. Lett.*, **105**, 125304, 2010.

- [124] R.N. PALMER AND J.K. PACHOS. Fractional quantum Hall effect in a $u(1) \times su(2)$ gauge field. *New J. Phys.*, **13**, 065002, 2010.
- [125] D. ZHANG. Exact Landau levels in two-dimensional electron systems with Rashba and Dresselhaus spin-orbit interactions in a perpendicular magnetic field. *J. Phys. A: Math. Gen.*, **39**, L477, 2006.
- [126] T.T. WU AND C.N. YANG. Dirac monopole without strings: monopole harmonics. *Nucl. Phys. B*, **107**, 365, 1976.
- [127] T.T. WU AND C.N. YANG. Some properties of monopole harmonics. *Phys. Rev. D*, **16**, 1018, 1977.
- [128] Z.F. EZAWA. *Quantum Hall Effects*. Singapore: World Scientific, 2nd edition, 2008.
- [129] S.L. SONDHI, A. KARLHEDE, S.A. KIVELSON, AND E.H. REZAYI. Skyrmions and the crossover from the integer to fractional quantum Hall effect at small Zeeman energies. *Phys. Rev. B*, **47**, 16419, 1993.
- [130] F.D.M. HALDANE. Stability of chiral Luttinger liquids and Abelian quantum Hall states. *Phys. Rev. Lett.*, **74**, 2090, 1995.
- [131] M. LEVIN. Protected edge modes without symmetry. *Phys. Rev. X*, **3**, 021009, 2013.
- [132] Y.-M. LU AND A. VISHWANATH. Theory and classification of interacting integer topological phases in two dimensions: A Chern-Simons approach. *Phys. Rev. B*, **86**, 125119, 2012.
- [133] L.-Y. HUNG AND Y. WAN. K matrix construction of symmetry-enriched phases of matter. *Phys. Rev. B*, **87**, 195103, 2013.
- [134] L.-Y. HUNG AND Y. WAN. Symmetry enriched phases via pseudo anyon-condensation. arXiv:1308.4673v1, 2013.
- [135] Y. GU, L.-Y. HUNG, AND Y. WAN. A unified framework of topological phases with symmetry. arXiv:1402.3356v2, 2014.
- [136] F.A. BAIS. The topology of monopoles crossing a phase-boundary. *Phys. Lett. B*, **98**, 437, 1981.
- [137] S.M. HAAKER. Phase transitions between fractional quantum Hall states: a Bose condensation approach. Master's thesis, University of Amsterdam, 2009.

-
- [138] S. DAS SARMA, M. FREEDMAN, AND C. NAYAK. Topologically protected qubits from a possible non-Abelian fractional quantum Hall states. *Phys. Rev. Lett.*, **94**, 166802, 2005.
- [139] P. BONDERSON, K. SHTENDEL, AND J.K. SLINGERLAND. Interferometry of non-Abelian anyons. *Ann. Phys.*, **323**, 2709, 2008.
- [140] E. GROSFELD AND K. SCHOUTENS. Non-Abelian anyons: when Ising meets Fibonacci. *Phys. Rev. Lett.*, **103**, 076803, 2009.
- [141] F.E. CAMINO, W. ZHOU, AND V.J. GOLDMAN. Realization of a Laughlin quasiparticle interferometer: Observation of fractional statistics. *Phys. Rev. B*, **72**, 075342, 2005.
- [142] F.E. CAMINO, W. ZHOU, AND V.J. GOLDMAN. Aharonov-Bohm superperiod in a Laughlin quasiparticle interferometer. *Phys. Rev. Lett.*, **95**, 246802, 2005.
- [143] C. NASH AND D. O'CONNOR. Zero temperature phase diagram of the Kitaev model. *Phys. Rev. Lett.*, **102**, 147203, 2009.
- [144] G. KELLS, A.T. BOLUKBASI, V. LAHTINEN, J.K. SLINGERLAND, J.K. PACHOS, AND J. VALA. Topological degeneracy and vortex manipulation in Kitaev's honeycomb model. *Phys. Rev. Lett.*, **101**, 240404, 2008.
- [145] J.R. WOOTTON, V. LAHTINEN, Z. WANG, AND J.K. PACHOS. Non-Abelian statistics from an Abelian model. *Phys. Rev. B*, **78**, 161102(R), 2008.
- [146] E. ARDONNE AND K. SCHOUTENS. New class of non-Abelian spin-singlet quantum Hall states. *Phys. Rev. Lett.*, **82**, 5096, 1999.
- [147] E. ARDONNE AND K. SCHOUTENS. Wavefunctions for topological quantum registers. *Annals of Physics*, **322**, 201, 2007.
- [148] N. Regnault. Private communication.
- [149] K. Schoutens. Private communication.
- [150] R. ILAN, E. GROSFELD, K. SCHOUTENS, AND A. STERN. Experimental signatures of non-Abelian statistics in clustered quantum Hall states. *Phys. Rev. B*, **79**, 245305, 2009.
- [151] P. BONDERSON AND J.K. SLINGERLAND. Fractional quantum Hall hierarchy and the second Landau level. *Phys. Rev. B*, **78**, 125323, 2008.
- [152] S.M. HAAKER, F.A. BAIS, AND K. SCHOUTENS. Noncompact dynamical symmetry of a spin-orbit-coupled oscillator. *Phys. Rev. A*, **89**, 032105, 2014.

Samenvatting

In de volgende pagina's zal ik een overzicht geven van het vakgebied waarbinnen het werk, beschreven in dit proefschrift, zich afspeelt. Aan het eind zal ik ingaan op specifieke details van mijn onderzoek, maar ik richt mij dus met name op het grotere plaatje.

Deze beknopte samenvatting is gericht op de lezer die geen achtergrond heeft in de natuurkunde, maar wel graag meer over dit onderwerp te weten wil komen. Om te voorkomen dat het geheel te lang wordt en het woord samenvatting geen recht meer doet aan dit stuk, zal ik in de tekst verwijzen naar kaders waarin bepaalde begrippen toegelicht worden. Deze kunnen derhalve overgeslagen worden om een korte versie te krijgen, of bestudeerd worden door de lezer die specifieke voorbeelden wil zien.

Het is alles behalve triviaal om een onderwerp uit de theoretische natuurkunde op zo'n manier uiteen te zetten dat het voor de lezer zonder enige wiskundige achtergrond begrijpbaar wordt. Ik zal dan ook mijn best doen om hier toch zoveel mogelijk in te slagen. Tegelijkertijd is een tekst zonder lezer zinloos en heeft de lezer in mijn ogen ook een belangrijke taak in het begrijpen van de tekst. Vertel uzelf niet bij voorbaat dat u niets van het onderwerp begrijpt, maar probeer bij alles wat onduidelijk lijkt te bedenken wát er precies onduidelijk is. Soms moet men over bepaalde onduidelijkheden heen stappen zonder bang te zijn dat de rest ook onbegrijpelijk zal zijn ①.

Theoretische natuurkunde Natuurkunde is de wetenschap die zich bezighoudt met het beschrijven van de natuur. Wat voor type deeltjes zijn er en wat voor krachten zijn er werkzaam? De meest voor de hand liggende manier om iets te testen is door een experiment uit te voeren, deze tak van de natuurkunde wordt dan ook experimentele natuurkunde genoemd.

① De angst voor natuurkunde komt vaak voort uit de wiskunde waarmee het beschreven wordt. Wiskunde is als een taal en het is niet verwonderlijk dat het niet zomaar te begrijpen valt. Ten onrechte denkt men vaak dat je er nu eenmaal goed of slecht in bent, terwijl zoals bij iedere taal men er veel mee moet oefenen om er vaardig in te worden.

Natuurkunde aan de andere kant, kan op een heel ander niveau begrepen worden. Vergelijk het met de Oeigoeren in China. We hoeven geen Oeigoers of Chinees te beheersen om toch een idee te krijgen van de geschiedenis van deze volkeren en hun conflict.

Op zo'n niveau kan de natuurkunde ook begrepen worden. Er zijn bijvoorbeeld verschillende type deeltjes in het universum en verschillende krachten werkzaam. Sommige deeltjes trekken elkaar aan, andere stoten elkaar af. Als er heel veel deeltjes samen kunnen ze bepaalde materialen vormen en ga zo maar door.

② Beschouwen we bijvoorbeeld de klassieke natuurkunde, dan vertelt Newton's tweede wet $\mathbf{F} = m\mathbf{a}$ ons dat als een kracht \mathbf{F} werkt op een object met massa m dat het een acceleratie krijgt gegeven door \mathbf{a} . Je zou kunnen zeggen dat je een natuurkundig fenomeen hebt omschreven met een wiskundige formule, maar nu zijn we er nog niet. We willen namelijk weten hoe het object zich gedraagt hoe ver we ook terug gaan in het verleden of vooruit kijken naar de toekomst. We kennen zijn versnelling, maar wat is de positie en zijn snelheid?

We kunnen bijvoorbeeld de tijd meten die een bal met een massa van 3 kg er over doet om van een bepaalde helling af te rollen. Maar wat vertelt dit resultaat ons? Het doet alleen een uitspraak over dit hele specifieke geval. Zijn we vervolgens geïnteresseerd in hetzelfde experiment maar dan met een bal met een massa van 3,1 kg, dan zouden we het moeten herhalen.

③ Ik wil twee voorbeelden uitlichten, één waarbij de experimentatoren voorop liepen en een ander waarbij de theoretici eerst waren.

In 1879 ontdekte Edwin Hall dat wanneer er een elektrische stroom loopt in een bepaalde richting door een geleidend materiaal en daar vervolgens loodrecht een magneetveld op wordt aangebracht, er een spanningsverschil ontstaat in de richting die loodrecht is op zowel de stroom als het magneetveld. Tegenwoordig wordt dit het Hall effect genoemd. Het spanningsverschil kunnen we nu verklaren doordat de elektronen die bewegen in een magneetveld worden afgebogen door de Lorentz kracht, waardoor er ophoping van lading ontstaat en dus een spanningsverschil dat evenredig is met het magneetveld. Maar bedenk dat Hall zijn ontdekking deed bijna 20 jaar voordat het elektron ontdekt werd.

Als voorbeeld waarbij de theorie iets nieuws voorspelde wil ik het Majorana deeltje bespreken. In 1928 formuleerde Paul Dirac een vergelijking die het elektron beschreef binnen de theorie van de quantummechanica, wat tot dan toe nog niet gelukt was. Eén van de implicaties was dat antimaterie zou moeten bestaan, maar dat terzijde. Een ander werd afgeleid in 1937 door Ettore Majorana. Hij beseftte dat er een oplossing bestond van de Dirac vergelijking waarbij een deeltje beschreven wordt dat zijn eigen antideeltje is, het zogeheten Majorana deeltje. Dat deze voorspelling uit zijn theorie komt rollen betekent niet dat het al waargenomen is. Een kandidaat is de neutrino, die in overvloed in ons universum aanwezig is, maar heel moeilijk te detecteren. Sinds een jaar of 10 is er in het vakgebied waar mijn onderzoek ook deel van uitmaakt het besef ontstaan dat Majorana deeltjes ook 'gemaakt' kunnen worden als er op een slimme manier materialen gecombineerd worden. In 2012 is een experiment gedaan in Delft waarbij het er op lijkt dat het Majorana deeltje voor het eerst is geobserveerd, hoewel het nog niet onomstotelijk is vastgesteld.

Dit is waar theoretische natuurkunde om de hoek komt kijken. Men probeert aan de hand van wiskundige structuren (de taal van de natuur) het gedrag van deeltjes en krachten te beschrijven en met name te voorspellen. Het opschrijven van een theorie is uiterst niet-triviaal. Men kan niet zomaar zijn fantasie erop loslaten, want het geheel moet zelf-consistent zijn, eventueel passen binnen andere bestaande theorieën en te rijmen zijn met wat er daadwerkelijk wordt waargenomen. (In dit opzicht loopt de vergelijking die sommige mensen maken tussen religie en wetenschap in mijn ogen spaak.) En als de theorie is *opgeschreven*, betekent het nog niet dat hij is *opgelost* ②. Vaak is de theorie te ingewikkeld als we alle effecten mee willen nemen en zal men een aantal aannames moeten doen, bijvoorbeeld dat de aanwezigheid van een vlinder in Brazilië geen invloed heeft op een experiment met een deeltjesversneller in Texas.

De experimentele en theoretische fysica hebben een mooie wisselwerking, welke ik nogmaals wil benadrukken, omdat dit in het speciaal iets is wat mij zo aantrekt binnen het veld waarin ik mijn onderzoek heb gedaan. Soms worden er tijdens een experiment ontdekkingen gedaan die theoretisch nog niet te verklaren zijn (er bestaan geen formules of modellen die dat fenomeen omschrijven). De gemeenschap van theoretische natuurkun-

digen doet er dan alles aan om het theoretisch kader aan te passen zodat het fenomeen

verklaard kan worden. Anderzijds kunnen formuleringen vanuit de theorie bepaalde implicaties hebben die experimenteel nog niet zijn waargenomen. Experimentele natuurkundigen zullen dan opstellingen willen bedenken om te testen of die theorie wel klopt, of kunnen de theorie gebruiken bij het ontwerpen van apparaten met een praktische toepassing voor de maatschappij **(3)**. Deze wisselwerking is een enorme drijvende kracht achter het vergaren van kennis.

Men zou kunnen zeggen dat het ultieme doel van de fysica is om één theorie te construeren die alles wat we om ons heen zien kan beschrijven. Helaas is dit nog niet het geval. Bij het oprekken van de grenzen van onze kennis, wordt er aan allerlei verschillende kanten gewerkt. Dit heeft als gevolg dat bepaalde hoeken van de natuurkunde steeds verder van elkaar verwijderd raken. Af en toe staat er een briljante natuurkundige **(4)** op die twee uitgewaaierde hoeken weer bijeen brengt, maar een theorie van alles lijkt nog ver weg. Niet iedereen houdt zich bezig met een theorie van alles, in mijn onderzoek was dit helemaal niet het grote doel. Ik ben met name bezig geweest met het oprekken van kennis in een specifieke hoek.

Gecondenseerde materie Het gebied waarbinnen mijn onderzoek heeft plaatsgevonden is de gecondenseerde materie. In tegenstelling tot hoge energie fysica waar men zich met name richt op de bouwstenen van het universum, de zogenaamde elementaire deeltjes, zoals het elektron en bijvoorbeeld het Higgs deeltje, draait het bij gecondenseerde materie om het samenspel van vele deeltjes met elkaar.

Een alledaags voorbeeld is water. Een glas water en een blok ijs bestaan beide uit

(4) In **(3)** noemde ik al de Dirac vergelijking om het Majorana deeltje in te leiden, maar de ontdekking van Paul Dirac is een mooi voorbeeld waarbij hij de relativiteitstheorie van Albert Einstein combineerde met de quantum mechanica, om zo een correcte bewegingsvergelijking voor het elektron op te stellen.

De relativiteitstheorie is nodig om de natuurkunde te beschrijven van objecten die de snelheid van het licht (= 300.000.000 m/s) benaderen. De quantum mechanica is een theorie die niet aan één natuurkundige toe te dichten is en werd ontwikkeld gedurende de eerste decennia van de vorige eeuw. Het beschrijft de natuurkunde wanneer we kijken op een schaal ter grootte van een atoom en kleiner.

In ons dagelijks leven halen we deze snelheden niet en zijn we groter dan een atoom, maar dat wil niet zeggen dat de relativiteitstheorie of de quantum mechanica niet opgaat voor ons. Het is slechts zo dat de klassieke mechanica goed genoeg is en makkelijker om mee te werken (waarom moeilijk doen als het makkelijk kan), maar voor een elektron gaat de klassieke mechanica niet meer op en zullen we toch echt de Dirac vergelijking moeten gebruiken.

(5) Supergeleiding is een fenomeen waarbij sommige materialen onder een bepaalde temperatuur (nabij het absolute nulpunt) in een fase komen waarbij de elektrische weerstand door het materiaal gelijk aan nul is. Het werd ontdekt in een experiment uitgevoerd door de Nederlandse onderzoeker Heike Kamerlingh Onnes in 1911, waar hij later de Nobelprijs voor ontving. Er wordt vandaag de dag nog volop onderzoek gedaan naar supergeleiders. Enerzijds omdat de theorie erachter nog steeds niet volledig begrepen is en anderzijds omdat het vele toepassingen kent in de industrie.

vele watermoleculen en toch gedragen deze systemen zich heel anders: in water kan je zwemmen en op ijs kan je zitten. Zonder de precieze posities van alle deeltjes te hoeven kennen (wat onmogelijk is met deze aantallen moleculen) en de krachten die ze op elkaar uitoefenen, kunnen de eigenschappen van het gehele systeem toch worden beschreven. Water is een voorbeeld van een vloeistof en ijs een voorbeeld van een vaste stof. Dit noemen we verschillende *fases* waarin een materiaal (zoals water) zich kan bevinden. In welke fase een materiaal zich bevindt is afhankelijk van bepaalde externe eigenschappen, zoals de druk of temperatuur van het systeem. Als de temperatuur van een vloeistof daalt is er een bepaalde temperatuur waarop het materiaal verandert van een vloeistof in een vaste stof, dit wordt een *faseovergang* genoemd. Het voorbeeld van water wat ik nu aanhaal is aan de ene kant intuïtief, aangezien we er in het dagelijks leven mee te maken hebben, maar tegelijkertijd beperkend want er zijn vele andere materialen die veel exotischere eigenschappen hebben, zoals bijvoorbeeld supergeleiding ⑤.

⑥ Groepentheorie is een tak van wiskunde die de eigenschappen van groepen bestudeert en classificeert. Een groep is een verzameling elementen samen met een operatie die werkt op deze elementen, die aan een aantal eisen moet voldoen. Dit klinkt heel erg abstract (het is dan ook wiskunde!), maar ik zal een voorbeeld geven dat hopelijk wat verheldering brengt. Een voorbeeld van een groep is de verzameling gehele getallen, die weergegeven wordt door het symbool \mathbb{Z} , waarbij de operatie gegeven wordt door optellen. \mathbb{Z} bestaat uit getallen zoals 3, 18, 49899, -1 , -886 , maar dus niet uit cijfers met cijfers achter de komma. Per definitie moet een groep aan de volgende eisen voldoen (anders mogen we het geen groep noemen).

Geslotenheid: Als we twee willekeurige gehele getallen nemen en ze optellen is het resultaat weer een geheel getal.

Associativiteit: Als we drie gehele getallen bij elkaar optellen maakt het niet uit in welke volgorde we dat doen, $(3 + 11) + 22 = 3 + (11 + 22)$.

Identiteit: Er is één element in de groep die triviaal werkt op alle andere elementen. Bij de gehele getallen is dit het getal 0, aangezien $-3 + 0 = -3$.

Inversie: Voor ieder element is er een element, zodanig dat wanneer ze optellen de identiteit verkregen wordt. In ons voorbeeld wordt de inverse van een getal verkregen door een minteken ervoor te zetten, $-11 + 11 = 0$.

Symmetrie Zoals gezegd bestaat een materiaal uit heel veel deeltjes en is het onmogelijk om een theorie op te schrijven waarbij we alle afzonderlijke deeltjes bijhouden en beschrijven wat voor kracht ze precies op elkaar uitoefenen. Gelukkig maakt de theoretische natuurkunde niet alleen gebruik van dit soort ‘microscopische’ beschrijvingen, maar ook van abstractere wiskundige noties.

Wederom keren we terug bij het voorbeeld van water. Zonder de precieze details van de fase waarin de watermoleculen zich bevinden te kennen, kunnen wij hem classificeren aan de hand van zijn *symmetrieën*. Laten we eerst het geval bekijken waarbij de materie een vloeistof vormt. Alle moleculen bewegen door elkaar, botsen en gaan weer hun eigen weg. Er zit hier weinig structuur in. Bekijken we de vloeistof op een bepaald punt in de ruimte en vergelijken het met een positie verderop dan zien we geen verschil. Dit noemen we een symmetrie van het systeem en om precies te zijn een translatie-

symmetrie. Hoe verhoudt dit zich dan tot ijs? De moleculen vormen een kristal en be-

wegen niet meer door elkaar heen, ze zitten op een rooster. Als we nu een punt bekijken bijvoorbeeld waar zich een watermolecuul bevindt, kunnen we niet zomaar een stukje verderop kijken om hetzelfde aan te treffen, dit kan alleen nog maar in stapjes ter grootte van de afstand tussen de moleculen. Er is meer structuur en daardoor minder symmetrie. De *continue* translatie symmetrie is gebroken naar een *discrete* translatie symmetrie. Aan het beschrijven van symmetrieën ligt een wiskundige theorie ten grondslag. Dat vakgebied heet groepentheorie ⑥ en het wordt in alle hoeken van de moderne natuurkunde gebruikt.

Topologische fase In dit proefschrift bekijk ik materialen die zich in een ander soort fase bevinden dan een vloeistof of kristal. Deze fases worden niet getypeerd door een symmetrie zoals bijvoorbeeld rotatie- of translatiesymmetrie. Het betreft een systeem dat zich in een topologische fase bevindt ⑦. Tot de jaren 80 van de vorige eeuw werd er gedacht dat alle fases en dus ook de faseovergangen, beschreven konden worden aan de hand van de symmetrieën die we eerder bespraken, totdat er een belangrijke ontdekking gedaan werd wat tegenwoordig bekend staat als het *quantum Hall effect* ⑧.

Een materiaal dat zich in de quantum Hall fase bevindt, wordt gekenmerkt door de kwantisatie van de Hall weerstand, dit kan uitgedrukt worden als $R_H = \frac{p}{q} \frac{h}{e^2}$, waarbij p en q gehele getallen zijn die de specifieke quantum Hall fase aangeven, h de constante van Planck en e de lading van een elektron. De getallen h en e zijn zogeheten natuurconstanten, wat wil zeggen dat ze altijd dezelfde waarde hebben in tegenstelling tot bijvoorbeeld druk of temperatuur.

Als we naar de symmetrieën kijken van twee materialen die gekenmerkt worden door verschillende waarden van de Hall weerstand, zich dus op andere plateaus bevinden, dan zien we geen verschil. En toch hebben ze een andere weerstand, wat een fysische eigenschap is. Hieruit moet men concluderen dat de classificatie aan de hand van de symmetrieën niet altijd voldoende is. De reden dat dit een topologische fase wordt genoemd is dat de kwantisatie van de weerstand zo precies is dat het niet uitmaakt of de vorm van

⑦ Topologie is een tak uit de wiskunde, die de eigenschappen van een object onderzoekt die niet veranderen (invariant zijn) onder vervormingen van het object. Een regel bij dit soort vervormingen is dat er niet geknipt of geplakt mag worden.

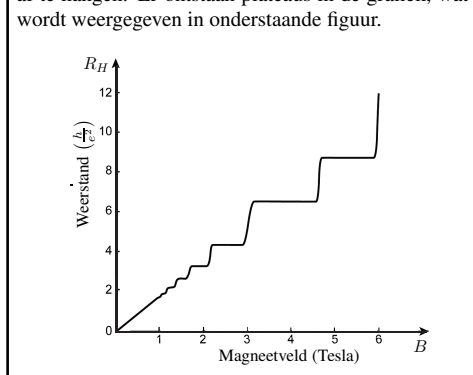
Een veelgebruikt voorbeeld is een koffiekop en een donut. Dit zijn op het eerste oog twee verschillende objecten, maar als we vervormingen toestaan zoals hierboven beschreven, dan kunnen we een koffiekop zo 'kneden' dat het gelijk wordt aan een donut. We zeggen dat ze topologisch equivalent zijn. De topologische invariant die hieraan toegekend kan worden is het aantal gaten in het object. De koffiekop en de donut hebben er beide één. Een bol heeft geen gaten en is niet equivalent aan een donut. Topologie is een globale eigenschap van een object. Lokaal kunnen we objecten vervormen zonder de topologie te veranderen, want het aantal gaten blijft gelijk ongeacht waar ze precies zitten.

Mocht zo'n soort equivalentie vreemd aanvoelen bedenk dan dat twee vrouwen heel erg verschillend zijn, maar dat we ze toch als vrouw kunnen classificeren aan de hand van hun geslachtschromosomen. Zo een classificatie kan handig zijn om bepaalde eigenschappen uit af te kunnen leiden zolang we maar beseffen waar de classificatie op gebaseerd is.

het materiaal iets anders is, of dat er hier en daar wat oneffenheden in het materiaal zitten. Zoals teruggelezen kan worden in ⑦ is de topologie van een object niet gevoelig voor lokale veranderingen, maar is het een eigenschap van het globale systeem. Naast het quantum Hall effect zijn er inmiddels vele andere topologische fases voorspeld en ontdekt, maar het quantum Hall effect staat nog steeds volop in de schijnwerpers en is één van de onderwerpen die behandeld worden in dit proefschrift.

Quasideeltjes Eén van de redenen om topologische fases te onderzoeken is dat sommige van deze systemen deeltjes hebben met bijzondere eigenschappen. Neem bijvoorbeeld het fractionele quantum Hall effect. Hierin kunnen deeltjes voorkomen met een elektrische lading die kleiner is dan de lading van het elektron. Wat hier wonderlijk aan is, is dat het systeem bestaat uit elektronen, wat elementaire deeltjes zijn, kleiner kan dus niet. En toch worden er deeltjes waargenomen met een kleinere lading.

⑧ In ③ besprak ik het Hall effect, maar dit fenomeen blijkt niet het complete verhaal te zijn. In 1980 werd er een experiment gedaan aan een systeem waarin de elektronen slechts in twee dimensies kunnen bewegen. Dit kan bewerkstelligd worden door twee slim gekozen materialen op elkaar te plaatsen, zodanig dat de elektronen slechts in het grensvlak tussen de materialen kunnen bewegen. Wanneer het geheel afgekoeld wordt tot ongeveer één graad boven het absolute nulpunt en er een heel sterk magneetveld gebruikt wordt dat loodrecht staat op het vlak waarin de elektronen bewegen, dan blijkt de weerstand niet langer linear van het magneetveld af te hangen. Er ontstaan plateaus in de grafiek, wat wordt weergegeven in onderstaande figuur.



De elektronen die een quantum Hall systeem vormen gedragen zich als een soort vloeistof. Plaatselijk kunnen er verdikkingen en verdunningen ontstaan en deze gedragen zich als deeltjes met fractionele lading. Aangezien het niet de deeltjes zijn waaruit het systeem is opgebouwd, worden ze ook wel quasideeltjes genoemd.

Wellicht is het tijd voor een kort intermezzo om de lezer die het niet meer ziet zitten moed in te praten. Het maakt niet uit als u het niet helemaal snapt. Om deze materie echt te doorgronden moet men kennis hebben van allerlei (veelal abstracte) theorieën, waar dan weer jaren van wiskundetraining aan vooraf gaat. Wat u op dit punt in de samenvatting moet begrijpen is dat er materialen (heel veel deeltjes bij elkaar) bestaan die onder hele extreme omstandigheden in een fase terecht komen, waarbij er ongebruikelijke fysische eigenschappen zich voordoen. In het geval van een materiaal dat zich in de quantum Hall fase bevindt is dat bijvoorbeeld een gequantiseerde weerstand en in

sommige gevallen het ontstaan van quasideeltjes in het materiaal.

Op deze quasideeltjes wil ik nog even doorgaan, omdat ze een grote rol spelen in mijn onderzoek, maar ook omdat ze een mooie toepassing hebben voor de industrie. De lading is niet het enige wat deze quasideeltjes bijzonder maakt, een andere eigenschap is dat ze een exotische *statistiek* hebben. Deze eigenschap zal ik nu toelichten. Stel we hebben twee identieke deeltjes, bijvoorbeeld twee elektronen. Met identiek bedoelen we dat we ze niet van elkaar kunnen onderscheiden. Nu draaien we één van de elektronen om de andere heen, wat schematisch weergegeven wordt in figuur 2.1 op pagina 30. De vraag is: kunnen we het verschil meten tussen een situatie waarbij de twee elektronen niet van plek veranderd zijn en waarbij ze wel de omcirkeling hebben doorgemaakt? Bij identieke elektronen en alle andere fundamentele deeltjes is dit verschil niet te meten, maar bij de quasideeltjes van het quantum Hall effect wel, ze hebben een niet-triviale statistiek. Nu zijn er bepaalde typen quasideeltjes voorspeld vanuit de theoretische natuurkunde (ze zijn nog niet met zekerheid waargenomen) die een bijzondere statistiek hebben die bruikbaar is om te dienen als hardware voor een topologische quantum computer ⑨.

Mijn proefschrift In het laatste deel van deze samenvatting wil ik kort toelichten wat er in de verschillende hoofdstukken van mijn proefschrift aan bod komt. Hoofdstuk 1 en 2 dienen als introductie en behandelen de bestaande kennis op het gebied van topologische fases en quantum Hall systemen. In hoofdstuk 1 wordt ook een ander vakgebied behandeld, dat nog niet de revue gepasseerd is in deze samenvatting, na-

⑨ Computeronderdelen worden almaar kleiner. Als die lijn wordt doorgetrokken komen we vanzelf in een regime waarbij de klassieke natuurwetten niet meer opgaan en de onderdelen zich volgens de quantum mechanica gaan gedragen ④. Dit lijkt op het eerste oog een probleem, maar in de jaren 80 van de vorige eeuw werd door een aantal natuurkundigen beseft dat het ook nieuwe mogelijkheden biedt. Een computer die gebruikt maakt van de quantum mechanica wordt een quantum computer genoemd en is in staat om (tot nu toe alleen in theorie) specifieke vraagstukken veel sneller op te lossen. Een voorbeeld hiervan is het factoriseren van getallen in priemgetallen, wat nu nog gebruikt wordt om op een veilige manier informatie te verzenden. Met de komst van de quantum computer zou deze manier van coderen veel sneller gekraakt kunnen worden.

Kort gezegd maakt een klassieke computer gebruik van *bits*, de toestand waarin een bit zich kan bevinden wordt weergegeven door een 0 of een 1. Met behulp van deze bits kan informatie worden opgeslagen en kunnen berekeningen worden gedaan. Een quantum computer werkt met *qubits* en het fundamentele verschil is dat een qubit een 0 of een 1 kan zijn, maar ook een 0 én een 1 tegelijkertijd. Dit fenomeen noemen we een superpositie en is aan de orde van de dag binnen de quantum mechanica. Pas als er een meting gedaan wordt, is de qubit een 0 of een 1, tot die tijd kunnen we alleen van kansen spreken of hij het één of het ander is. Van dit fenomeen kan handig gebruik gemaakt worden, aangezien berekeningen nu parallel uitgevoerd kunnen worden.

Het nadeel van een quantum computer is dat hij erg gevoelig is voor invloeden van de omgeving, wat kan leiden tot fouten in de informatie die opgeslagen is. Een oplossing voor dit probleem zou de topologische quantum computer zijn. De qubits van dit type computer worden gevormd door de quasideeltjes die leven in een topologische fase. Deze deeltjes hebben als eigenschap dat ze niet gevoelig zijn voor invloeden van hun omgeving. Als hun positie iets verandert of het materiaal vervormt, dan blijft de informatie behouden, aangezien de topologie van het geheel niet gevoelig is voor dit soort lokale veranderingen ⑦.

melijk systemen van koude atomen. Dit is een redelijk nieuw vakgebied en kan onder andere dienen als een simulator voor bijvoorbeeld quantum Hall materialen. Door een slimme opstelling te kiezen van lasers, kan een wolk van koude atomen zich zo gedragen dat het precies de eigenschappen van een quantum Hall systeem nadoet. Hoofdstuk 2 is met name gericht op het bespreken van faseovergangen tussen verschillende topologische fases. Er wordt uiteen gezet hoe zulke overgangen beschreven kunnen worden aan de hand van de specifieke quasideeltjes die in de fase voorkomen.

In hoofdstuk 3 wordt een specifiek systeem besproken waarin een geladen deeltje kan bewegen in drie dimensies, terwijl het een kracht voelt veroorzaakt door een opgelegd magnetisch veld. Deze configuratie is voorgesteld als een kandidaat voor een nieuw soort topologische fase [105]. Wij (Sander Bais, Kareljan Schoutens en ik) hebben de symmetrieën van dit systeem achterhaald en gebruiken vervolgens groepentheorie om de energieniveaus van het deeltje te vinden. Een soortgelijk vraagstuk wordt beschouwd in hoofdstuk 4. Het verschil is dat het deeltje nu nog maar in twee dimensies mag bewegen. Hierbij bekijken we (Benoit Estienne, Kareljan Schoutens en ik) het platte vlak, maar ook een deeltje dat op het oppervlak van een bol beweegt.

Het onderwerp van hoofdstuk 5 en 6 is faseovergangen tussen verschillende topologische fases. De bestaande theorie breiden we (Sander Bais, Joost Slingerland en ik) uit en we behandelen specifieke voorbeelden van dit soort processen. Verder bekijken we wat er gebeurt als men twee systemen die zich in een verschillende topologische fase bevinden naast elkaar plaatst. We leiden af wat er precies op de rand gebeurt en welke quasideeltjes daar kunnen bestaan. Eén van de voorbeelden die bekeken worden is een fase waarbij de quasideeltjes van het type zijn dat bruikbaar is voor een quantum computer.

Summary

In the following pages I will give an overview of the field, which the work described in this thesis is part of. Towards the end, I will discuss specific details of my research, but I will mainly focus on the bigger picture here.

This summary is aimed at the reader who has no background in physics, but would like to know more about this topic. To prevent this text from becoming too long, which would do no justice to the word ‘summary’, I will refer to frames in the text with which I elaborate on certain concepts. These can be skipped to obtain a short version or can be examined by the reader who wants to see specific examples.

It is far from trivial to explain a topic in theoretical physics in such a way that it is comprehensible for a reader without any background in mathematics. I will do my best to succeed in this task as much as possible. At the same time a text without a reader is pointless and in my opinion the reader has an important role in this process too. Do not tell yourself in advance that you do not understand anything about the topic, but try to think of what it is exactly that seems unclear. Sometimes one must pass over certain uncertainties without worrying too much that the rest will be incomprehensible too ①.

Theoretical physics Physics is the science which studies how nature behaves. Which types of particles exist and which forces act? The most obvious way to test something is by carrying out an experiment, and this branch of physics is called experimental physics. For example, we can measure the time it takes for a ball with a mass of 3 kg to roll down a certain incline. But what do these results tell us? We can only draw conclusions for this particular case. Should we be interested in the same experiment, but with a ball with a mass of 3.1 kg, we would have to repeat it.

① The fear of physics often stems from the underlying mathematics. Mathematics is like a language and therefore it is not surprising that it is not so easy to understand. Often you hear people claim that you are simply either good or bad at it. However I think that as with any language it takes a lot of practise to become skilled at it.

Physics, on the other hand, can be understood on a very different level. Compare it with the Uyghur people in China. We do not have to be familiar with Uyghur or Chinese to understand parts of the history of these peoples and their conflict.

In my opinion physics can also be understood at such a level. For example, there are different types of particles in the universe, and various forces are present. Some particles attract each other, others repel. If many particles come together, they may form specific materials and so on.

② For example, when we consider classical mechanics, Newton’s second law $\mathbf{F} = m\mathbf{a}$ tell us that if a force \mathbf{F} acts on an object with mass m it will have an acceleration given by \mathbf{a} . One could claim that a physical phenomenon is now described by a mathematical formula, but that is not the case yet. We want to know how the object behaves no matter how far we go back in the past or how far we look forward in time. We know its acceleration, but what is its position and velocity?

③ I want to highlight two examples, one in which the experimentalists led the way, and another in which the theorists were first.

In 1879, Edwin Hall conducted an experiment in which he discovered that a small voltage difference arises in a conductive material when an electric current flows in one direction, and a magnetic field is applied perpendicularly to the current. The voltage difference is observed in the direction which is perpendicular to both the current and the magnetic field. Nowadays this phenomenon is called the Hall effect and with our present knowledge the voltage difference can be explained as follows. Without a magnetic field, the electrons that make up the current would follow a straight path. When a magnetic field is applied the path gets curved by the Lorentz force and charge starts to accumulate at the edge of the sample, resulting in a voltage difference that is proportional to the magnetic field and the current. The explanation is fairly simple, but realize that Hall did this experiment almost 20 years before the electron was discovered.

As an example of a prediction that came from theoretical physics I would like to discuss the Majorana particle. In 1928 Paul Dirac formulated an equation which describes the electron within the theory of quantum mechanics. One implication of his theory was that antimatter should exist. Another was derived in 1937 by Ettore Majorana. He realized that a solution to the Dirac equation could be found which corresponds to a particle that is its own antiparticle, the so-called Majorana particle. Even though the theory allows for such a particle to exist that does not mean that it has been observed yet. Some physicists believe that the neutrino could be a Majorana particle. The neutrino is present in abundance in our universe, but it is also very difficult to detect. Another candidate can be found in the same realm of my field of research. Approximately 10 years ago it was realized that Majorana particles can be 'built' when certain materials are combined in a clever way. In 2012, a group in Delft conducted an experiment along those lines and they have strong evidence that they did indeed observe a Majorana particle, although I must say it has not yet been indisputably proven.

not yet been observed experimentally. Experimentalists will design setups and perform measurements to test if the theory is indeed correct, or they may use the theory to design devices with practical applications for society ③. This interaction is a major driving

This is where theoretical physics enters the stage. By using mathematical structures (the language of nature), one tries to explain and predict the behavior of particles and forces. Writing down a theory is highly nontrivial. Simply using your imagination is not good enough, because the theory must be self-consistent, it should potentially fit within other existing theories and be reconciled with what is actually observed. (In this respect, the comparison that some people make between religion and science does not hold in my opinion.) And even if a theory can be written down that does not mean that it has been solved ②. Oftentimes the theory is too complicated if we want to take all the effects into account and a number of assumptions have to be made. For instance, that the presence of a butterfly in Brazil has no effect on an experiment with a particle accelerator in Texas.

Once more I would like to emphasize the power of the interaction between experimental and theoretical physics, as this is the main reason why the field in which my research took place is so appealing to me. Sometimes an experimental discovery occurs, which was unexpected and cannot be explained from theory (there are no formulas or models that describe this phenomenon). The community of theoretical physicists will try their very best to adjust the theoretical framework or come up with something new in order to explain the observation. On the other hand, a new theory may have implications which have

force behind the acquisition of knowledge.

One could claim that the ultimate goal of physics is to construct one theory which accounts for everything we observe around us. Unfortunately this is not yet the case. When stretching the limits of our knowledge, scientists work in many different areas. As a result the different corners of physics drift away from each other. Occasionally a brilliant physicist ^④ enters the stage and manages to connect two different theories, but it seems that a theory of everything will not be developed in the near future. Even so, not every physicist is concerned with building a theory of everything, and for me this was never the main goal. I have been working in one specific area and have been trying to add to the knowledge of it.

Condensed matter The area in which my research took place is called condensed matter theory. As opposed to high-energy physics which focuses in particular on the building blocks of the universe - the so-called elementary particles, such as the electron and for example the Higgs particle - condensed matter theory studies the interplay of particles when you bring many of them close together.

A common example is water. A glass of water and a block of ice both consist of many water molecules and yet these systems behave very differently: you can swim in water and sit on ice. Without having to know the exact position of all the molecules (which is impossible with these numbers of particles), and the forces which they exert on each other, the properties of the entire system can still be described. Water is an example of a liquid and ice an example of a solid. This is what we call different *phases* of matter. The phase a specific material is in depends on certain external features, such as the pressure or temperature of the system. As the temperature

^④ I mentioned the Dirac equation in ^③ mainly to introduce the Majorana particle, but the discovery of Paul Dirac is a good example of a theory which merges two previously different areas. He combined the theory of relativity of Albert Einstein with quantum mechanics in order to get a correct equation of motion for the electron.

The theory of relativity is necessary to describe objects that travel with a speed that approaches the speed of light (= 300,000,000 m/s). Quantum mechanics is a theory which was developed during the first decades of the last century by many different physicists. It describes physics when we go to a scale the size of an atom or even smaller.

In our daily lives we do not reach these speeds and we are definitely bigger than an atom, but that does not mean that the theory of relativity or quantum mechanics does not apply to us. It is just that classical mechanics is good enough and far more easy to work with, but for an electron classical mechanics breaks down and we have to appeal to the Dirac equation.

^⑤ Superconductivity is a phenomenon in which some materials below a certain temperature (close to absolute zero) are in a phase in which the electric resistance through the material becomes equal to zero. It was discovered in 1911 in an experiment conducted by the Dutch scientist Heike Kamerlingh Onnes, for which he later received the Nobel Prize. Nowadays superconductivity is still an active area of research. Firstly, because the theory behind it is not entirely understood and secondly, because it has many applications in industry.

of a liquid decreases, there is a certain temperature at which the material changes from a liquid into a solid, which is referred to as a *phase transition*. I have used water as an example because we encounter it in our everyday lives and therefore it is easier to grasp, but at the same time it is limiting because there exist many other materials with far more exotic properties, for instance superconductivity (5).

(6) Group theory is a branch of mathematics that studies the properties of groups and classifies them. A group is a set of elements together with an operation that acts on these elements, which have to obey four conditions. This might sound very abstract (it is mathematics after all!), but I will give one specific example of a group, which hopefully makes it more tangible. The set of all integers, which is represented by the symbol \mathbb{Z} , together with addition (the operation) is an example of a group. The set \mathbb{Z} is composed of numbers such as 3, 18, 49899, -1 , -886 , but excludes numbers with decimal places. By definition a group must meet the following requirements (otherwise it cannot be classified as a group).

Closure: If we take two arbitrary integers their sum always results in another integer, i.e. another element of the group.

Associativity: When adding three integers the order in which we do so does not matter, $(3 + 11) + 22 = 3 + (11 + 22)$.

Identity element: There is one element in the group which acts trivially on all the other elements. In the case of the integers, the identity element is the number 0, since for instance $-3 + 0 = -3$.

Inverse element: For each element in the group, there is an element such that they add to the identity. In our example, the inverse of a number is obtained by acting with a minus sign, i.e. $-11 + 11 = 0$.

Symmetry As mentioned before a material consists of a lot of particles and it is impossible to write a theory that keeps track of every separate particle and the kind of forces they exert on each other. Fortunately, theoretical physics does not only solely make use of these kinds of ‘microscopic’ descriptions.

Once more we return to the example of water. Without knowing the exact details of the phase the water molecules are in, we can classify water by its *symmetries*. Let us first have a look at the case where the material forms a liquid. All the molecules move around, they collide and each go their own way again. This is a situation with very little structure. When we consider the liquid at a certain point in space and we compare that with a position farther along, we will not see any difference. This is what we call a symmetry of the system and in this particular case it is a translational symmetry. How does this compare to ice? The molecules form a crystal and no longer move around,

they are fixed to a grid. Now when we look at a certain point in space, for instance where a water molecule is located, we will not find the same situation when we translate to a different position in space. It is only a symmetry when translating by steps equal to the distance between the water molecules. In the case of ice there is more structure and therefore less symmetry. The *continuous* translation symmetry of the liquid is broken to a *discrete* translation symmetry. There is a mathematical theory at the root of describing symmetries. This field is called group theory (6) and is used in all corners of modern physics.

Topological phase In this thesis, I investigate materials that are in a different type of phase than those described for water. It concerns phases that are not characterized by a symmetry such as rotation or translation. This type of phase is referred to as a topological phase (7). Until the 1980's it was believed that all phases and phase transitions could be described by the underlying symmetries that were discussed before, until an important discovery was made which is nowadays known as the *quantum Hall effect* (8).

A material which is in a quantum Hall phase is characterized by the quantization of the Hall resistance, which can be expressed as $R_H = \frac{p}{q} \frac{h}{e^2}$, where p and q are integers that denote the specific quantum Hall phase, h is Planck's constant and e denotes the charge of an electron. The numbers h and e are so-called constants of nature, which means that they always have the same value in contrast to, for instance, pressure or temperature.

When considering two materials that are characterized by different values of the Hall resistance (different values of p and q), their symmetries are the same. And yet they have a different resistance, which is a physical property. From this, one must conclude that the classification of phases on the basis of its symmetries is not always sufficient. The reason that these phases are called topological phases is because of the exact quantization of the resistance. It does not matter whether the shape of the material is different, or there are impurities in the sample. As has been explained in (7), the topology of an object is not sensitive to local changes, but it is a feature of the global system. After the discovery of the quantum Hall phases many more topological phases have been predicted in theory and observed in experiments, nonetheless the quantum Hall effect is still an active area of research and is one of the topics treated in this thesis.

(7) Topology is a branch of mathematics which investigates the properties of an object that do not change (remain invariant) under smooth deformations of the object. Not all deformations are permitted, for instance one is not allowed to tear or glue.

A well-known example is a coffee cup and a donut. At first glance these are two different objects, but if we allow deformations such as described above, we may bend and stretch a coffee cup in such a way that it is transformed into a donut. Therefore these objects are topologically equivalent. The topological invariant that characterizes them is the number of holes in the object. The coffee cup and donut both have one hole, but a sphere for instance has no holes and is not topologically equivalent to a donut. Topology is a global property of an object. Locally we can distort the object without changing its topology. The number of holes remains the same regardless of where they are exactly.

If this kind of equivalence seems unnatural, remember that two women are very different, but we can still choose to classify them as women based on their sex chromosomes. Such a classification can be helpful to distill certain properties as long as we remember what the classification is based on.

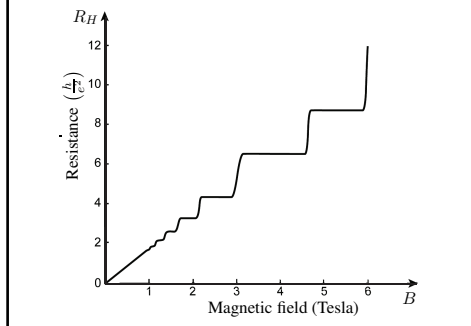
Quasiparticles One of the reasons to study topological phases is that in some of these systems particles emerge with special properties. Consider for example the fraction quantum Hall effect. In this system particles can exist with a smaller charge than that of an electron. The astounding thing about this is that this system is built up of electrons, which are elemental particles, so smaller should not be possible. Yet particles with a smaller

charge are being observed.

The electrons that form a quantum Hall system behave as if they were a sort of liquid. Locally there can be changes in density, which behave as particles of fractional charge. Considering that the system comprises electrons and not these particles, we speak of quasiparticles.

⑧ In ③ the Hall effect was discussed, but this phenomenon is not the whole story. In 1980, a similar experiment was conducted, but now a system was created in which the electrons could move in only two dimensions. This was achieved by placing two suitable materials on top of each other, in such a way that the electrons can only move along the interface between the two materials.

When the system was cooled down to approximately one degree above absolute zero and a very strong magnetic field was applied in the direction perpendicular to the plane in which the electrons can move, it was found that the resistance no longer depended linearly on the strength of the magnetic field. Instead, plateaus arise in the graph, which is depicted in the figure below.



electrons. Identical means that they are indistinguishable from one another. Now we bring one of the electrons around the other in a full circle, which is schematically depicted in figure 2.1 on page 30. We can ask ourselves the question: can we somehow measure the difference between the situation where the two electrons did not move and the situation where one circulation has been made? With electrons and any other fundamental particle this difference is not measurable, but with the quasiparticles of the quantum Hall phase it is, this is what we call nontrivial statistics. Certain types of quasiparticles have been predicted from theoretical physics (they have not yet been observed with complete certainty) that have special statistics which makes them useful as a kind of hardware for a

It might be time for a short intermezzo to encourage the reader who has lost track. It does not matter if you do not understand every bit of the text so far. To be able to thoroughly understand this, you need knowledge of many abstract theories, which is preceded by many years of practice in mathematics. What you need to understand at this point is that there exist materials (many particles together) that under certain conditions end up in a phase where unusual physical properties occur. In the case of a material that is in a quantum Hall phase, the resistance becomes quantized and in some cases exotic quasiparticles emerge in the material. I would like to focus somewhat more on these quasiparticles, because they play a big role in my research, but also because they have an exciting application for industry.

Their fractional charge is not the only aspect that makes these quasiparticles special; another property is that they have exotic *statistics*. I will explain this property in the following. Imagine that we have two identical particles, for instance two

topological quantum computer ⑨.

My thesis In the last part of this summary I would like to summarize what is discussed in the separate chapters of my thesis. Chapters 1 and 2 serve as an introduction and discuss the existing knowledge concerning topological phases and quantum Hall systems. In chapter 1 another field is discussed as well, that has not yet been mentioned in this summary, namely cold atom systems. This is a fairly new field and it can be used as a simulator of, for example, quantum Hall materials. By cleverly choosing an array of lasers, a cloud of cold atoms can be made to behave as if it is a quantum Hall system. Chapter 2 concentrates mainly on discussing phase transitions between different topological phases and how such transitions can be described using the specific quasiparticles that exist in that phase.

In chapter 3 a system is discussed that has a charged particle moving in three dimensions, while subject to a magnetic field. This configuration is proposed as a candidate for a new kind of topological phase [105]. We (Sander Bais, Kareljan Schoutens and I) have determined the symmetry of this system and have used group theory to find the energy levels of the particle. A similar issue is discussed in chapter 4. The difference there is that the particle can only move in two dimensions. We (Benoit Estienne, Kareljan Schoutens and I) consider a particle confined to the plane, but also a particle moving on the surface of a sphere.

Chapters 5 and 6 discuss phase transitions between different topological phases. We (Sander Bais, Joost Slingerland and I) expand the existing theory and discuss specific examples of these kinds of processes. Furthermore we look at what happens when two

⑨ Computer parts are getting smaller and smaller. As this trend continues we will automatically reach a regime where classic laws of physics no longer apply and the computer parts start to behave according to the laws of quantum mechanics ④. At first glance this seems to be a problem, but in the 1980's a number of physicists realized that this also brings forth great new possibilities. A computer that uses quantum mechanics is called a quantum computer and is (still only in theory) capable of solving specific problems much faster. An example is the factorization of prime numbers, which is nowadays being used for the encryption of information so that it can be sent safely. Quantum computers would make this way of encryption useless because they can easily crack it.

In short, a classic computer uses *bits* where the state a bit is in can be indicated by either 0 or 1. These bits can be used to store and process information. A quantum computer uses *qubits* and the fundamental difference is that a qubit can be either 0 or 1, but also 0 and 1 at the same time. This phenomenon is called superposition and is very common in quantum mechanics. Only when we measure which state the qubit is in do we find 0 or 1, until that time we can only talk about the probability of finding 0 or 1. This phenomenon has practical uses: considering calculations can now be done parallel.

A disadvantage of the quantum computer is that it is highly sensitive to its surroundings, which can cause errors in storing information or computing. A solution to this problem could be a topological quantum computer. The qubits of this type of computer are formed by the quasiparticles that exist in a certain topological phase. These particles have the disposition of being insensitive to the influences of their surroundings. If their position changes a bit or the shape of the material that carries them changes, the information is still stored, as the topology of the system is insensitive to these kinds of local changes ⑦.

systems that carry different topological phases are adjacent to each other. We derive what occurs at the boundary between the two phases and which quasiparticles can exist there. One of the examples is a phase with the sort of quasiparticles which are useful for a topological quantum computer.

Dankwoord

De laatste pagina's van dit proefschrift zijn de vrolijkste! Dit is de plek om iedereen te bedanken die op één of andere manier heeft bijgedragen bij de totstandkoming van dit werk.

Op de eerste plaats natuurlijk Kareljan Schoutens. Bedankt dat je me deze promotieplek gegund hebt. Helaas heb ik niet volop van jouw kennis gebruik kunnen maken, omdat je op andere plekken ook nodig was, maar ik wil je bedanken voor de vrijheid die je me gegeven hebt en je grenzeloze vertrouwen in me.

Het plezier dat ik tijdens mijn master's scriptie ervoer, heeft ertoe geleid dat ik aan deze promotie begonnen ben. Dit heb ik aan Sander Bais te danken mijn begeleider in die periode. In de eerste jaren van mijn promotie is het contact tussen ons sporadisch geweest (geheel aan mij te wijten), maar de laatste twee jaar hebben we weer intensief samengewerkt. Toen Kareljan mij niet meer kon begeleiden heb jij je over mij ontfermd en het is grotendeels aan jou te danken dat ik deze promotie uiteindelijk toch goed volbracht heb. Mijn dankbaarheid hiervoor is vele malen groter dan ik hier kan uitdrukken. Ook kijk ik met plezier terug op de vele gezellige middagen die we hebben gehad en voor al het 'vaderlijk' advies dat je me gaf omtrent mijn toekomstplannen. Ik waardeer je openhartigheid en bewonder je ongebreidelde enthousiasme voor zoveel verschillende onderwerpen.

The start of my PhD coincided with the arrival of a new postdoc: Benoit Estienne. In the first two years of my PhD I had the pleasure of working with you. I feel lucky that our paths crossed, not only are you a gifted physicist, but most of all I will remember you for the friend that you are. Conferences with you were never dull and I will fondly remember the numerous adventures that we have had.

Vanaf het begin van mijn master scriptie tot het eind van mijn promotie heb ik het genoeg gehad om met Joost Slingerland samen te werken. Dank je Joost dat je mijn vele vragen altijd vol geduld en feilloos wist te beantwoorden. En dat laatste paper dat komt er nog!

Jan de Boer wil ik bedanken voor het meedenken aan één van mijn projecten wanneer ik vastliep. Het paper [152] had zonder jouw hulp niet tot stand kunnen komen.

One of the best parts of being a PhD candidate is getting to meet so many bright, fun and inspiring people. Jesper and Miłosz, being your office mate felt like winning the jackpot. I could not have wished for anything better. When I think about the two of you, it always makes me smile.

I would like to thank the ID group for accepting me into their loving family, even though I had one dimension too many. Jacopo, Sebas, Rianne, Giuseppe (a.k.a Daddy), Thessa, Davide (a.k.a. the ASOIAF oracle), Omar, Rogier and Bram. Thanks for the many fun lunch breaks and all the other social stuff that happened after work.

And there are so many other physicists from my institute that I am grateful for for having met: Bahar, Liza, Balt, Xerxes, Thomas, Kristian, Michael, Antoine, J.-S., Ville, Guillaume, Balázs, Vladimir, Jelena, Milena, Paul, Daniel, Benjamin, Hamish, Marco, György, Ido, Natascia, Juan, Michiel, João, Bernard Nienhuis, Jan Pieter van der Schaar, Erik Verlinde, Tom Hijmans.

En dan was er nog de ondersteunde staff op ons instituut: Yocklang, Bianca, Anne-Marieke, Sandra, Natalie en Joost. Jullie ondersteunden niet alleen op het gebied van administratieve zaken, maar boden ook altijd een luisterend oor of maakten tijd voor gewoonweg een gezellig gesprek, wat een welkome afwisseling was op het vaak nogal eenzame werk dat ik moest verrichten.

I have met so many pleasant and fun people at conferences: Jildou, Ties, Erik, Sander, the guys from Delft, the Saclay guys (Jérôme, Jean-Marie and Roberto), Enrique, Zohar, Klaus, Iota, Olaf, Andrei, Fiona, Steve, Ady, Eddy, Rembert, Vicenze, and many many more. Thanks for the fun times we have had.

Johannes en Lucas bedankt voor alle fijne momenten en met name voor het samen opzetten van Nerd Nite. Wie had ooit gedacht dat het zo een succes zou worden! Lisa jij ook bedankt voor het meewerken aan Nerd Nite, maar met name voor de vriendin die je bent. Eén van de grootste voordelen aan deze PhD is dat ik jou heb ontmoet.

I want to mention a couple of people who helped me write this manuscript. Thijs bedankt voor je advies over Illustrator. Veronica and Lisa, thanks for reading and correcting parts of the manuscript. Milena, I cannot express how grateful I am for your effort. You read the ENTIRE manuscript and gave me so much helpful feedback. It did not just improve the text, but most of all it gave me so much moral support knowing that I was not alone in working at night. You are a true friend and I am grateful for that.

Teresa Mom bedankt voor de steun die je hebt geboden om mijn planning weer op de rails te krijgen. Je hebt me ontzettend veel goed advies gegeven en ik ben blij dat ik je ontmoet heb.

Kraker, thanks for your endless hospitality. The two months that I spent working at your place, was the best recipe for the physics blues I was experiencing at that time and it helped me finishing a paper I had been struggling with for more than two years. It was the best office I have had, say hi to the squirrels for me.

Mijn naaivrienden wil ik bedanken voor de heerlijke donderdagochtenden met koffie, koek, verhalen, wijze lessen en af en toe wat genaai. Zo had ik altijd iets leuks om naar uit te kijken. Van jullie heb ik zoveel geleerd wat misschien nog wel belangrijker dan natuurkunde is! Bedankt daarvoor lieve Eva, Ans, Loes, Sandy, Paula, Redina en met name natuurlijk Truus.

Mijn niet-natuurkunde vrienden bedankt voor alle fijne momenten die we samen gedeeld hebben. En in het bijzonder wil ik Emma en Liesbeth noemen, mijn niet-natuurkunde PhD vriendinnen die precies begrijpen wat een PhD doen inhoudt.

Gijs jij mag hier niet ontbreken. De eerste twee jaren van mijn promotie was jij mijn

steun en toeverlaat. Ik ben je dankbaar voor alles wat we samen hadden en simpelweg voor wie je bent.

Ik wil mijn familie bedanken voor alle steun en alle begrip. Het geeft een fijn gevoel om te weten dat jullie er altijd voor me zijn, ongeacht welke keuzes ik maak. Dit betekent zo ontzettend veel voor mij en geeft mij de basis voor het leven dat ik leid.

Lieve Lau, allereerst bedankt voor alle praktische steun die je me geboden hebt. Het helpen met het schrijven en vertalen van de samenvatting en je fantastische idee voor mijn cover design hebben me door de laatste stressdagen gesleept. Maar meer dan alles ben ik dankbaar voor alle liefde die je me geeft. Wanneer ik totaal opgezogen werd door mijn werk gaf je me die ruimte en stond je vervolgens klaar wanneer het me teveel werd. Je voelt precies aan wat ik nodig heb en geeft me dat zonder iets terug te verwachten. Door jou kan ik alles aan, zelfs een promotietraject!